

Doctoral thesis

**Neutralization Resistance and Post-Neutralization Properties of
Fly Ash and Blast Furnace Slag Based Geopolymer Concrete**

(フライアッシュと高炉スラグ微粉末を用いたジオポリマー
コンクリートの中酸化抵抗性及び中酸化後の性能変化)

September, 2018

LI SHA

Department of Information and Design Engineering
Graduate School of Science and Engineering

Yamaguchi University
Japan

Acknowledgements

I would like to thank my supervisor professor Zhuguo Li, Graduate School of Science and Technology for Innovation of Yamaguchi University, for his invaluable support, guidance, and constructive suggestion throughout this research.

I would like to thank Y. Tanigawa, an emeritus professor at Nagoya University, for his valuable advise.

The GP concrete specimens were produced mainly in the Mie Prefecture Testing Center for Construction Materials, Mie province, Japan. I am grateful to H. Takagaito and T. Nagai in the center, for providing the concrete production site, devices, tools and the human support during the production of GP concrete specimens.

Many thanks to S. Hashizume et al. in Toho Chemical Industry Co., Ltd.. for their assistance in the production of the cement specimens.

I would like to thank my senior Guodong Cao, and the team members Kun Guo and Zhisong Xu, for their kind help in producing the GP mortar specimens in laboratories of Yamaguchi University.

I would like to thank the scholarship support from Yamaguchi University, that gave me enough time to do my research.

Last but not the least, I have to thank to my families for their mental and physical supports.

Abstract

Geopolymer (GP), produced with industrial waste or by-product of rich Si, Al oxides and alkali activator, is thought as a potential alternative to ordinary Portland cement (OPC) for its less carbon dioxide emissions and mass waste recycling. Other advantages of concrete using GP as binder over OPC concrete also include early strength growth, fire and sulfate resistances, and no alkali aggregate reaction etc. However, detailed investigation of GP concrete's durability, especially carbonation resistance has been seldom conducted. For the practical use of GP concrete in reinforced concrete, the clarification of carbonation resistance of ambient-cured GP concrete is very important.

The most readily available GP source materials are fly ash (FA) and ground granulated blast furnace slag (BFS) in Japan, and the most commonly used alkali activators are sodium silicate, hydroxide or their mixture. Although FA and BFS can be used independently to produce GP, FA-based GP concrete, cured in the ambient air, has low compressive strength. Hence, in case of curing the ambient air, the addition of BFS is recommended for achieving a practical strength. In this study, the neutralization resistance and post-neutralization properties of FA&BFS-based GP concrete activated by sodium hydroxide and sodium silicate were investigated.

Carbonation reaction is always considered as a main reason of alkalinity drop of OPC concrete. Correspondingly, the carbonation resistance was firstly investigated for FA&BFS-based GP concrete, and was compared with OPC concrete with the same compressive strength. The experimental results showed that FA&BFS-based GP concrete, using 30% BFS, had a lower carbonation resistance than the normal OPC concrete.

Then, the carbonation depths of various FA&BFS-based GP concretes and GP mortars were measured by the accelerated carbonation test at different elapsed times. After discussing the relationship between the carbonation depth and the carbonation period based on the experimental results and by theoretical analysis, two root functions ($x=at^{1/n}$, a : carbonation rate coefficient) were proposed to describe the carbonation rate of FA&BFS-based GP concrete, and GP mortar, respectively. The reciprocal number of root values ($1/n$) are 0.31 for GP concrete and 0.22 for GP mortar, differentiating from OPC concrete, of which the $1/n$ value is 0.5.

The influencing factors of carbonation resistance of FA&BFS-based GP concrete were further investigated in detail, through comparing the carbonation rate coefficients of different GP concretes or mortars. It can be mainly concluded that the carbonation resistance increases with increasing BFS ratio in active fillers (AF), NaOH content in active activator solution (AS), and BFS fineness, or with reducing AS/AF ratio and

water/AF ratio. Moreover, heat-curing and addition of the retarder showed benefits to the improvement of the carbonation resistance of FA&BFS-based GP concrete.

In moisture environment, alkali activating matters, remained in the pores of GP concrete, may dissolve out through continuous pores opening to the outside, which are formed during dehydration polymerization reaction of GP. The neutralization behaviors of FA&BFS-based GP concrete in different environments, including water environment, wet-dry repeating environment besides CO₂ atmosphere, were thus investigated by measuring neutralization depth and pH value. And the neutralization resistances of GP mortar in different environments were compared with the OPC mortar cured under the same conditions. The experimental results indicate that GP concrete can also be neutralized to great degree under wetting, or in wet-dry repeating conditions, which implies that water absorption and evaporation would result in the neutralization of GP concrete. And FA&BFS-based GP concrete had a lower neutralization resistance than OPC concrete in water, and wet-dry repeating environments. However, curing at high temperature can improve the neutralization resistance of GP concrete.

Furthermore, the effects of neutralization on the compressive strength of FA&BFS-based GP mortar, and the changes in the ingredients and micro-structure of GP mortar were investigated together with OPC mortar under four kinds of environmental conditions. As the results, it is found that except in the wet-dry repeating environment, the compressive strength of ambient-cured FA&BFS-based GP mortar increased after neutralized in other three environments. After being neutralized in water immersion and wet-dry repeating environments, cubic-shaped calcite crystals with different sizes were found in the OPC mortar samples. However, many crystals shaped like flower in bloom were observed in GP mortar neutralized in the wet-dry repeating environment. The main elements of the flower-shaped crystals were C, Ca, O, and Si. But Na₂CO₃ crystal was judged as the main carbonation product of GP mortar in the accelerated carbonation (constant humidity and CO₂ concentration) and carbonation-dry repeating environments.

Contents

1	Introduction.....	1
1.1	Background of research.....	1
1.2	Objectives of the research.....	4
1.3	Frame of the research.....	5
	References.....	6
2	Literature Review.....	7
2.1	Geopolymer.....	7
2.1.1	Definition.....	7
2.1.2	Reaction mechanism.....	7
2.1.3	Raw Materials.....	9
2.1.4	Admixtures.....	12
2.1.5	Production.....	12
2.2	Performance characteristics of GP concrete.....	14
2.2.1	Microstructures.....	14
2.2.2	Properties.....	15
2.2.3	Influencing factors of mechanical properties.....	22
2.3	Neutralization resistance of GP concrete	27
2.3.1	AAS.....	27
2.3.2	FA-based GP.....	24
2.3.3	FA&BFS-based GP.....	25
2.4	The carbonation rate model.....	30
2.5	Summary.....	32
	Reference.....	33
3	The Carbonation Resistance of FA&BFS-based GP Concrete.....	41
3.1	Introduction.....	41
3.2	Experimental program.....	44
3.2.1	Materials.....	44
3.2.2	Mix proportions of GP concrete and mortar.....	44
3.2.3	Specimen preparation.....	46
3.2.4	Accelerated carbonation and compressive strength test.....	47
3.3	Results and the proposing of carbonation rate function.....	49
3.3.1	Pink color range on the specimen section after spraying phenolphthalein solution.....	49
3.3.2	Variation of carbonation depth with elapsed time.....	51
3.3.3	Carbonation Rate of GP Concrete.....	52
3.3.4	Carbonation rate model.....	53
3.4	Influencing factors of carbonation resistance.....	61

3. 4. 1	Addition of retarder.....	61
3. 4. 2	WG to AS ratio.....	62
3. 4. 3	AS to AF ratio and AS content.....	62
3. 4. 4	BFS to AF ratio.....	63
3. 4. 5	BFS fineness.....	64
3. 4. 6	Curing temperature.....	64
3. 4. 7	Na to Si ratio.....	65
3. 5	Relationship between compressive strength and carbonation resistance.....	66
3. 6	Conclusions.....	67
	References.....	69
4	The Neutralization Resistance of FA&BFS-based GP Concrete in Conditions with Water Movement.....	72
4. 1	Introduction.....	72
4. 2	Experimental program.....	74
4. 2. 1	Raw materials.....	74
4. 2. 2	Mix proportions.....	74
4. 2. 3	Production and curing of specimens.....	75
4. 2. 4	Neutralization environment conditions.....	75
4. 2. 5	Measurement methods of neutralization depth, pH and compressive strength.....	77
4. 3	Neutralization resistance of GP concrete.....	80
4. 4	Neutralization resistance of GP mortar comparing with OPC mortar.....	84
4. 5	Conclusions.....	88
	References.....	89
5	The Post-Neutralization Properties of FA&BFS-based GP Concrete.....	90
5. 1	Introduction.....	90
5. 2	Experimental program.....	92
5. 3	The post-carbonation properties.....	93
5. 3. 1	The compressive strength of specimens with and without carbonation.....	93
5. 3. 2	The micro-structure of specimens before and after carbonation.....	95
5. 4	The post-neutralization properties.....	97
5. 4. 1	The compressive strength of specimens neutralized and non-neutralized.....	97
5. 4. 2	The changes in micro-structure after neutralization.....	102
5. 5	Conclusions.....	107
	Reference.....	108
6	Conclusions and Future Works.....	109
6. 1	Conclusions.....	109
6. 2	Future works.....	111
	Paper List.....	112

List of terms and abbreviations

Terms /Abbreviations	Meaning
GP	Geopolymer
OPC	Ordinary portland cement
GPM	Geopolymer mortar
GPC	Geopolymer concrete
AGPC	Geopolymer concrete cured in the ambient air
HGPC	Heat curing geopolymer concrete
OPCM	Ordinary portland cement mortar
FA	Fly ash
BFS	Ground granulated blast furnace slag
AAS	Alkali activated slag
AAM	Alkali activated materials
AF	Active filler
AS	Alkali activator solution
S	Fine aggregate: Sea sand for mortar and river sand for concrete
G	Coarse aggregate:Crushed lime stone
WG	Water glass aqueous solution
NH	Sodium hydroxide solution
R	Retarder
W	Water content
C	Cement content
R-WRA	AE retarding type water-reducing agent
E_w/e_w	Environment of water immersion
E_{w+d}/e_{w+d}	Environment of wet-dry repeating
E_c/e_c	Environment of carbonation
E_{c+d}/e_{c+d}	Environment of carbonation-dry repeating
SEM	Scanning electron microscopy
EDS	Energy Dispersive Spectroscopy

List of symbols

Symbols	Meaning	Unit
f_c	Compressive strength	MPa
x	Carbonation diffusing depth	mm
t	Carbonation period	day
a	Carbonation rate coefficient	mm/ $\sqrt{\text{day}}$
Q	Diffusion flux of carbon dioxide	g/m ² ·s
φ	Carbon dioxide concentration	g/m ³
φ_0	CO ₂ concentration at the surface of concrete	g/m ³
D	Diffusion coefficient of CO ₂	m ² /s
J	The mass of chemically bound CO ₂ in concrete	g
S	Surface through which the diffusion occurs	m ²
q	CO ₂ absorption capacity	g/m ³
t_c	The age of concrete	day
a_∞	The ultimate degree of hydration	
M_{CO_2}	The molecular weight of CO ₂ ($M_{\text{CO}_2}=44$)	g/mol
n	Positive number of root function	
R^2	Determination coefficients	
R^2_m	The mean of R^2	
σ	Standard deviation	

List of Figures

Fig. 1.1	The CO ₂ emissions of GP concrete and OPC concrete in Japan.....	1
Fig. 1.2	The schematic of the opening-pores in GP concrete	3
Fig. 2.1	The stability of N-A-S-H gels due to Ca ²⁺ content and solution pH	15
Fig. 2.2	Compressive strength of 70%FA + 30%BFS (3000 cm ² /g)-based GPC.....	16
Fig. 2.3	Erosion situation of GP mortar and OPC mortar (4 months).....	18
Fig. 2.4	The polymer nanostructure of GP.....	20
Fig. 2.5	Weight loss of geopolymer mortars after 25 of freeze-thaw cycles.....	21
Fig. 2.6	Unclear carbonation boundary of FA-based GP concrete after spraying phenolphthalein indicator.....	28
Fig. 3.1	Experimental procedure.....	46
Fig. 3.2	Specimen's section sealed with waterproof tape.....	47
Fig. 3.3	Measurement positions of carbonation depth.....	47
Fig. 3.4	Color change after spraying the phenolphthalein solution.....	48
Fig. 3.5	Relationship between the carbonation depth of GP concrete and the elapsed time	51
Fig. 3.6	Relationship between the carbonation depth of GP mortar and the elapsed time...	52
Fig. 3.7	Carbonation coefficient of GP concrete with different AS content.....	52
Fig. 3.8	The SEM images of series No.1 before and after carbonation.....	54
Fig. 3.9	The changes of R ² _m and σ with 1/n of concrete.....	58
Fig. 3.10	The changes of R ² _m and σ with 1/n of mortar	59
Fig. 3.11	Effect of retarder on the <i>a</i> value of GP concrete and mortar.....	61
Fig. 3.12	The <i>a</i> -WG/AS ratio relationship of GP concrete and mortar.....	62
Fig. 3.13	The <i>a</i> -AS/F ratio relationship of GP concrete.....	62
Fig. 3.14	The <i>a</i> -AS content relationship of GP concrete.....	63
Fig. 3.15	The <i>a</i> -BFS/F ratio relationship of GP concrete.....	63
Fig. 3.16	The effect of BFS fineness on the <i>a</i> value of GP mortar.....	64
Fig. 3.17	The effect of curing temperature on the carbonation resistance of GP mortar	65
Fig. 3.18	The change of the <i>a</i> value of GP concrete with Na/Si ratio.....	65
Fig. 3.19	Relationship between the <i>a</i> value and compressive strength.....	66
Fig. 4.1	pH measurement positions for GP concrete	77
Fig. 4.2	Three pH measurement positions for mortar.....	77
Fig. 4.3	The effect of sample concentration on the pH values of GP and OPC mortar	78
Fig. 4.4	The effect of dissolving time in water on the pH values.....	79
Fig. 4.5	The flexural strength test (left) and compressive strength test (right) for mortar specimens.....	79
Fig. 4.6	The pH change with the elapsed time of the GP concretes under three conditions.....	81
Fig. 4.7	The pH change with the elapsed time in the three positions: 0 mm, 10mm, and 30mm of OPCM and GPM in the environments “E _w ” and “E _{w+d} ”.....	85

Fig. 4.8	The pH change with the elapsed time in the three positions: 0 mm, 10mm, and 30mm of OPCM and GPM in the environments “E _c ” and “E _{c+d} ”.....	86
Fig. 5.1	The compressive strength of GP concrete with and without 56 days carbonation.....	93
Fig. 5.2	The compressive strength of GP mortar with and without 42 days carbonation....	93
Fig. 5.3	The EDS mapping of GP concrete Series 11A carbonated 2 weeks.....	96
Fig. 5.4	The EDS mapping of GP concrete Series 11A carbonated 6 weeks.....	96
Fig. 5.5	Micro-structure of Na ₂ CO ₃	96
Fig. 5.6	The compressive strengths of specimens at the age of 28days, 68days, and after neutralizing in the four environments.....	97
Fig. 5.7	The element distribution of the crystals in the O _w , O _{w+d} , G _{w+d} and O _{c+d} samples....	103
Fig. 5.8	The SEM images (×100) of O _w and O _{w+d}	104
Fig. 5.9	EDS mapping of the G _c sample after carbonation.....	105
Fig. 5.10	EDS mapping of the G _{c+d} sample after carbonation-dry repeating.....	106

List of Tables

Table 2.1	The change after firing of metakaolin and FA based geopolymer.....	20
Table 2.2	Influencing factors effects on the compressive strength and setting time of FA&BFS-based GP concrete (1).....	23
Table 2.3	Influencing factors effects on the compressive strength and setting time of FA&BFS-based GP concrete (2).....	23
Table 2.4	Substances in AAS and OPC before and after carbonation.....	27
Table 2.5	Carbonation products of various GP concretes.....	29
Table 3.1	Physical properties and chemical compositions of active fillers.....	44
Table 3.2	Alkali activator's components and density.....	44
Table 3.3	Mix proportions and compressive strength of GP concrete.....	45
Table 3.4	Mix proportions and curing temperature of GP mortar.....	45
Table 3.5	Pink color ranges of concrete specimens before and after the	49
Table 3.6	Carbonation rate coefficient of GP concrete and OPC concrete with same compressive strength (mm/ $\sqrt{\text{week}}$).....	53
Table 3.7	The carbonation rate coefficient a of FA&BFS-based GP concrete.....	57
Table 3.8	The Determination coefficient R^2 of FA&BFS-based GP concrete.....	57
Table 3.9	The carbonation rate coefficient a of FA&BFS-based GP mortar.....	59
Table 3.10	The Determination coefficient R^2 of FA&BFS-based GP mortar.....	59
Table 4.1	Chemical compositions and physical properties of OPC.....	74
Table 4.2	Mixtures of GP mortar and GP concrete.....	74
Table 4.3	Mixtures of OPC mortar.....	74
Table 4.4	Environment conditions of neutralization (one cycle).....	76
Table 4.5	Color change and neutralization depth of GP concrete specimens in three neutralization environments.....	80
Table 4.6	Color change of mortar specimens processed in the four environments.....	83
Table 5.1	Mix proportions of FA&BFS-based GP concrete (C).....	92
Table 5.2	The SEM images of 4 kinds of GP mortars before and after carbonation..	95
Table 5.3	The SEM images ($\times 500$) of GPM and OPCM before and after neutralization in the 4 kinds of environments.....	99
Table 5.4	The SEM images ($\times 2000$) of GPM and OPCM before and after neutralization in the 4 kinds of environments.....	101

1 Introduction

1.1 Background of research

As the population grows, the demand of concrete used in construction also increases. The usage of concrete has been considered as the second only to the water around the world. Ordinary Portland cement (OPC) was always used as the main raw materials in concrete. However, If we want to produce one tonne OPC, almost 1 tonne CO₂ will be released into the atmosphere in the meantime^{[1][2]}. The CO₂ generated from the Portland cement industry has been as high as 5%~7% of the anthropogenic CO₂ production in the global^{[3][4][5]}. Searching for the alternatives of OPC, with a large reduction in CO₂ emissions, become increasingly necessary.

Geopolymer (GP), which some researchers named as alkali activated materials (AAM), is one kind of amorphous matrix, produced by raw materials highly containing Si/Al oxides, reacted with alkaline activator solutions. GP has been considered as the potential alternatives of OPC for enabling a significant reduction of CO₂ emission. GP cement can reduce 70%~90% CO₂ emissions compared to OPC for requiring a less amount of calcium-based raw materials^[6]. The CO₂ emissions statistical data of GP concrete in Japan confirms this result and presents 20% CO₂ emissions of OPC concrete as Fig. 1.1 shows^[7].

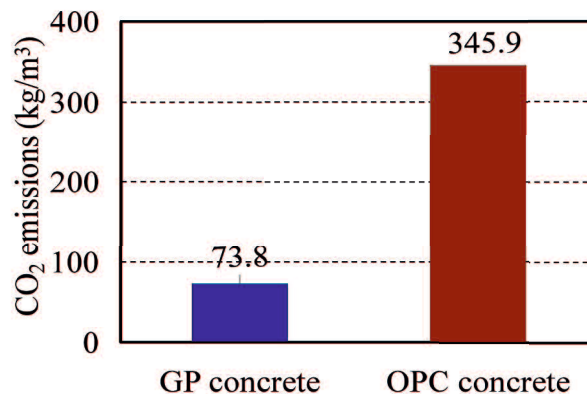


Fig. 1.1 The CO₂ emissions of GP concrete and OPC concrete in Japan

Meanwhile, Geopolymer utilize the waste materials as source material, can also solve the problem of disposing of industrial wastes and by-products^[8]. As we all know that the construction industry consumes amounts of minerals and produces amounts of industrial wastes and by-products^[4]. These waste materials such as bottom ash produced from power generation and mine wastes, by-products such as fly ash (FA), ground granulated blast furnace slags (BFS) and bauxite processing residues, not only take up many land, pollute environment but also waste a lot of resource. Those solids

are rich in silicate and aluminum.

Among them, the annual discharge of FA has been reported over 56.5 million tons in China, and over 12 million tons in Japan. The volume of fly ash would increase as the growing need of powder. Recently, the recycling rate of FA in China is just about 60%. Even though, in Japan, it is up to 98%, over 60% use of FA is to produce OPC cement as the replacing of clay ^[9]. This kind of usage has no effect on reducing the CO₂ emission of cement for limestone is still used. So, high value-added recycles of FA are expected. The usage of FA in GP can make it true for GP reduce less CO₂ emissions compared to OPC.

Up to now, FA-based GP concrete, used in research is always of heat curing. If we want to widely use GP in concrete especially for construction on site, GP concrete had better be cured at ambient temperature. However, the ambient-cured FA-based GP concrete have low compressive strength, BFS is always added to increase its compressive strength. Fly ash (FA, a pozzolanic material) and ground granulated blast furnace slag (BFS, a latent hydraulic material) are always blended as the main source material of GP ^[10].

GP concretes have been reported have the characteristics of high early compressive strength, strong acid corrosion, strong fire resistance, convenient maintenance, small hydration heat, and non-alkali aggregate reaction ^{[11][12][13]}. The application of this GP concrete so far is mainly focused on repairing materials, water tanks, retaining walls, precast structures and pavements. That is to say GP is mainly used in the precast concrete without steels. For reinforced concrete, in addition to ensuring the excellent properties of the concrete itself, we should also ensure the security of steel bars. For example, carbonation will decrease the pH of concrete and leads to steel corrosion. As the steel bar expands due to corrosion, the concrete will crack then peel off. The process of carbonation and steel corrosion are shown in Eqs. (1.1) and (1.2).



So for using GP in reinforced concrete, the more properties, especially the carbonation resistance, of GP concrete have to be considered. However, there is few studies on carbonation resistance of GP concrete. The existing studies on carbonation resistance of GP concrete are sometimes lower than that of OPC concrete. The carbonation resistance may be a problem to use GP in reinforced concrete.

For FA&BFS-based GP concrete with ambient curing, we have investigated its properties of compressive strength, sulfuric acid resistance, dry shrinkage, freeze-thaw resistance etc.. However, the carbonation resistance of this GP concrete is still unclear. Especially its carbonation rate model so far is not mentioned. Only really realizing the neutralization process of the GP concrete, can we widely use GP replacing of OPC in the reinforced concrete.

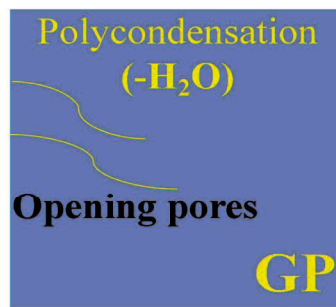


Fig. 1.2 The schematic of the opening-pores in GP concrete

On the other hand, since the polycondensation of GP concrete release water that may cause opening-pores in the concrete as shown in Fig. 1.2. Also because that the main carbonation substances in GP concrete may be the alkali activators. For geopolymer reinforced concrete, carbonation may be not the only way that reduce the alkalinity in the normal environment. That internal alkaline substance move out with water may also reduce the internal alkalinity of concrete. Like the the damage of normal concrete in the water environment, we speculate that water immersion and wet-dry repeating may cause large alkalinity decrease of geopolymer concrete. In this study, we defined the alkalinity decrease of GP concrete in the general environments without high acid or alkalinity as neutralization. Carbonation is only a way to neutralize GP concrete. So, neutralization resistance not just carbonation resistance should be considered for GP concrete.

Neutralization resistance of concrete decide the service life period of a building. Not only the neutralization resistance but also the post-neutralization properties, such as the compressive strength and micro-structures of GP concrete after neutralization should also be investigated. Only all the properties of FA&BFS-based GP concrete present well can this GP concrete can be used in the practical construction.

Hence, it is necessary to in detail investigate the neutralization resistance of FA&BFS-based GP concrete with ambient curing.

1.2 Objectives of the research

The ultimate aim of our research is to practically use the FA&BFS-based geopolymer as an alternative of ordinary Portland cement (OPC) in the construction industry. The neutralization resistance is an indispensable part for practical application of FA&BFS-based GP concrete, hence we will start with it first.

The study on neutralization resistance of FA&BFS-based GP concrete will be promoted as following 3 steps.

1. The thesis will find out whether carbonation (The most important one in neutralization conditions) can cause the decrease of FA and BFS based GP alkalinity and factors influencing the carbonation rate. Based on the carbonation results, we will further derive the carbonation rate formula suiting for FA&BFS-based GP concrete.

2. Due to the alkaline soluble substance is probably contained in the FA&BFS-based geopolymer, this research discussion will concentrate on whether the neutralization reaction of geopolymer concrete will be generated in the different environments, especially in the humid environment, as well as the test methods for judging it.

3. Except the study on neutralization resistance of the FA&BFS-based GP concrete, the effect of neutralization on other properties, especially on the compressive strength of the GP concrete, will also be investigated. Meanwhile, the SEM and EDS will be used to observe the micro-structure and ingredients of GP concrete before and after neutralization.

1.3 Frame of the research

This thesis is organized into 6 chapters. The main content of every chapter is summarized here.

Chapter 1 relates the reason, the necessary and the objects of conducting this research on the neutralization resistance of FA&BFS-based GP concrete.

Chapter 2 concludes the previous research achievements containing the definition, reaction mechanism and source raw materials of GP, the mechanical properties, and the influencing factors on mechanical properties of GP concrete based on BFS, FA and blending of them. The neutralization resistance of BFS, FA and blending of them based GP concrete is summarized and discussed principally.

Chapter 3 relates the carbonation rate of FA&BFS-based GP concrete and mortar with different recipes. According to the experimental results of carbonation depth this chapter proposes the carbonation rate function, meanwhile compares and analyzes the effect of different recipes on the carbonation rate of FA&BFS-based GP concrete.

Chapter 4 clarifies the neutralization depths and pH values of FA&BFS-based GP concrete and mortar compared with OPC mortar, after subjected to wetting, wet-dry repeating, carbonation, and carbonation-dry repeating, respectively. Depending on these results, the effect of water and carbonation in the ambient atmosphere on FA&BFS-based GP concrete can be understood.

Chapter 5 relates the effect of carbonation on the compressive strength of FA&BFS-based GP concrete by comparing the compressive strength change of the GP concrete with and without neutralization. Meanwhile, chapter 5 reports the micro-structure characteristics and the ingredient changes of FA&BFS-based GP mortar before and after neutralization based on scanning electron microscopy (SEM) and Energy Dispersive Spectroscopy (EDS) to explain the reason of compressive strength change.

Finally, chapter 6 relates the conclusions of this research and the further works .

References

- [1] M. C. G. Juenger, et al., Advances in alternative cementitious binders, *Cement and concrete research*. 41(12) (2011) 1232-1243.
- [2] J. Davidovits, False Values on CO₂ Emission for Geopolymer Cement/Concrete published in *Scientific Papers*, Geopolymer Institute Library Technical paper #24. (2015) 1-9.
- [3] E. Gartner, Industrially interesting approaches to low-CO₂ cements, *Cement and Concrete Research*. 34(9) (2004) 1489-1498.
- [4] D. N. Huntzinger, T. D. Eatmon, A life-cycle assessment of Portland cement manufacturing: comparing the traditional process with alternative technologies, *Journal of Cleaner Production*. 17 (7) (2009) 668-675.
- [5] C. Meyer, The greening of the concrete industry, *Cement and Concrete Research*. 31 (8) (2009) 601-605.
- [6] Technical paper #21 GP_CEMENT2013, Geopolymer cement review. 2013.
- [7] 上原 元樹, ジオポリマー法でコンクリートの環境負荷を低減する, *材料技術*, (2011) 10-13.
- [8] K. I. Song, J. K. Song, B. Y. Lee, K. H. Yang, Carbonation characteristics of alkali activated blast-furnace slag mortar, *Advances in Materials Science and Engineering*. (2014) 1-11.
- [9] JCOAL 一般財団法人石炭エネルギーセンター, 石炭灰全国実態調査報告書 (平成 26 年度実績), 2018.
- [10] A. A. Adam, Strength and durability properties of alkali activated slag and fly ash-Based geopolymer concrete, RMIT University Melbourne, Australia. (2009)
- [11] D. A Crozier, J. G. Sanjayan, Chemical and physical degradation of concrete at elevated temperatures, *Concrete in Australia*. 25(1) (1999) 18-20.
- [12] S. Thokchom, P. Ghosh, S. Ghosh, Performance of fly ash based geopolymer mortars in sulphate solution, *Journal Engineering Technology Review*. 3(1) (2010) 36-40.
- [13] B. V. Rangan, Geopolymer concrete for environmental protection, *The Indian Concrete Journal*. 88(4) (2014) 41-59.

2 Literature Review

2.1 Geopolymer

2.1.1 Definition

The term “geopolymer (GP)” is proposed in 1978 by Davidovits. According to Davidovits^[1], geopolymers are polymers, a type of amorphous 3D materials with complex composition, that is different to the crystal of $\text{Ca}(\text{OH})_2$ and C-S-H in OPC.

There has been a controversy on the definition between GP and alkali-activated materials (AAM). According to Palomo et al. ^[2], alkali-activation should be divided into two models. One is the (Si+Ca) model, represented by blast furnace slag activation, with a mild alkaline solution. The other is alkali activation (Si+Al), example is the alkali-activation of metakaolin or FA with medium to high alkaline solutions. The final product of second model is characterized by a polymeric model and high mechanical strength. And it is the alkali-activated metakaolin or FA that always considered as the geopolymer. And GP usually present great advantages over AAS.

The general rule is to use the name alkali-activated binders, and the name geopolymer should only be used when we are really in the presence of a geopolymer, a zeolite with amorphous to semi-crystalline characteristics^[3].

So, geopolymer is one kind of amorphous matrix, produced by raw materials highly containing Si and Al oxides reacted with alkaline liquid. Up to now, the most acceptable viewpoint for judging GP is that GP must meet the following two points.

- (1) The constituent material must be amorphous;
- (2) The $[\text{SiO}_4]^-$ and $[\text{AlO}_4]^-$ tetrahedral units must be high polycondensed and having a three-dimensional (3D) network.

However, in Japan, all products reacted with raw materials, containing aluminum and silicate as the main component, and alkaline liquid can be defined as GP. That is to say, AAS can also be defined as GP based on slag.

2.1.2 Reaction mechanism

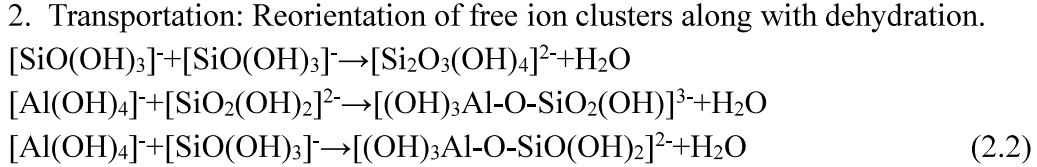
The polymerization process (geopolymerization) involves a substantially fast chemical reaction under alkaline conditions with Si and Al minerals that results in a three-dimensional polymeric chain and ring structure consisting of Si-O-Al-O bonds.

There are researchers divided the synthesis of geopolymers into two steps: fast dissolution and fast polycondensation. But, the more acceptable saying thought that synthesis of GP consists of three basic steps^{[4][5]}:

1. Dissolution: Dissolution of aluminosilicate in a strong alkali solution



Under highly alkaline conditions, reactive aluminosilicates are rapidly dissolved and free $[SiO_4]^-$ and $[AlO_4]^-$ tetrahedral units are released in a strong alkali solution as shown in Eq. (2.1).



The tetrahedral units are alternatively linked to polymeric precursor, as shown in the right of Eq. (2.2), by sharing part of the oxygen atoms, along with dehydration.

3. Polycondensation: Condensation and hardening of the structure in an inorganic polymeric system.

As the polymerization proceeds, polymeric precursor further translates to polymeric Si-O-Al-O bonds (silicate). Positive ions, like Na^+ , K^+ etc. is needed to balance the negative charge of Al^{3+} in tetrahedral coordination. The empirical formula of silicate is as follows:



where n is the degree of polymerization, z is 1, 2 or 3, and M is an alkali cation, such as Na or K, generating different types of poly(sialates).

One kind of three-dimensional network gel can be divided into the following 3 types.

- PS: Poly (sialate:Si/Al=1) -Si-O-Al-O-
- PSS: Poly (sialate-siloxo:Si/Al=2)-Si-O-Al-O-Si-O-
- PSDS: Poly (sialate-disiloxo:Si/Al=3) -Si-O-Al-O-Si-O-Si-O-

The open framework 3D structure is a proposed structure for the N-A-S-H gel (using Na based alkaline activator) arising from the “geopolymerisation”, in which the degree of condensation is somewhat greater than that found in hydrated Portland cement systems [6].

Besides, from the process of geopolymers’ synthesis, it can be found that the dissolution of aluminosilicate uses water, but the polymerization releases water. That is to say, the water during the geopolymerization just acts as a reagent or as a reaction process[7]. According to Davidovtis[11], the water used in the dissolution and hydrolytic process will balance the water produced by geopolymer. So, the author insist that there was no bound water within the geopolymer. But, releasing water in the hardening time may cause interconnected open-pores in GP that decrease the permeability resistance of GP strongly. That also a reason why we have to conduct this research on neutralization resistance of GP concrete.

2. 1. 3 Raw Materials

(1) Source materials

The source materials for geopolymers could be natural minerals, such as kaolinite, clays, micas, andalusite, spinel, etc, or by-product materials, such as fly ash, silica fume, slag, rice-husk ash, red mud, etc, whose empirical formula contains Si, Al, and oxygen (O)^[1]. The choice of the source materials depends on cost, application or specific demand of the users. Most recently used in research or actual construction are metakaolin, fly ash and blast furnace slag.

Metakaolin is looked as a preferred source materials of geopolymer due to its high rate of dissolution in the reactant solution, easier control on the Si/Al ratio and the white color^[8]. However, metakaolin is expensive. Using Metakaolin based GP as the binder of concrete is unrealistic. Moreover, metakaolin has higher liquid demand due to its finer particle size. The workability of metakaolin based GP is difficultly controlled.

Blast furnace slag (BFS) and fly ash (FA) are two kinds of by-products from steel plant and coal-fired power plant respectively. Their massive accumulation, especially for FA, has already caused an ecological burden. From the Fly Ash Industry Development Report of China (2017) and Japan (2016), the annual discharge of fly ash in China is over 56.5 million tons, and over 12 million tons in Japan. But the recycling rate of fly ash for China is only about 60%, that is much less than 98% of Japan. Rational use of BFS and FA will not only cost less but also solve the problem of disposing of industrial waste.

It has been proved that alkali-activated slag concrete has the advantages of low energy consumption, excellent physical and mechanical properties and durability. However, the composition of alkali-activated slag concrete is complex, the early hydration speed is very fast^[9]. The hydration product is complex, the dry shrinkage is big, and it is easy to produce cracks^[10]

It is found that the low calcium (ASTM Class F) FA is preferred as a source material than high calcium (ASTM Class C) FA, for high calcium may interfere with the polymerisation process and alter the micro-structure^[6]. Low-calcium FA (Class F) has been investigated as a suitable material for geopolymer because of its wide availability, pertinent silica and alumina composition and less water demand. Besides, the special spherical shape particles in FA exert good effect on binders' workability. Heat-cured low-calcium FA based geopolymer concrete has shown excellent mechanical and durability properties in short and long term tests^{[11][12]}.

In contrast, FA-based GP concrete cured at ambient temperature is reported having a long setting time but a low 28 days compressive strength. The requirement of curing at elevated temperature largely limit the wide use of FA-based GP concrete in the construction engineering. For solving this problem, FA-based GP concrete blended with

various admixtures and additives such as metakaolin, silica fume, blast-furnace slag, Portland cement, rice husk ash and waste by-products from different industries were investigated. Among these admixtures and additives, blast furnace slag has been tested with great results for the ambient-cured Class F FA-based GP concrete [13]. BFS accelerated the setting time with significant improvement of strength, but the workability and handling time reduced rapidly with the increase of slag content [14]. In our experiment the mechanical strength of FA&BFS-based GP concrete specimens with ambient curing were investigated. The specimens blended 30% BFS had a better compressive strength than that blended less BFS, but the setting time of specimens containing 30% BFS was less than 40 min. In order to ensure the strength and workability of concrete, one kind of retarder was added into the concrete [15].

FA and BFS have been confirmed as the potential source materials for making geopolymers [16]. Recently, there are more and more researchers focused their studies on FA&BFS-based GP concrete.

One more question is that, for the alkaline activated blending of FA and BFS, it is difficult to determine whether it is a GP or not. According to the study of M. Criado et al. [17], who detected the micro-structures of fillers with BFS ratio from 0 to 80%, it was found that the main products of active fillers (F) blended above 60% BFS is C-A-S-H gels (Ca, Al, Si, H₂O), but when BFS occupied below 40%, the main products became N-A-S-H (Na, Al, Si, H₂O). That is to say, the BFS to total fillers ratio of blended FA and BFS GP must be less than 60%. Depending on this theory, the BFS content in FA and BFS GP of my research is considered not above 50%.

(2) Alkaline activators

Alkaline activator solution plays a vital role in the initiation of the polymerization process. Palomo et al. [2] considered that the type of alkaline liquid is also significantly affected the mechanical strength.

Puertas et al. [18] studied blast furnace slag activated with NaOH, and has reported using the activator NaOH leads to reaction products with the molar ratio Al/Si higher than the one obtained with the activator NaOH mixed with water glass.

Katz [19] and Patankar [20] et al. studied alkali-activated FA and reported an increase in mechanical strength when the concentration of the NaOH activator increases. However, also for the alkali-activation of fly ashes, Palomo et al. [2] concluded that an activator with a 12 M concentration leads to better results than a 18 M concentration. Gorhan and Kurklu [21] and Somna et al. [22] investigated NaOH concentration effect on the compressive strength of FA-based GP mortar and paste respectively curing at different temperatures. They also got the same result as Palomo et al., that the compressive strength of FA-based GP concrete increased first, then flatten, and finally even declined with the increase of NaOH concentration. That is to say, the concentration of activator is not the more the better.

The sodium based alkaline activator ($\text{pH} > 11.5$) consisting of anions of Cl^- and SO_4^{2-} is reported effective to facilitate the reaction process and enhance the mechanical strength of alkali-activated FA^[20]. Li^+ and Na^+ was concluded to promote gelling because this “structural” water coordinates hydrogen bonding between silicates, while the weakly hydrated K^+ and larger alkali metal cations cannot^[23].

Komljenovic et al.^[24], utilized five different type of alkaline activators, i.e. $\text{Ca}(\text{OH})_2$, NaOH , $\text{NaOH} + \text{Na}_2\text{CO}_3$, KOH and Na_2SiO_3 with various concentrations, to assess the compressive strength of FA-based geopolymer mortars and concluded that the highest compressive strength was obtained from GP concrete using Na_2SiO_3 , followed by $\text{Ca}(\text{OH})_2$, NaOH , $\text{NaOH} + \text{Na}_2\text{CO}_3$ and KOH . The authors considered that sodium silicate is the most suitable as alkaline activator because it contains dissolved and partially polymerized silicon which reacts easily, incorporates into the reaction products and significantly contributes to improving the mortar characteristics.

The most common alkaline liquid used in geopolymerisation is a combination of sodium hydroxide (NaOH) or potassium hydroxide (KOH) and sodium silicate or potassium silicate. The previous researches have shown that potassium hydroxide (KOH) gave little better results in terms of the compressive strength and the extent of dissolution than sodium hydroxide. Phair et al.^{[25][26]} also stated that: using K_2SiO_3 as the alkaline activators can produce the GP with early strength. Whereas, this author, also reported the good silicon aluminum phase solubility of GP produced by Na_2SiO_3 solution.

Similarly, Palomo et al.^[2] gave a similar conclusion that alkaline liquid contained soluble silicates could better increase reaction rate compared to alkaline solutions that contained only hydroxide. Moreover, sodium is cheaper than potassium. So, in the previous researches sodium alkaline activator is more used.

Besides, considering the definition of geopolymer (GP) as a paste matrix composed of an amorphous substance having a three-dimensional (3D) network, the presence of SiO_3^{2-} in the alkaline activator solution is considered as a key factor for the generating of 3D amorphous substance^[27]. This conclusion was also reported in the study of palomo^[28], who thought that when activator solution contained only with NaOH , AlO_4^- tetrahedral unit will replace the cross linked SiO_4 tetrahedral unit of C-S-H gel and generate a C-A-S-H gel (low Ca/Si ratio) with longer linear chain but still 1D structure. Only after adding SiO_3^{2-} in the alkaline activator solution, 2D C-A-S-H gel generated.

Furthermore, the activator solution only containing Na_2SiO_3 is proved to result in low mechanical properties and durability of GP concrete curing at ambient temperature. GP concrete only using NaOH showed a limited workability and low early compressive strength^[29]. However, the blending of NaOH and Na_2SiO_3 activator solution presented great potential in the structural stability and physical properties^[28].

Hence, FA&BFS-based GP concrete alkaline activated by blending of NaOH and

Na_2SiO_3 will be a potential alternative to OPC, and the study on this material is significant.

2. 1. 4 Admixtures

For the FA&BFS-based GP, BFS accelerated the setting time with significant improvement of strength, but the workability and handling time reduced rapidly with the increase of slag content^[14]. In order to ensure the strength and workability of concrete, few researchers added retarder into the concrete^[15].

The naphthalene based superplasticizer, once used in OPC concrete, rendered 136% increase in relative slump without any decrease in compressive strength of FA-based GP^[30]. The use of naphthalene based admixture in the case of slag-based geopolymer also extended the setting time up to 180 min^[31]. Modified polycarboxylate based superplasticizer was reported with good effect on improving the workability of fly ash and slag blended system^[32], but the use of this superplasticizer in FA-based GP concrete also lead to a decrease in compressive strength of 29%^[34].

A new retarding admixture for FA&BFS-based GP concrete was also added in our experiments. It has confirmed having a good effect on the workability, meanwhile no bad effects on mechanical properties of FA&BFS-based GP concrete^[33]. But, the effect of the retarder on the neutralization resistance of FA&BFS-based GP concrete have not been observed. So, in my thesis, the retarder's effect will also be considered.

2. 1. 5 Production

The always used mixture procedure for GP specimens is as following 3 steps:

(1) Mixing dry binders and aggregates: The dry saw materials and the aggregates were first mixed in a mixer.

(2) Alkaline activator solution preparing: Mixing the alkaline liquid with the super plasticiser and the extra water, if any. Something should be mentioned is that alkaline liquid had better be mixed before use at least 1 day. NaOH and KOH was always used to mediate the molar of alkaline liquid.

(3) Adding the alkaline liquid: the alkaline solutions were added into the dry materials mentioned in procedure(1) and the mixing continued for another minutes.

However, the mix program for GP binder or GP based mortar and concrete has not been standardized. There are 2 minutes for mixing dry materials then adding the alkaline solution for a other 2 minutes in an industrial mixer^[34], also 3 minutes then 3 minutes^[35], even 1 min. then 1 min.^[31], respectively for the procedure (1) and procedure (3).

The mix time especially for the procedure (3) should be strictly controlled depending on the setting time of GP binders. The mix time in my study is described after amount of tentative experiments.

According to amount of experimental results, Davidovits^[36] gave his suggestions for binder execution using average molar ratios to the composition of the hardened material as follows:

$$\text{Si/Al} = 2.854 (2.047-5.57);$$

$$\text{K/Al} = 0.556 (0.306-0.756);$$

$$\text{Si/K} = 6.13 (3.096-9.681);$$

$$\text{Ca/Al} = 0.286 (0.107-0.401);$$

$$\text{Si/Ca} = 15.02 (4.882-41.267).$$

Later researchers based on this suggestion reported another optimum composition as $\text{Na}_2\text{O/SiO}_2 = 0.25$; $\text{H}_2\text{O/Na}_2\text{O} = 10$ and $\text{SiO}_2/\text{Al}_2\text{O}_3 = 3.3$.

It can be seen that calculating the ratio of chemical element is difficult. In the actual construction, the more sample operation the better. So, our research is more inclined to use the formulation method used directly in practice as a influencing factor. For example, when making one kind of activator solution, what we mainly considered is not the Si/Al ratio etc but how much water glass or sodium hydroxide, and water will be used.

2. 2 Performance characteristics of GP concrete

2. 2. 1 Microstructures

For FA-based GP binders, Criado et al.^[37] surveyed the reaction products of them activated by sodium hydroxide and blends of sodium silicate and sodium hydroxide using XRD test. The chief crystalline phases in products are quartz, mullite and magnetite, which were also found in the initial ash and apparently remained unaltered after activation. Other signals found corresponded to zeolite structures are hydroxysodalite ($\text{Na}_4\text{Al}_3\text{Si}_6\text{O}_{12}\text{-OH}$) and herschelite ($\text{NaAlSi}_2\text{O}_6\cdot 3\text{H}_2\text{O}$) or alkaline bicarbonates. Krivenko and Kovalchuk^[38], produced the alkali activation of fly ashes with NaOH and waterglass also reported the formation of zeolites like analcime and hydroxysodalite with high molar ratios, $\text{SiO}_2/\text{Al}_2\text{O}_3$ (4.55).

The studies on AAS are more than that on FA-based GP and FA&BFS-based GP. Pan et al.^{[39][40]} studied the alkali activation of blast furnace slag mixed with red mud, having noticed that the hydration products are CSH with a molar ratio, Ca/Si (0.8-1.2). They did not detect any zeolitic phase or even portlandite. Brough and Atkinson^[41] studied the activation of blast furnace slag, and reported that XRD analysis shows no crystalline products, however, the SEM analysis reveal the formation of hydrotalcite after a month.

Puertas et al.^[18] studied blast furnace slag activated with NaOH using XRD analysis and reported the presence of hydrotalcite ($\text{Mg}_6\text{Al}_2\text{CO}_3(\text{OH})_{16}\cdot 4\text{H}_2\text{O}$), calcite (CaCO_3) and CSH. Those authors have noticed that when using the activator NaOH, it leads to reaction products with the molar ratio Al/Si higher than the one obtained with the activator NaOH mixed with waterglass, due to the replacement of Si by Al in the tetrahedral location of the silicate chain.

As for Song et al.^[42] the main reaction product of blast furnace slag hydration is CSH gel with minor amounts of hydrotalcite, that was detected by XRD analysis, which are formed only when the slag achieves a high level of hydration ^[43]. As for Wang and Scrivener^[44] they confirmed that CSH gel is the main reaction product of alkali activation of blast furnace slag, having also noticed a low C/S ratio.

Up to know, there is no a standard that can be used to judge whether a alkali-activated material is GP or not. It is normal thought that alkali-activated BFS (AAS) is not a geopolymer, but, the alkali-activated FA was usually marked as FA-based GP with heat curing. The unclear thing is the alkali-activated blending of FA and BFS.

For FA and BFS based GP binder, Ismail et al.^[45] conducted the studies similar to Criado et al.^[17], in which the phase evolution of FA and BFS binder with different BFS concentrations were detected. From the ternary representations of EDX date, it can be

clear found that C-A-S-H dominate the system when BFS>50%, as the decrease of BFS/total binder less than 50%, N-A-S-H will increase and a hybrid type gel described as N-(C)-A-S-H is also identified. But, when BFS content in binder turned to 0, the N-(C)-A-S-H disappeared. According to the results, 50% BFS can be used as the demarcation point distinguishing GP or not.

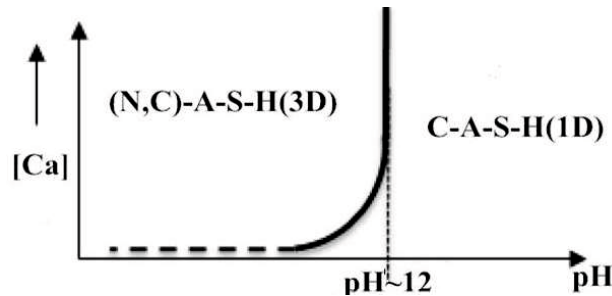


Fig. 2.1 The stability of N-A-S-H gels due to Ca^{2+} content and solution pH

Fig. 2.1 shows the effect of Ca content and pH on the structure of GP concrete. It is found that the N-A-S-H gel was disappeared when the solution pH over 12, because that Ca^{2+} is very aggressive to the three dimensional N-A-S-H structure at high pH. But, if pH lower than about 11.5, Ca^{2+} becomes insufficiently aggressive to degrade the three dimensional structure and may adsorb onto its surface in an ion exchange with Na^+ to give (N,C)-A-S-H gels^[46]. This conclusion is agree with the finding by Ismail et al., and explained why the GP concrete activated by only sodium hydroxide can't be regarded as geopolymer. Palomo et al.^[2] who found that a high calcium content and pH level favour C-A-S-H over N-A-S-H gel formation, also proved the viewpoint from Fig. 2.1.

For FA & BFS based geopolymer concrete, Davidovits^[47] stated that, the improved compressive strength and setting times can be explained by the formation of the CSH gel. The gel increases the compressive strength of the FS&BFS based geopolymer concrete and accelerates the setting time. Besides, another study indicated the importance of temperature on reaction. The author concluded that in the case of FA&BFS blends, the reaction is dominated by the slag activation at 27 °C, whereas at 60 °C the reaction is depended on combined activation of fly ash and slag^[48].

2.2.2 Properties

(1) Compressive strength

Wardhono^[49] tested the compressive strength of AAS mortars (water curing + ambient curing) and FA-based GP mortars (heat curing) compared to OPC mortars. It is found that the AAS mortars obtained a comparable strength result with OPC mortars. The compressive strength of FA geopolymer mortars with heat curing were considerably higher than that of the OPC mortars. But, for the ambient-cured FA GP based mortars, the results were not good. So the further study of the author also investigated the

mechanical properties of FA&BFS-based GP mortar with different BFS/FA ratio, and found the great contribution of BFS on increasing the strength of FA-based GP mortar with ambient curing. Test results showed that the compressive strength of ambient-cured geopolymer concrete significantly increased with the age. This trend is in contrast to the effect of age on the compressive strength of heat-cured geopolymer concrete. Heat-curing FA-based GP concrete was reported having a high early strength, but remaining unchanged or decreasing as age increase^[11]. But Nagai et al. got a similar growth trend of compressive strength of FA&BFS-based GP concrete no matter with heat-curing or ambient-curing as shown in Fig. 2.2. it can be seen the 7d-compressive strength of the GP concrete can reach 60-80% of the 28d-compressive strength. FA&BFS-based GP concrete is confirmed having a high early compressive strength.

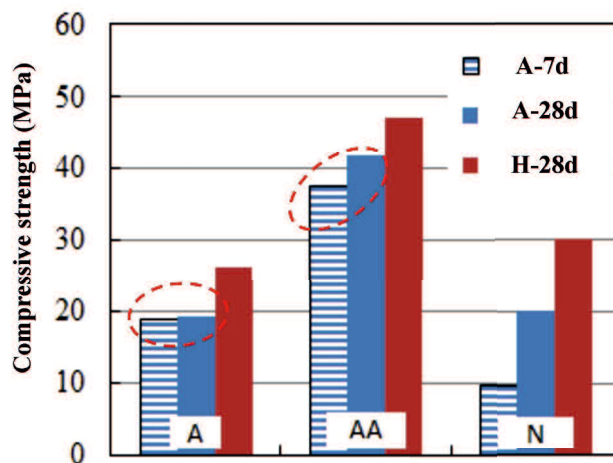


Fig. 2.2 Compressive strength of 70%FA + 30%BFS (3000 cm²/g)-based GPC (A: Na₂SiO₃ solution; N: NaOH solution; AA: blending of A and N)

High-early strength gain is a characteristic of geopolymer concrete when dry-heat or steam cured, although ambient temperature curing is possible for geopolymer concrete. It has been used to produce precast railway sleepers, sewer pipes, and other prestressed concrete building components. However, high compressive strength of FA-based GP concrete were always got when cured at a high temperature, that limit the application of FA-based GP concrete except to produce precast railway sleepers and other pre-stressed concrete building components.

(2) Low creep and drying shrinkage

The drying shrinkage of concrete can be evaluated by dry shrinkage rate using the following formula Eq. (2.3).

$$S_d = \frac{(X_{0l} - X_{tl})}{L_0} \times 100\% \quad (2.3)$$

S_d---Dry shrinkage of concrete in the age of d (%)

L₀---Specimen measurement range (mm)

X_{01} ---Initial length of the specimens (mm)

X_{t1} ---Average length of the specimens after t days (mm)

Increasing slag content in FA&BFS mix increased the expansion of resulting systems^[50]. There was no significant expansion in fly ash based geopolymer mortars. The formation of crystalline zeolites was very slow and since these minerals are usually found in the gaps of the matrix, the existence of stress that might generate cracking is unlikely^[51]. However, the cause of expansion in slag-based geopolymer mortars is the formation of sodium calcium silicate hydrate reaction product with rosette-type morphology^[52].

Test results showed that heat-cured fly ash-based geopolymer concrete undergoes very little drying shrinkage in the order of about 100 micro strains after one year. This value is significantly smaller than the range of values of 500 to 800 micro strains experienced by Portland cement concrete. And it is said that the specimens shrinkage cured in ambient conditions are larger than those experienced by the heat-cured because of water evaporation^[60].

However, there is also a previous research that suggested that fly ash based geopolymer concrete, cured at elevated temperatures, yields higher modulus of elasticity values compared to FA&BFS-based geopolymer concrete that cures at ambient temperatures^[53].

(3) Durability

On one side, Glukhovsky^[54] the first author who had investigated the binders used in ancient Roman and Egyptian constructions. He concluded that they were composed of aluminosilicate calcium hydrates similar to the ones of Portland cement and also of crystalline phases of analcite, a natural rock that would explain the durability of those binders. The other study Campbell and Folk^[55] showed that the durability of ancient binders was due to its high level of amorphous zeolitic compounds. XRD diffraction patterns of pyramid specimens also indicate that an amorphous material composed of aluminosilicates and a zeolite like material ($\text{Na}_2\text{O} \cdot \text{Al}_2\text{O}_3 \cdot 4\text{SiO}_2 \cdot 2\text{H}_2\text{O}$) were also found^[56].

Malinowsky^[57] had investigated ancient constructions repaired with OPC, having noticed that the repairing material was disintegrated just after 10 years, showing its low durability when compared with the repaired structures.

On the other side, Glukhovsky^[58] had already made crucial investigations about the activation of blast furnace slag: (a) identifying hydration products as being composed by calcium silicate hydrates and calcium and sodium aluminosilicate hydrates and (b) noticing that clay minerals when submitted to alkali-activation formed aluminium silicate hydrates which is similar to that of zeolites. This can be explain the good durability of GP like ancient structures. The performance of GP in different environment present as follows

❖ *Sulfate and acid resistance*

By immersing GP in different acid or sulphate solution, and comparing with OPC, it can be proven that GP have a higher acid and sulphate resistance than OPC. Thokchom et al. [59] found the specimens with higher alkali content were observed to lose more weight than specimens with lower alkali content. In the 5% sulfuric acid, the dissolution of GP is about 1/13 times to OPC, and at 1/12 times when in HCl solution[60]. According to Bakharev and Singh et al.[61][62], more crystalline geopolymer material prepared with sodium hydroxide was more stable in the aggressive environment of sulfuric and acetic acid solutions than amorphous geopolymers prepared with the sodium silicate activator.

Shankar and Khadiranaikar[63] studied the durability characteristics of geopolymer concrete compared with OPC specimens. The two kinds of specimens were fully soaked in 10% sulphuric acid solution after 7 days of casting. After regularly monitoring through visual inspection, and measuring the weight and strength change of GP and OPC specimens. It was concluded that the compressive strength loss for the specimens exposed in sulphuric acid was in the range of 10 to 40% in OPC, however it was about 7 to 23% in GPC. From the specimens' change of GP mortar and OPC mortar before and after sulfuric acid immersion as shown in Fig. 2.3, the good acid resistance of GP mortar can be easily understood[64].

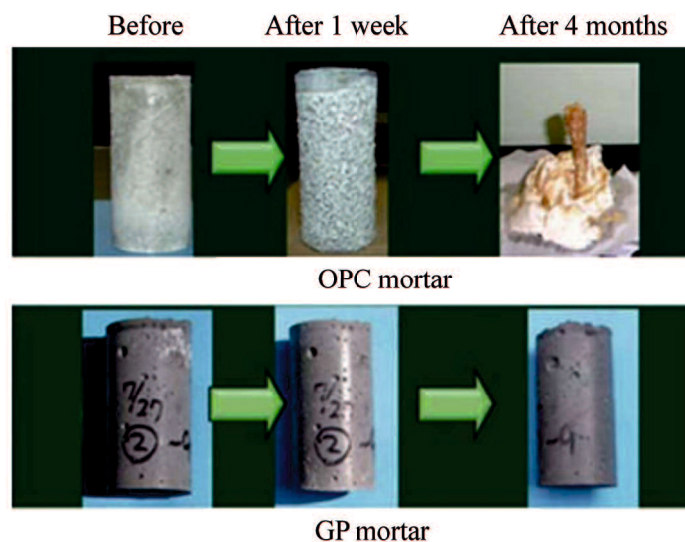


Fig. 2.3 Erosion situation of GP mortar and OPC mortar (4 months)

Sathia et al.[65] found the weight loss in FA-based GP concrete samples was less than 5% after 3 months exposure in 3% H₂SO₄ solution, superior to ordinary Portland cement pastes. Davidovits et al. [66] also reported that fly ash-based geopolymer pastes retained a dense microstructure after 3 months exposure in HNO₃. Rajamane et al. [67] reported sulphate resistance of fly ash-based GPC in 5% Na₂SO₄ and 5% MgSO₄

solutions. There was 2-29% loss of compressive strength as compared to 9-38% in the OPC concrete. And the weight loss in samples was 2.4% only.

The deterioration of OPC concrete can be attributed to the formation of expansive gypsum and ettringite which can cause expansion, cracking and spalling in the concrete. Contrary to this, there is no or few ettringite and aluminum silicate minerals in the GP products. Because of that, the GP materials have good acid resistance. The deterioration in GP pastes was connected to depolymerisation of the aluminosilicate network and formation of zeolites [61].

However, an extensive physical deterioration of FA&BFS-based GP pastes was observed during immersion in $MgSO_4$ solution after 3 months exposure but not in Na_2SO_4 solution. The calcium sulphate dihydrate formed in paste was identified as being particularly damaging to the materials in $MgSO_4$ [68].

For slag-based GPC, Bakharev et al. [69] found that exhibited about 33% reduction in strength compared to 47% decrease in OPC concrete when exposed in acetic acid solution (pH=4) for 12 months. When immersing in a 2% H_2SO_4 solution, the strength loss was about 11% for GPC compared to 36.2% for OPC concrete. It can be concluded that the low calcium C-S-H with average Ca/Si ratio of 1 is more stable in the acid solution than the constituents of the OPC pastes.

Geopolymer concrete has shown to have superior acid resistance and may be suitable for applications such as mining, some manufacturing industries and sewer systems.

✧ *Fire resistance*

High temperatures lead to changes in chemical structure and the dehydration of free and chemically-bound water. Moisture because of high temperature rapidly escapes towards the surface of the specimen, that in turn causes surface-cracking and internal damage in the overall structure of the concrete.

It is known that after exposing high temperature between 800°C and 1000°C, the residual strength of OPC concrete less than 20-30% normally because of dehydration and destruction of C-S-H and other crystalline hydrates, aggregate types, permeability etc. However, The fire resistance of geopolymer, especially for fly-Ash based GP, is likely to be superior to OPC concrete and other materials which loses most of their strength after firing^[70]. According to Bakharev^[71], exposing to high temperature resulted in an increase in the average pore size of OPC but reduced average pore size and improved compressive strength of geopolymer.

So, does all alkali-activated materials have high fire resistance. The answer may be no. In the study of Daniel, which detected and compared the reaction of metakaolin and Fly-Ash based geopolymer by subjecting to temperatures of up to 800 °C from room temperature. It can be found as shown in Table 2.1, the Fly-Ash based geopolymer has a better fire resistance than that of metakaolin based geopolymer^[72]. The high fire

resistance of FA-based geopolymers was explained by the large numbers of small pores that facilitate the escape of moisture caused by high temperature and leads to a minimal damage^{[73][74]}.

Table 2.1 The change after firing of metakaolin and FA based geopolymer

Influencing factors	Metakaolin	Fly-Ash
Color	A slight lightening of color	Significant change of color
Cracks	Macro-cracks	No cracks
Strength	A strength drop of 34%	A strength increase of 6%
Mass	30% mass reduction	11% mass reduction

For the FA&BFS-based GP concrete, it was also observed showing a significant resistance at 300°C and 600°C^[75].

Lee et al.^[34] investigated the gel structures and strength of alkali-activated FA&BFS pastes with different BFS/total binder ratio, under high temperature. The results indicated that specimens adding less BFS have a better fire resistance for the higher residual strength and more porous after exposure to elevated temperature. And the reason was thought due to the inherited high thermal stability of the highly cross-linked gel with Q3 and Q4 structures such as N-A-S-H, anorthite ($\text{CaAl}_2\text{Si}_2\text{O}_8$) or nepheline ($(\text{Na,K})\text{AlSiO}_4$), formed by exposure to 800 °C, rather than the presence of C-(A)-S-H.

(4) Others

✧ *Solidification of various radioactive residues*

Davidovits^[1] concluded that the GP solidification rate of various metals, such as As, Fe, Mn, Ar, Co, Pb, is not less than 90%. Its network skeleton structure is relatively stable even under the effect of radiation for the metal cations balance the negative charge of tetrahedral coordination (Al^{3+}) as shown in Table 2.4.

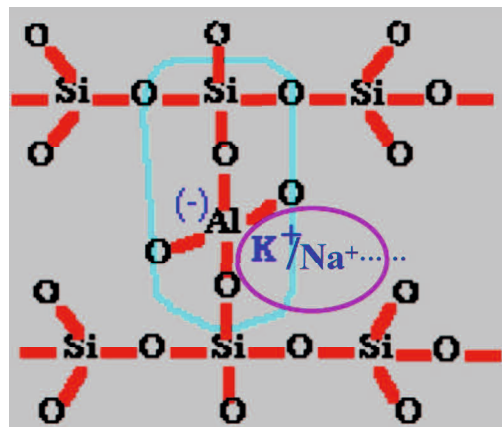


Fig. 2.4 The polymer nanostructure of GP

Metal ions influence the geopolymer structure differently, mainly because of

differences in the atomic ratio, electronegativity and reactivity^[76]. Fly ash based geopolymers provide a satisfactory method for heavy metal immobilization with low permeability, good resistance to acid and chloride attack and long durability^[77]. Heavy metals can also react with Al- and Si- species dissolved from Al source forming new phases. Meanwhile, research results indicated that NaOH comparing to Na-silicate has more effective activation properties regarding ion immobilization. This is correlated with the higher alkalinity of NaOH which favors minerals dissolution and consequently creation of new phases with ions inside the structure^[78].

Besides, the Si/Al molar ratio is important for the ion immobilization, for example, it was shown that leaching of Cr and Cu decreased as the Si/Al ratio increased, while Zn reached its lowest point at an intermediate Si/Al ratio^[79]

Geopolymers are also reported to stabilize hazardous and radioactive wastes better than Portland cement^[80].

The ability in solidification of various radioactive residues of GP concrete is much better than that of OPC concrete.

✧ *Bond between reinforcing bars and geopolymer concrete*

The bond between reinforcing bars and geopolymer concrete also reported good. Sarker^[81] found that the FA-based GPC has higher bond strength than the OPC concrete because of higher splitting tensile strength and dense interfacial transition zone between the aggregate and geopolymer paste. The design provisions mentioned in the Standards for OPC concrete can be used for designing geopolymer concrete columns also^[82].

✧ *Freeze-thaw resistance*

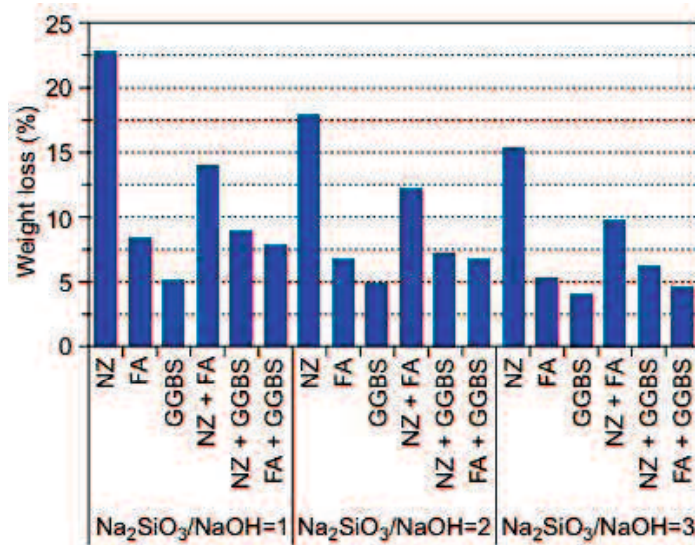


Fig. 2.5 Weight loss of geopolymer mortars after 25 of freeze-thaw cycles.
(NZ: zeolite-clinoptilolite)

In the cold region, the ability of freeze-thaw resistance must be considered. It is reported that the cycle time of freeze-thaw for FA based polymer concrete is 98 times, which is 2.2 times of that for portland cement concrete. Degirmenci^[83] compared the freeze-thaw resistance of FA, BFS and FA&BFS-based GP mortars cured at ambient temperature but with different $\text{Na}_2\text{SiO}_3/\text{NaOH}$ ratio, and found that, as shown in Fig. 2.5, the weight loss after freeze-thaw cycle of FA-based GP mortars is slightly larger than that of FA&BFS-based GP mortars, but much larger than the weight loss of BFS based GP mortars. Besides, As the $\text{Na}_2\text{SiO}_3/\text{NaOH}$ ratios of the alkaline activator solution increase, the weight losses of geopolymer mortars decrease.

However, whether the general air-entraining agent is applied to geopolymer concrete and its suitable air content and size distribution of the pores should be further studied. Moreover, the development of new additive material will be performed, which can generate bubbles into geopolymer concrete by chemical reaction to improve the freeze-thaw resistance.

✧ *Corrosion and chloride resistance*

Accelerated corrosion results of Sathia et al.^[65] showed that FA-based GP concrete mixes exhibited low level corrosion activity and time to failure that were 3.86-5.70 times longer than those of the OPC concrete. The large amounts of fly ash and alkaline activators in the GP concrete mix increased the availability of ions that can produce high electrical resistance at high impressed voltage. This enhanced the cathodic reaction and reduces the rate of corrosion, which in turn, reduces the tensile stress of the specimens, thus decreasing the risk of cracking and clearly extending the time to failure^[84] Also Reddy et al.^[85] compared the durability of FA-based GPC with that of OPC concrete exposed to marine environment for a period of 21 days. The initial corrosion current measured for GPC (71-91 mA) was much lower than that of OPC concrete (772 mA).

FA and BFS based GP concretes showed high chloride resistance. When comparing with OPC concrete, the penetration depth of the GP concretes were at most 4 times lower than that of OPC concrete^[86].

2. 2. 3 Influencing factors of mechanical properties

(1) Ratio of BFS and alkaline activator solution to total binder

Xu and Deventer^[7] reported that factors such as the percentage of CaO, K_2O , and the molar Si-to-Al ratio in the source material, the type of alkali liquid, the extent of dissolution of Si, and the molar Si-to-Al ratio in solution significantly influenced the compressive strength of geopolymers.

In the study of Nath^[14], influencing factors such as BFS/total binder, alkaline

activator solution (AS)/total binder, sodium hydroxide ratio/water glass (NH/WG), curing temperature were considered to investigate their effects on compressive strength and setting time of FA&BFS-based GP concrete as listed in table 2.2. The similar results were obtained in the study of Sundar Kumar et al.^[87] as shown in table 2.3. From tables 2.2 and 2.3, it can be concluded that, influencing the BFS/total binder ratio and NH/WG (mole amount of NH) or decrease the AS/total binder ratio leads to a increase of compressive strength but shorter setting time. Heat curing resulted in a high compressive strength especially the early strength.

Table 2.2 Influencing factors effects on the compressive strength and setting time of FA&BFS-based GP concrete (1)

Influencing factors	Compressive strength	Setting time
BFS/Total binder (↑)	↑	↓
NH/WG($\text{Na}_2\text{O}/\text{SiO}_2$) (↑)	↑	↓
AS/Total binder (↑)	↓	↑
Curing temperature (↑)	↑	-

Notes: ↑: Increase, ↓: Decrease.

Table 2.3 Influencing factors effects on the compressive strength and setting time of FA&BFS-based GP concrete (2)

No.	BFS/Filler (%)	NaOH solution molar (M)	Curing temperature ($^{\circ}\text{C}$)	Setting time (hours)	Compressive strength (MPa)
1	0	10	20	≥ 48	-
2	0	10	65	8	20
3	0	8	65	8	16
4	10	8	20	-	38
5	50	8	20	-	50

For the effect of AS/total binder, Olivia and Nikraz^[84] also reported that the water-geopolymer solids ratio was the most influential parameter that affects the properties of GPC. The liquid to solid ratio affects the volume of voids and porosity in the pastes which directly influences the strength of geopolymer. Increased porosity causes a decline in strength. The the activator solution /FA ratio ratio also exert a greet influence on the workability of mixture.

(2) Curing

Curing condition is a important influencing factor for geopolymer.

Hardjito et al.^[88] produced fly ash-based GPC with the compressive strength ranging between 30 and 80 MPa with the slump varied from 100 to 250 mm as curing temperature from 30 to 90 $^{\circ}\text{C}$. Also, Palomo et al.^[2] studied curing temperature effect on alkali-activated fly ash with liquid/solid ratio as 0.25 and 0.30. It is indicated that the compressive strength of geopolymers cured at 85 $^{\circ}\text{C}$ for 24 h was much higher than

those cured at 65°C. But, after 24 hours, the rise of strength became much smaller.

Jaarsveld et al.^[5], focused their study on alkali-activated metakaolin/fly ash mixtures, concluded that long curing time weakens the material structure due to excessive shrinkage. Other authors^[89] also noticed the strength decrease for long heat curing time and suggests that some water may remains in the hardened binder, keeping the “gelular” character of geopolymers. But Wang et al.^[44] concluded that the effect of curing temperature on alkali-activated slag is almost irrelevant when high concentration .

Criado et al.^[37] studied the alkali-activation of fly ashes suggesting the isolation of the specimens for avoiding carbonation process lowering the pH and the mechanical strength. Collins and Sanjayan^{[90][91]} compared the strength of AAS using water glass, with air curing , curing with isolation and water curing, and found that strength of water curing AAS is slightly better than curing with isolation but far better than air curing. But Kirschener and Harmuth^[92] confirmed that water curing leads to a strength decrease.

And it is proven that heat-curing can be achieved by either steam-curing or dry-curing. Test data show that the compressive strength of dry-cured geopolymer concrete is approximately 15% larger than that of steam-cured geopolymer concrete^[93].

The above can be concluded as that heat curing with isolation may be the best curing condition for GP concrete.

(3) The Blaine fineness of BFS

Talling and Brandstetr^[94] obtained optimum strength for a slag with Blaine fineness of 4000 cm²/g. Wang et al. Reported that the optimum Blaine fineness depends on the type of slag and varies between 4000 and 5500 cm²/g. Brough and Atkinson^[41], those authors studied alkali-activated slag mixtures, also reporting that an increase in Blaine fineness from 3320 to 5500 cm²/g leads to an increase in mechanical strength from 65 to 100MPa. The compressive strength of FA&BFS-based GP concrete effected by varies influencing factors were also tested in our experiment. Except the influencing factors mentioned above, BFS fineness, retarder were also considered^[33]. The results is concluded that the compressive strength of FA&BFS-based GP concrete increased as increasing the BFS fineness, but after 4000 cm²/g, the increase became hard to found.

Increase of Blaine fineness raises the available amount of aluminium. More aluminium means more [Al(OH)₄]⁻ tetrahedral groups, being able to attract negatively charge groups and therefore, increasing the reacted species amount.

(4) Others

◇ *The content of H₂O*

The H₂O content can accelerate the dissolution and hydrolysis, however, interact with the process of polymerisation^[95]. H₂O in raw materials determines geopolymer’s volume density and open porosity. On the other hand, the geopolymer activated by

sodium alkaline activator can absorb more water for containing more structure pores^[96].

Perera et al.^[97] found that the H₂O in geopolymer can be divided into three types:

1. Free water, existing between the particle and its surface.
2. Interstitial water, which is mainly bonded with alkali metal ion and formed a hydrated ion.
3. Exist With hydroxyl form.

From this point of view, having the mastery between water content and the curing mechanism can get high performance of polymer products. .

✧ *The content of Ca*

Van Jaarsveld et al^[98] found that fly ash with higher amount of CaO produced higher compressive strength, due to the formation of calcium-aluminate-hydrate and other calcium compounds, especially in the early ages. For Xu, Phair, Lee and Minarikova, they all stated that as the Ca content increasing, porosity in the GP is decreased and finally led to an enhanced compressive strength.

✧ *The ratio of Si to Al*

There is a rapid increase in the compressive strength, but a decrease in pore size^[99], of geopolymers with increasing Si/Al ratio. However, specimens with Si/Al = 2.15, exhibit a reduced strength compared to those with Si/Al = 1.90. That is believed to be a result of the effects of unreacted material, as a defect in the binder phase^[100].

Si/Al ratio in the solution will always be greater than unity, since the concentrations of silicon initially in the solution are large compared to the amount of aluminum initially dissolved. Higher lability promoted by low silicon concentration. Fernandez-Jimenez et al.^[101] studied several types of fly ashes, and reported for the reactive phase Si/Al molar ratio between 1.42 and 2.38, Al has a less reactive phase than Si. Therefore, what matters most is the Si/Al molar ratio in the reactive phase, but not so much the Si/Al molar ratio of the original prime material.

Furthermore, the ratio of Si-to-Al determines the GP concrete formation and properties. Increasing SiO₂/Al₂O₃ ratio generally decreases the initial rate of reaction^[102]. The more content of Al, the faster speed of early strength, on the contrast, the post-strength increase faster, if have more Si content.

✧ *The effect of pores*

Pores in different size have various influence on the product's properties. Gel pores do not influence the strength of concrete through its porosity, although these pores are directly related to creep and shrinkage. Capillary pores and other large pores are responsible for reduction in strength and elasticity. The GP with more micro pores is better than that with few large pores. And the presence of pores give GP a good property to resist high temperature.

Pore size in geopolymers decreases with increasing Si/Al ratio^[103].The pore is also

related to the content of alkaline ions. The products made by Na^+ ion can get more pores than that using K^+ ion, so the Na^+ ion made products can absorb more water.

it is worth mentioning that we have investigated the influencing factors of compressive strength, workability, sulfate resistance etc, of FA&BFS-based GP concrete at ambient temperature, and got the conclusion that BFS/total binder ratio, alkali activator solution and curing temperature may be the most important influencing factors for FA&BFS-based GP concrete^{[29][33][104]}.

2.3 Neutralization resistance of GP concrete

Using GP concrete as a structural material requires the assessment and verification of its durability. The most important factor for a durability evaluation is the degree of carbonation resistance^[37].

2.3.1 AAS

Alkali-activated ground granulated blast-slag (AAS) is the most obvious alternative material for ordinary Portland cement (OPC). Recently, many studies showed that concrete made by AAS has a lower carbonation resistance than OPC concrete. Bakharev et al.^[105], assessed the carbonation resistance of AAS concrete comparing with OPC concrete, by measuring the pH values and compressive strength as increase of carbonation time, in a NaHCO₃ solution (0.352 M) and the atmosphere high in carbon dioxide (CO₂%=10%). It is found that, AAS concrete has a lower carbonation resistance than OPC concrete. Moreover, different to OPC concrete, the compressive strength of AAS concrete decreased after carbonation. The reason leading to a low carbonation resistance of AAS concrete was explained for the low calcium in AAS.

Song et al.^[35] investigated the carbonation rate of AAS concrete, with different alkaline activator content, and the concrete's strength and micro-structure change after carbonation. The carbonation resistance of AAS concrete is also verified lower than that of OPC concrete. The author gave the ingredients in AAS and OPC before and after carbonation as shown in Table 2.4. It can be found albite and sodium aluminium silica in AAS completely disappeared after carbonation. Meanwhile, the authors found that increasing the activator amount leads to a higher amount of CSH and a increase of the strength and carbonation resistance.

Table 2.4 Substances in AAS and OPC before and after carbonation

Source material	Before	After
AAS	Albite ((Na, Ca)Al(Si, Al)3O8), Sodium aluminum silica, Calcite, Quartz, and CSH	Calcite(a little increase), Quartz, and CSH
OPC	Calcium hydroxide, CSH	Calcite

The conclusions of Rodríguez et al.^[106] also proved that the AAS concretes is more vulnerable to carbonation, with a front three times wider than frond of the OPCs. Also strength loss was considerably greater in AAS than OPC.

2.3.2 FA-based GP

Adam et al.^[107] investigated the carbonation resistance of AAS and FA-based GP concrete (with heat curing). Except the similar results regarding to AAS, the FA-based

GP concrete can not find the colour change after spraying phenolphthalein solution as shown in Fig. 2.6. And the author guessed that this may be because the carbonation products of FA-based GP concrete also have high pH values as described in Eq. (2.4).

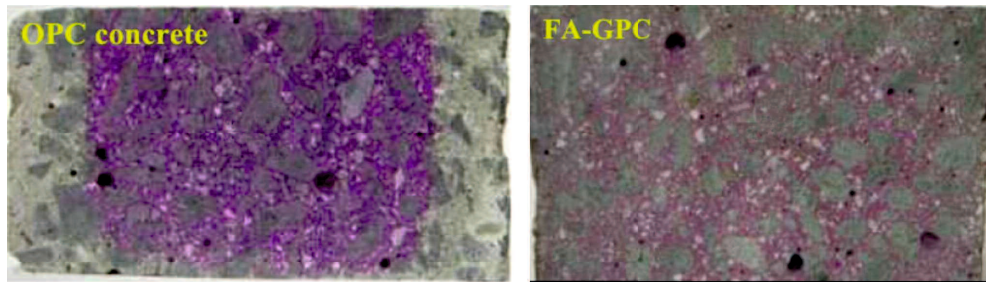
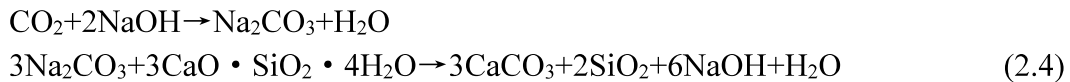


Fig. 2.6 Unclear carbonation boundary of FA-based GP concrete after spraying phenolphthalein indicator

Law et al.^[108] further investigated the carbonation front of FA-based GP mortars using pH measurement and found that the pH values of the GP mortars were maintained above 10 as the growth of carbonation time. It is guessed that the steel in FA-based GP concrete couldn't be corroded even without any protection for the different carbonation products from OPC. If just pore solution in FA-based GP mortar can be carbonated, a high final pH value after carbonation can be expected. In fact, the study of Benal et al.^[109] just proved the hypothesis above and reported that the carbonation for alkali-activated FA-based binders (ambient sealed curing) mainly through precipitation of alkali bicarbonate salts from the pore solution, but coexisting with the largely unaltered binder gel (N-A-S-H) as measured by thermogravimetry and NMR analysis. Even though for the alkali-activated FA&BFS binders, the gel been carbonated is C-A-S-H formed by alkali silicate activation of BFS, but, with almost no change to the N-A-S-H gel caused by activation of FA.

Besides, Olivia and Nikraz^[83] reported FA-based GP concretes have lower water permeability with heat curing, than the OPC concrete due to its denser paste and smaller pore inter-connectivity. The author also proposed that there will form a dense layer of oxide film on GP concrete surface to prevent concrete from permeation, oxidation and carbonation.

2.3.3 FA&BFS-based GP

Recently, there is relatively little existing studies on the carbonation process in low-calcium FA-based GP concrete, less on the FA&BFS-based GP concrete.

The research by Benal et al.^[109], on effect of carbonation on gel nanostructure in FA&BFS-based paste compared with AAS and FA-based GP, proposed the carbonation

substances and carbonation products of these GP concrete as listed in the Table 2.5. This is a very valuable article, but it needs more experiments to support.

Table 2.5 Carbonation products of various GP concretes

	FA based GP concrete	Alkali activated BFS	(FA/BFS=1) based GP concrete
Before carbonation	N-A-S-H +Na+ alkali solution	C-A-S-H +Na+ alkali solution	N-A-S-H + C-A-S-H +Na+ alkali solution
After carbonation	N-A-S-H Na ₂ CO ₃ -NaHCO ₃ -H ₂ O	CaCO ₃ Na ₂ CO ₃ -NaHCO ₃ -H ₂ O	N-A-S-H+CaCO ₃ Na ₂ CO ₃ -NaHCO ₃ -H ₂ O

Hakata et al.^[110], investigated the FA&BFS-based GP mortars using two kinds FA sorts of Japan, and proved the lower carbonation resistance of GP mortars than OPC mortars. At the same time, the authors pointed out that the interface between carbonated and non-carbonated zones of GP specimens is unstable after spraying phenolphthalein solution.

Khan et al.^[111] investigated the carbonation resistance of GP concrete, blended 10% BFS and 90% low-calcium FA, with heat curing, under natural condition and accelerated carbonation conditions with carbon dioxide concentration of 1% or 3%, by measuring and comparing the carbonation depth and pH values. The carbonation degree in the natural condition, 1% and 3% accelerated carbonation conditions were determined to be 2.57 mm/year^{0.5}, 6.3 mm/year^{0.5} and 55.6 mm/year^{0.5} respectively. This work contributes to the assessment of the actual risk of carbonation-induced reinforcement corrosion in low-calcium FA-based GP concrete using accelerated carbonation test, but cannot predict carbonation progress yet.

Pasupathy, et al.^[112] investigated the carbonation degrees of two kinds of FA&BFS-based GP concretes in the air for 8 years. On basis of supposing that the carbonation depth of GP concrete is a root function of elapsed time (t, year) as $x = K\sqrt{t}$, the authors concluded that the carbonation rate coefficient K (mm/ $\sqrt{\text{year}}$) is positively correlated to the permeability, porosity, and pore size of GP concrete. The author also explained why phenolphthalein sometimes provided unclear identification of carbonation front, due to the carbonate products content of calcium carbonation from BFS based GP and the sodium carbonate from FA-based GP. The effects of alkaline activator sorts on the carbonation resistance of FA&BFS-based GP concrete were also considered in this study. Only using NaOH or KOH solution as alkaline activator obtained a greater carbonation resistance than that using NaOH or KOH together with sodium silicate. This is also the study on the carbonation resistance of GP in the condition that is closest to the actuality up to now.

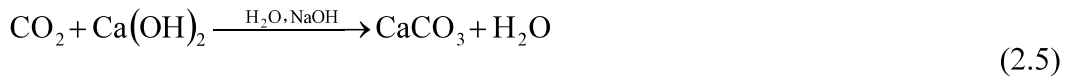
2.4 The carbonation rate model

The carbonation models used to predict the carbonation procedure of GP concrete have not been involved in. Sometimes carbonation model of cement concrete were used to compare the carbonation rate between GP concrete and normal concrete.

The source of carbonation models can be divided into three

- (1) Empirical model based on the carbonation test;
- (2) Theoretical derivation model based on the Fick's diffusion theory;
- (3) A model based on diffusion theory and experimental results.

Carbonation in normal concrete is regarded as a reaction shown in Eq.(2.5) that takes place between carbon dioxide (CO₂) and Ca(OH)₂.



The carbonation model of normal concrete is based on Fick's diffusion theory as shown in Eq.(2.6).

$$Q = -D \frac{\partial \varphi}{\partial x} \quad (2.6)$$

Where, Q is diffusion flux of carbon dioxide into concrete throw unit cross section at unit time (g/m²·s);

φ is carbon dioxide concentration (g/m³).

If we assume that Fick's first law allows to describe the diffusion process under a constant, unchanging in time, density of the diffusion flux^[113], meanwhile, the diffused carbon dioxide will be completely used for carbonation, the Eq. (2.6) can be finally derived to Eq. (2.7).

$$x = \sqrt{\frac{2D\varphi_0}{q}} \sqrt{t} \quad (2.7)$$

Where, x is the carbonation depth (mm);

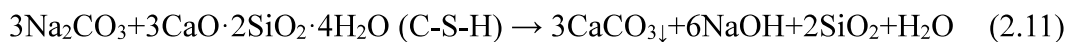
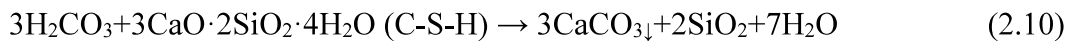
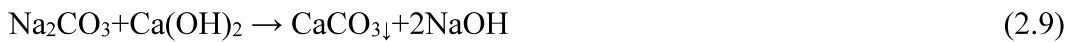
q is CO₂ absorption capacity of concrete due to carbonation through a unit surface area in unit time (g/m³);

φ_0 is carbon dioxide concentration at the surface of concrete (g/m³).

In function (2.7), D is finally determined by water/cement (W/C), aggregate-to-cement ratio (a/C) and time(t). Besides, it is said that D can be represented by the porosity of the cement paste. q is mainly effected by W/C and cement content(amount of reactant).

That is to say, if we want to propose the carbonation rate function of GP concrete, the concrete's porosity, carbonation reaction mechanism should be realized. Otherwise, amount of experiments on the relation ship between x and t have to be conducted.

For GP concrete, Adam et al.^[106] thought the dissolved carbon dioxide will react with sodium hydroxide forming sodium carbonate and releasing water (Eq. 2.8). The sodium carbonate will then react with calcium hydroxide producing calcium carbonate and release hydroxide ions which will react again with carbon dioxide according to Eq. (2.9). Because of the less Ca concentration in FA and BFS compared too OPC, the presence of calcium silicate hydrate (CSH) becomes possible. Carbonation reaction shown in Eqs. (2.10) and (2.11) may also occurred.



However, from the previous researches, it can be concluded that the reactants in FA&BFS-based GP concrete are far more than $\text{Ca}(\text{OH})_2$ and C-S-H. Some scholars even believe that there is no calcium hydroxide in the GP. Moreover, the source materials coming from different plants, and the blending alkali activator of sodium hydroxide and sodium silica, made it more difficult to realize the reaction mechanism of GP. So, up to now, carbonation reaction mechanism of FA and BFS based GP is still unclear.

Hence, amount of experiments on the carbonation resistance of GP concrete may be the fastest and much effective method to practically apply GP concrete. The porosity effected by carbonation should also be tested.

2.5 Summary

In Chapter 2, the current researches on geopolymer (GP) and alkali-activated materials (AAM) based binder, mortar or concrete were in detail summarized and discussed. It could be concluded that fly ash (FA) and blast furnace slags (BFS) are the most popular materials used in GP and AAM. The accepted alkaline activator are Na based hydroxide, silicate or blending of them. Most of GP concrete especially FA-based GP concrete were cured at high temperature. GP based concrete does show good mechanical properties and durability in fire, acid and sulphate resistance. The influencing factors on the mechanical properties of GP concrete based on BFS, FA and blending of FA and BFS, mainly contain BFS/total solid ratio, alkaline activator solution (AS) sorts and the ratio of AS to binders and curing conditions.

However, up to now, the neutralization resistance (a important factor for the practical use of GP in the reinforce concrete) of FA&BFS-based GP concrete has not been widely concerned, especially for the ambient-cured GP concrete. And, most of studies are inclined to using binder and mortar but not concrete to solve the concrete problem. Researchers seem to care more about what GP is but not how to use it widely. So many people put their research on GP's nanostructures. Predicting the neutralization rate of FA&BFS-based GP concrete, and the neutralization resistance of FA&BFS-based GP concrete suffered from water submission and movement have not been involved.

Reference

- [1] J. Davidovits, Geopolymers of the First Generation: SILIFACE-Process. Paper presented at the Geopolymer'88, First European Conference on Soft Mineralogy, Compiègne, France. (1988)
- [2] A. Palomo, M. W. Grutzeck, M. T. Blanco. Alkali-activated fly ashes a cement for the future. *Cement And Concrete Research*, 29(8) (1999) 1323-1329.
- [3] F. Pacheco-Torgal, J. Castro-Gomes, S. Jalali, Alkali-activated binders: A review: Part 1. Historical background, terminology, reaction mechanisms and hydration products. *Construction and Building Materials*. 22(7) (2008) 1305-1314.
- [4] J. Davidovits, Geopolymer chemistry and properties, In: *Proceedings of 1988 geopolymer conference*. 1 (1988) 25-48.
- [5] J. G. S. Jaarsveld, J. S. J. Deventer, G. C. Lukey, The effect of composition and temperature on the properties of fly ash and kaolinite based geopolymers. *Chemical Engineering Journal*. 89 (2002) 63-73.
- [6] V. F. F. Barbosa, K. J. D. MacKenzie, C. Thaumaturgo, Synthesis and characterisation of materials based on inorganic polymers of alumina and silica: sodium polysialate polymers. *Journal of Inorganic Materials*. 2 (2000) 309-317.
- [7] H. Xu, J. S. J. Deventer, S. J. Jannie, The effect of alkali metals on the formation of geopolymeric gels from alkali-feldspars, *Physicochemical and Engineering Aspects*. 216(1-3) (2003) 27-44.
- [8] J. T. Gourley, *Geopolymers Opportunities for Environmentally Friendly Construction Materials*. Paper presented at the *Materials 2003 Conference: Adaptive Materials for a Modern Society*, Sydney. (2003).
- [9] Y. Lee, J. Choi, K. H. Kim, B. Y. Lee, Effects of a defoamer on the compressive strength and tensile behavior of alkali-activated slag-based cementless composite reinforced by polyethylene fiber, *Composite Structures*. 172 (2017) 166-172.
- [10] W. Long, J. Wei, Y. Gu, F. Xing, Research on dynamic mechanical properties of alkali-activated slag concrete under temperature-loads coupling effects, *Construction and Building Materials*. 154 (2017) 687-696.
- [11] S. Wallah, B. V. Rangan, *Low-calcium fly ash-based geopolymer concrete: Long-term properties*, research report GC 2. Perth (Australia): Faculty of Engineering, Curtin University of Technology; 2006.
- [12] A. Fernandez-Jimenez, I. Garcí'a-Lodeiro, A. Palomo, Durability of alkali-activated fly ash cementitious materials, *Journal of Materials Science*. 42(9) (2007) 3055-3065.
- [13] M. L. Granizo, S. Alonso, M.T. Blanco-Varela, A. Palomo. Alkaline activation of metakaolin: effect of calcium hydroxide in the products of reaction, *Journal of the American Ceramic Society*. 85(1) (2002) 225-231.
- [14] P. Nath, P. K. Sarker, Effect of GGBFS on setting, workability and early strength

- properties of fly ash geopolymer concrete cured in ambient condition, *Construction and Building materials*. 66 (2014) 163-171.
- [15] 佐藤隆恒、上原元樹、南浩輔、山崎淳司, ジオポリマー硬化体の種々の配合, 作製法における生成物と pH 等諸性質との関係, *コンクリート工学年次論文集*. 38(1) (2016) 2325-2330.
- [16] H. Xu, J. S. J. van Deventer. The Geopolymerisation of Alumino-Silicate Minerals. *International Journal of Mineral Processing*. 59(3) (2000) 247-266
- [17] M. Criado, W. Aperador, I. Sobrados, Microstructural and mechanical properties of alkali-activated Colombian raw materials, *Materials*. 9(3) (2016) 158.
- [18] F. Puertas, A. Fernandez-Jimenez, M. T. Blanco-Varela. Pore solution in alkali-activated slag cement pastes. Relation to the composition and structure of calcium silicate hydrate. *Cement and Concrete Research*. 34 (2014) 195-206.
- [19] A. Katz, Microscopic study of alkali-activation fly ash. *Cement and Concrete Research*. 28 (1998) 197-208.
- [20] S. V. Patankar, Y. M. Ghugal, S. S. Jamkar, Effect of concentration of sodium hydroxide and degree of heat curing on fly ash-based geopolymer mortar, *Indian Journal of Materials Science*. (2014).
- [21] G. Gorhan, G. Kurklu, The Influence of the NaOH solution on the properties of the fly ash-based geopolymer mortar cured at different temperatures. *Composites Part B: Engineering*. 58 (2013) 371-377.
- [22] K. Somna, C. Jaturapitakkul, P. Kajitvichyanukul, P. Chindapasirt, NaOHactivated ground fly ash geopolymer cured at ambient temperature. *Fuel*. 90(6) (2011) 2118-2124.
- [23] J. Depasse, Coagulation of Colloidal Silica by Alkaline Cations: Surface Dehydration or Interparticle Bridging?. *Journal of Colloidal & Interface Science*, 194 (1997) 260-262.
- [24] M. Komljenovic, Z. Bascarevic, V. Bradic. Mechanical and microstructural properties of alkali-activated fly ash geopolymers. *Journal of Hazardous Materials*. 181(1-3) (2010) 35-42.
- [25] J. W. Phair, J. S. J. Van Deventer, Effect of silicate activator pH on the leaching and material characteristics of waste-based inorganic polymers. *Miner Engineering*, 14(3) (2001) 289-304.
- [26] J. W. Phair, J. S. J. Van Deventer, Characterization of fly ash-based geopolymeric binders activated with sodium aluminate, *Industrial & Engineering Chemistry Research*. 41(17) (2002) 4242-4251.
- [27] A. Matsuda, I. Maruyama, S. Pareek, Y. Araki, Reaction and resultant physical properties of fa-based alkali-activated materials and geopolymer cured at 80 °C, *Proceedings of the Japan Concrete Institute*. 39(1) (2017) 2041-2046.
- [28] A. Palomo, et al., A review on alkaline activation: new analytical perspectives,

- Material and Construction, 64(315) (2014) 1-24.
- [29] T. Nagai, Z. Li, H. Takagaito, A. Suga, Experimental study on the mechanical properties of geopolymer concrete using fly ash and ground granulated blast furnace slag, *Proceedings of the Japan Concrete Institute*. 39(1) (2017) 2077-2082.
- [30] B. Nematollahi, J. Sanjayan, Effect of different superplasticizers and activator combinations on workability and strength of fly ash based geopolymer, *Materials & Design*. 57 (2014) 667-672.
- [31] M. Palacios, P. F. G. Banfill, F. Puertas. Rheology and setting of alkali-activated slag pastes and mortars: effect of organic admixture. *ACI Materials Journal*. 105 (2008) 140-148.
- [32] J. G. Jang, N. K. Lee, H. K. Lee, Fresh and hardened properties of alkali-activated fly ash/slag pastes with superplasticizers. *Construction and Building Materials*. 50(1) (2014) 69-76.
- [33] T. Okada, Z. Li, S. Hashizume, T. Nagai, Experimental study on the properties of fly ash and ground granulated blast furnace slag based geopolymer concrete using retarder, *Proceedings of the Japan Concrete Institute*. 38(1) (2016) 2295-2300.
- [34] N. K. Lee et al. Influence of binder composition on the gel structure in alkali-activated fly ash/slag pastes exposed to elevated temperatures, *Ceramics International*. 43(2) (2017) 2471-2480.
- [35] K. I. Song, J. K. Song, B. Y. Lee, K. H. Yang, Carbonation characteristics of alkali-activated blast-furnace slag mortar, *Advances in Materials Science and Engineering*. (2014) 1-11.
- [36] J. Davidovits, Geopolymer chemistry and sustainable development. The poly (sialate) terminology: a very useful and simple model for the promotion and understanding of green-chemistry. In: *Proceedings of 2005 geopolymer conference*, 1 (2005) 9-15.
- [37] M. Criado, A. Palomo, A. Fernandez-Jimenez, Alkali activation of fly ashes. Part 1: Effect of curing conditions on the carbonation of the reaction products. *Fuel*. 84 (2005) 2048-2054.
- [38] P. Krivenko, G. Kovalchuk, Heat-resistant fly ash based geocements. In: *Proceedings of 2002 geopolymer conference*. (2002).
- [39] Z. Pan, D. Li, J. Yu, N. Yang. Hydration products of alkali-activated slag red mud cementitious material. *Cement and Concrete Research*. 32 (2002) 357-362.
- [40] Z. Pan, D. Li, J. Yu, N. Yang. Properties and microstructure of the hardened alkali-activated red mud-slag cementitious material. *Cement and Concrete Research*. 33 (2003) 1437-1441.
- [41] A. R. Brough, A. Atkinson, Sodium silicate-based alkali-activated slag mortars. Part I. Strength, hydration and microstructure. *Cement and Concrete Research*. 32 (2002) 865-879.

- [42] S. Song, D. Sohn, H. M. Jennings, Mason TO. Hydration of alkaliactivated ground granulated blast furnace slag. *Materials Science*. 35 (2004) 249-257.
- [43] S. Song, H. M. Jennings. Pore solution chemistry of alkali-activated ground granulated blast furnace slag. *Cement and Concrete Research*. 29 (1999) 159-170.
- [44] S. D. Wang, K. Scrivener, P. Pratt. Factors affecting the strength of alkali-activated slag. *Cement and Concrete Research*. 24(10) (1994) 33-43.
- [45] I. Idawati, et al, Modification of phase evolution in alkali-activated blast furnace slag by the incorporation of fly ash, *Cement and Concrete Composites*. 45 (2014) 125-135.
- [46] D. Macphee, I. Garcia-Lodeiro, Activation of aluminosilicates-some chemical considerations. In *Proceedings of Slag Valorisation Symposium*. (2011) 51-61.
- [47] J. Davidovits, *Geopolymer chemistry and applications*. France: Geopolymer Institute. 2011.
- [48] B. Singh, I. G., M. Gupta, S. K. Bhattacharyya, Geopolymer concrete: A review of some recent developments. *Construction and Building Materials*, 85 (2015) 78-90.
- [49] A. Wardhono, D. W. Law, A. Strano, The strength of alkali-activated slag/fly ash mortar blends at ambient temperature, *Procedia Engineering*. 125 (2015) 650-656.
- [50] B. Singh, G. Ishwarya, M. Gupta, S. K. Bhattacharyya. Performance evaluation of geopolymer concrete through alkali-silica reaction. In: *Advances in chemically activated materials*, Changsha, China. (2014) 1-3.
- [51] I. Garcia-Lodeiro, A. Palomo, A. Fernandez-Jimenez. The alkali-aggregate reaction in alkali-activated fly ash mortars. *Cement and Concrete Research*. 37 (2007) 175-183.
- [52] A. Fernandez-Jimenez, F. Puertas. The alkali-silica reaction in alkali-activated granulated slag mortars with reactive aggregate. *Cement and Concrete Research*. 32 (2002) 1019-1024.
- [53] N. K. Lee, H. K. Lee, Setting and mechanical properties of alkali-activated fly ash/slag concrete manufactured at room temperature. *Construction and Building Materials*, 47 2013 1201-1209.
- [54] V. D Glukhovsky. *Soil silicates*. Kiev, USSR: Gostroiizdat Publish. 1959.
- [55] D. H. Campbell, R. L. Folk. Ancient Egyptian pyramids-concrete or rock. *Concrete International*. (1991) 29-44.
- [56] J. Davidovits, Ancient and modern concretes: what is the real difference. *Concrete International*. 12 (1987) 23-25.
- [57] R. Malinowsky, Concretes and mortars in ancient aqueducts. *Concrete International*. 1 (1979) 66-76.
- [58] V. D. Glukhovsky, G. S. Rostovskaja, G. V. Rumyna, High strength slag alkaline cements, In: *Proceedings of the seventh international congress on the chemistry of cement*. 3 (1980) 164-168.

- [59] S. Thokchom, P. Ghosh, S. Ghosh. Performance of Fly ash Based Geopolymer Mortars in Sulphate Solution. *Journal of Engineering Science and Technology Review*, 3(1) (2010) 36-40.
- [60] E. Wang, W. Ni, Q. Sun. The principle and development of GP technology using industrial solid waste. *Comprehensive Utilization of Mineral Resources*, 2005
- [61] T. Bakharev, Resistance of geopolymer materials to acid attack. *Cement and Concrete Research*. 35 (2005) 658-670.
- [62] B. Singh, S. Sharma, M. Gupta, S. K. Bhattacharyya, Performance of fly ash-based geopolymer pastes under chemical environment. In: *International conference on advances in construction materials through science and engineering*, Hong Kong. (2011) 5-7.
- [63] H. S. Shankar, R.B. Khadiranaikar,, Performance of geopolymer concrete under severe environmental conditions, *International Journal of Civil and Structural Engineering*, 3(2) (2012) 396-407.
- [64] 上原 元樹, ジオポリマー法でコンクリートの 環境負荷を低減する, 材料技術, (2011) 10-13.
- [65] R. Sathia, K. Ganesh Babu, M. Santhanam, Durability study of low calcium fly ash geopolymer concrete. In: *3rd ACF international conference*, Ho chi minh city, Vietnam. (2008).
- [66] J. Davidovits, Geopolymers: inorganic polymeric new materials. *Journal of Thermal Analysis and Calorimetry*. 37 (1991) 1633-1656.
- [67] N. P. Rajamane, M. C. Natraja, J. K. Dattatreya, N. Lakshmanan, D. Sabitha. Sulphate resistance and eco-friendliness of geopolymer concretes. *Indian Concrete Journal*. 86 (2012) 13-21.
- [68] I. Ismail, S. A. Bernal J. L. Provis, S. Hamdan, J. S. J. van Deventer, Microstructural changes in alkali-activated fly ash/slag geopolymers with sulphate exposure, *Materials and Structures*. 46 (2013) 361-373.
- [69] T. Bakharev, J. G. Sanjayan, Y. Cheng, Resistance of alkali-activated slag concrete to acid attack. *Cement and Concrete Research*. 33 (2003) 1607-1611.
- [70] D. A. Crozier, J. G. Sanjayan, Chemical and physical degradation of concrete at elevated temperatures, *Concrete in Australia*. 25(1) (1999) 18-20.
- [71] T. Bakharev, Thermal behaviour of geopolymers prepared using class F fly ash and elevated temperature curing. *Cement and Concrete Research*. 36 (2006) 1134-1147.
- [72] D. L. Kong, J. G. Sanjayan, Damage behavior of geopolymer composites exposed to elevated temperatures. *Cement and Concrete Composites*, 30(10) (2008) 986-991.
- [73] R. Zhao, J. G. Sanjayan. Geopolymer and Portland cement concretes in simulated fire. *Magazine of Concrete Research*. 63 (2011) 163-173.
- [74] D. L. K. Kong, J. G. Sanjayan, Effect of elevated temperatures on geopolymer

- paste, mortar and concrete. *Cement and Concrete Research*. 40 (2010) 334-339.
- [75] B. Patil, V. K. M, D. H. Narendra, Durability studies on sustainable geopolymer concrete, *International Research Journal of Engineering and Technology (IRJET)*. 2(4) (2015) 671-677.
- [76] J. G. S. Van Jaarsveld, J. S. J. Van Deventer, L. L. Lorenzen, Factors affecting the immobilization of metals in geopolymerized flyash *Metall. Metallurgical and Materials Transactions B*, 29 (1998) 283-291.
- [77] B. I. El-Eswed, R. I. Yousef, M. Alshaer, I. Hamadneh, S. I. Al-Gharabli, F. Khalili, Stabilization/solidification of heavy metals in kaolin/zeolite based geopolymers *International Journal of Mineral Processing*, 137 (2015) 34-42,
- [78] J. W. Phair, J. S. J. Van Deventer, J. D. Smith, Effect of Al source and alkali activation on Pb and Cu immobilisation in fly-ash based “geopolymers”. *Applied Geochemistry*, 19 (2004) 423-434.
- [79] N. Waijarean, S. Asavapisit, K. Sombatsompop, Strength and microstructure of water treatment residue-based geopolymers containing heavy metals, *Construction and Building Materials*. 50 (2014) 486-491.
- [80] C. Shi, A. Fernández-Jiménez, Stabilization/solidification of hazardous and radioactive wastes wit alkali-activated cements, *Journal of Hazardous Materials*. 137 (2006) 1656-1663.
- [81] P. K Sarker. Bond strength of reinforcing steel embedded in fly ash-based geopolymer concrete. *Materials and Structures*. 44 (2011) 1021-1030.
- [82] D. M. J. Sumajouw, D. Hardjito, S. E. Wallah, B. V. Rangan. Fly ash-based geopolymer concrete: study of slender reinforced columns. *Journal of Materials Science*. 42 (2007) 3124-3130.
- [83] F. N. Degirmenci, Freeze-thaw and fire resistance of geopolymer mortar based on natural and waste pozzolans, *Ceramics-Silikáty*. 62 (1) (2018) 41-49
- [84] M. Olivia, H. Nikraz, Properties of fly ash geopolymer concrete designed by taguchi method. *Materials & Design*. 36 (2012) 191-198.
- [85] D. V. Reddy, J. B. Edouard, K. Sobhan, A. Tipni, Experimental evaluation of the durability of fly ash-based geopolymer concrete in the marine environment. 9th Latin American and Caribbean Conference for Engineering and Technology. (2011) 1-10.
- [86] D. K. Arbi, Durability of geopolymer concrete, *Materials & Environment in Delft University of Technology*. (2016).
- [87] S. Sundar Kumar et al. Development and Determination of Mechanical properties of fly ash and slag blended geopolymer concrete. *International Journal of Scientific & Engineering Research*. 4(8) (2013).
- [88] D. Hardjito, S. E. Wallah, D. M. J. Sumajouw, Rangan BV. On the development of fly ash-based geopolymer concrete. *ACI Mater J* 2004;101(4) (2004) 67-72.

- [89] M. Khalil, E. Merz, Immobilisation of intermediate-level waste in geopolymers. *Journal of Nuclear Materials*. 2(14) (1994) 1-8.
- [90] F. Collins, J. Sanjayan, Strength and shrinkage properties of alkali- activated slag concrete placed into a large column. *Cement and Concrete Research*. 29 (1999) 659-666.
- [91] F. Collins, J. Sanjayan, Microcracking and strength development of alkali-activated slag concrete. *Cement and Concrete Research*. 23 (2001) 345-352.
- [92] K. Andrea, H. Harald. Investigation of geopolymer binders with respect to their application for building materials. *Journal Ceramics-Silikáty*. 48 (2004) 117-120.
- [93] D. Hardjito, B. V. Rangan, Development and Properties of Low-Calcium Fly Ash-based Geopolymer Concrete, Research Report GC1, Faculty of Engineering, Curtin University of Technology, Perth, (2005).
- [94] B. Talling, J. Brandstetr, Present state and future of alkali-activated slag concretes. In: 3rd International conference on fly ash, silica fume, slag and natural pozzolans in concrete. Trondheim Norway; 1989 1519-1546.
- [95] Z. Zhang et al. Role of water in the synthesis of calcined kaolin-based geopolymer, *Applied Clay Science*. 2009, 43(2): 218-223.
- [96] L. Maricela, G. Andres, B. Sandip et al. Effects of water content and chemical composition on structural properties of alkaline activated metakaolin-based geo-polymers. *Journal of the American Ceramic Society*, 95(7) (2012) 2169-2177.
- [97] D. S. Perera, E. R. Vance, K. S. Finnie, et al. Disposition of water in metakaolinite based geopolymers. *Advanced Ceramic Matrix Composites*. 185 (2005) 225-236.
- [98] J. G. S. van Jaarsveld, J. S. J. van Deventer, G. C. Lukey, The characterisation of source materials in fly ash-based geopolymers. *Materials Letters*. 57(7) (2003). 1272-1280.
- [99] P. Duxson, G. C. Lukey, F. Separovic, J. S. J. van Deventer, Effect of alkali cations on aluminum incorporation in geopolymeric gels, *Industrial & Engineering Chemistry Research*. 44(4) (2005) 832-839.
- [100] B. V. Rangan, D. Hardjito, S. E. Wallah, D. M. J. Sumajouw, Fly-ash based geopolymer concrete: a construction material for sustainable development. *Concrete in Australia*. 31 (2005) 25-30.
- [101] A. Fernandez-Jimenez, J. Palomo, I. Sobrados, J. Sanz, The role played by reactive alumina content in the alkaline activation of fly ashes. *Microporous and Mesoporous Materials*. 91 (2006) 111-119.
- [102] J. L. Provis, J. S. J. Deventer. Geopolymerisation kinetics. In situ energy-dispersive X-ray diffractometry, *Chemical Engineering Science*. 62(23) (2007) 18-29.
- [103] P. Duxson, G. C. Lukey, F. Separovic, J. S. J. van Deventer, Effect of alkali cations on aluminum incorporation in geopolymeric gels, *Industrial & Engineering Chemistry Research*. 44 (4) (2005) 832.

- [104] H. Takagaito, Z. Li, T. Nagai, T. Okata, Experimental study on the sulfate resistance of geopolymer concrete using fly ash and ground granulated blast furnace slag, *Proceedings of the Japan Concrete Institute*. 39(1) 2017 2017-2022.
- [105] T. Bakharev, J. G. Sanjayan, Y. B. Cheng, Resistance of alkali-activated slag concrete to carbonation, *Cement and Concrete Research*, 31(9) (2001) 1277-1283.
- [106] E. Rodríguez, S. Bernal, R. M. de Gutiérrez, F. Puertas, Alternative concrete based on alkali-activated slag. *Materiales de Construcción*. 58(291), (2008) 53-67.
- [107] A. A. Adam, Strength and durability properties of alkali activated slag and fly ash-Based geopolymer concrete, RMIT University Melbourne, Australia. (2009)
- [108] D. W. Law, A. A. Adam, T. K. Molyneaux, I. Patnaikuni, A. Wardhono, Long term durability properties of class F fly ash geopolymer concrete, *Materials and Structures*. 48(3) (2015) 721-731.
- [109] S. A. Bernal, et al. Gel nanostructure in alkali-activated binders based on slag and fly ash, and effects of accelerated carbonation. *Cement and Concrete Research*. 53 (2013) 127-144.
- [110] K. Harada, I. Ichimiya, S. Tsugo, K. Ikeda, Fundamental study on the durability of geopolymer mortar, *Proceedings of the Japan Concrete Institute*. 33(1) (2011) 1937-1942.
- [111] M. Khan, A. Castel, A. Akbarnezhad, Utilisation of steel furnace slag coarse aggregate in a low calcium fly ash geopolymer concrete, *Cement and Concrete Research*. 89 (2016) 220-229.
- [112] K. Pasupathy, M. Berndt, A. Castel, J. Sanjayan, R. Pathmanathan, Carbonation of a blended slag-fly ash geopolymer concrete in field conditions after 8 Years, *Construction and Building Materials*. 125 (2016) 661-669
- [113] A. Muntean, On the interplay between fast reaction and slow diffusion in the concrete carbonation process: a matched-asymptotics approach, *Meccanica*. 44 (1) (2009) 35-46.

3 The Carbonation Resistance of FA&BFS-based GP Concrete

3.1 Introduction

Geopolymer have excellent mechanical properties and durability in fire and acid^{[1][2][3][4]}. Compared with normal concrete, it shows great advantages to the environment^{[5][6]}. However, the carbonation resistance of GP has not been clearly understood.

The most readily available source materials of GP are fly ash (FA) and ground granulated blast furnace slag (BFS), which are aluminosilicate minerals composed of aluminium, silicon, and oxygen, etc. FA-based geopolymer can cut down about 60% CO₂ emission, compared to OPC ^[7]. However, in order to improve the strength of FA-based geopolymer cured at room temperature, BFS has to generally be blended. In addition, alkali-activated slag is also thought to be an alternative to OPC.

There are many investigations on the three kinds of alkali-activated materials-FA, BFS, and FA&BFS-based GP concrete. But these investigations are mainly focused on recipes, mechanical properties, and reaction products. However, for putting GP to practical use in reinforced concrete, detailed investigation of GP concrete's durability, especially carbonation resistance, is very necessary ^[8].

Adam, et al. ^[9] compared the carbonation resistances of FA-based GP concrete cured at 80 °C, BFS-based GP concrete, and BFS-OPC blended concrete by the accelerated carbonation test in the ambient air of 20°C, 70% R.H., and 20% of CO₂ concentration. The latter two concretes were cured at room temperature. They found that the FA-based GP concrete didn't show a clear boundary between the carbonated and non-carbonated area after sprayed the phenolphthalein solution. Also, it was found that BFS-based GP concrete has a lower carbonation resistance than FA-based GP and OPC-BFS blended concretes since BFS-based GP concrete specimen had more inside micro-cracks, and its C-S-H gel has in general a lower Ca/Si ratio than the C-S-H in OPC concrete. The C-S-H gel with low Ca/Si ratio is thought to carbonate faster than the general C-S-H gel. Adam, et al. ^[10] also measured the pH changes of FA-based GP mortars, which were mixed with different alkali activators, during accelerated carbonation under 20°C, 70% R.H., and 5% of CO₂ concentration. The pH values of the GP mortars fell from 12 to 11 after carbonated. Initial pH (=12) of GP mortar was smaller than that (pH=13) of OPC concrete, but final pH (=11.0) was higher than OPC concrete (pH=9.0). This results are nearly consistent with the Davidovit's finding that pH ranges of GP concrete are 11.5~12.5, and 10.0~10.5, respectively before and after carbonation ^[11]. Based on this result, Adam, et al. concluded that GP concrete with the

pH value of over 11, which is a safe value for preventing reinforcing steel from corrosion, would be achieved by using adequate alkali activator and aluminosilicate materials.

Song, et al. [12] investigated the carbonation resistance of BFS-based GP mortars, mixed with different amounts of alkali activator and cured in sealed state, by measuring their carbonation depths and the micro-structures before and after carbonated. They found that before carbonation, there were C-S-H gel and few aluminum compounds but no portlandite ($\text{Ca}(\text{OH})_2$) in the BFS-based GP mortars. However, the C-S-H gel is more vulnerable to CO_2 than that in OPC paste. After carbonation, the C-S-H gel changed to silica gel, and the aluminum compounds completely disintegrated. Thus, the carbonation resistance of BFS-based GP is lower than that of OPC. However, they suggested that as the alkali activator content increased, the carbonation resistance of BFS-based GP was improved.

Bernal, et al. [13] detected and compared the changes in the nano-structures of BFS-based GP, FA-based GP, and FA&BFS-based GP before and after carbonation in detail. It was found that N-A-S-H is a main product in FA-based GP and almost can't be disintegrated by carbonation, and only the alkali activator in the pores is neutralized by CO_2 . However, once BFS is blended in GP, the C-A-S-H gel is also formed. The C-A-S-H gel would be decalcified in CO_2 environment to cause the structural transformation at a relatively greater degree.

Criado, et al. [14] examined the effect of curing condition on the early carbonation, and concluded that heat curing with surface sealing can prevent the early carbonation and make the alkali activated FA paste to reach a high degree of polycondensation reaction. The reaction degree affects GP paste's strength and carbonation resistance.

Pasupathy, et al. [15] investigated continuously the carbonation degrees of two kinds of FA&BFS-based GP concretes in the air for 8 years. On basis of supposing that the carbonation depth of GP concrete is a root function of elapsed time (t , year) as $x = K\sqrt{t}$, the authors concluded that the carbonation rate coefficient K ($\text{mm}/\sqrt{\text{year}}$) is positively correlated to the permeability, porosity, and pore size of GP concrete. They also found that the GP concrete, only using NaOH or KOH solution as alkali activator, had a greater carbonation resistance than that using NaOH or KOH together with sodium silicate.

In summary, up to now, 1) there are still few studies on the carbonation resistance of GP concrete, 2) most of studies are for the GP concretes cured at elevated temperature, 3) influencing factors of carbonation resistance were not yet clarified, and 4) there is no carbonation rate model to predict the carbonation depth of GP concrete at any age. However, the carbonation rate of concrete correlates closely with the service life of reinforced concrete.

In fact, if curing in the ambient air, FA-based GP concrete sets slowly, and has a small ultimate strength [16]. In order to attain a practical compressive strength, BFS is

generally mixed together with FA. With the mix of BFS, the setting time becomes short but the strength increases ^[16] ^[17]. The similar results were observed in our experiments ^[18]. Even if FA&BFS-based concrete has practical strength, too short setting time or handling time less than one hour would result in a difficulty of practical use in construction site. Li, et al. successfully developed a retarding admixture for FA&BFS-based GP concrete ^[19]. The retarder can prolong the setting time of FA&BFS-based GP concrete by 1.5~2.3 times, together with almost not giving bad effect on the compressive strength. However, the carbonation resistance of FA&BFS-based GP concrete using retarder has not yet been investigated.

FA&BFS-based GP concrete not only can recycle much waste discharged from thermal power station, but also it has a practical strength even though cured in the ambient air. In order to clarify the carbonation resistance of FA&BFS-based GP concrete, in this study we first investigated the carbonation depths of FA&BFS-based GP concretes and mortars by the accelerated carbonation test. Then a carbonation rate model was proposed to describe the relationship between the carbonation depth and the elapsed time. Furthermore, the influencing factors of the carbonation rate of FA&BFS-based GP concrete were discussed, including alkali activator content, replacing ratio of BFS, alkali activator sort, fineness of BFS, retarder, ratio of alkali activator to active filler, curing temperature, and compressive strength, etc.

3.2 Experimental program

3.2.1 Materials

Table 3.1 Physical properties and chemical compositions of active fillers

Active Filler (AF)	Physical property		Chemical composition (%)								
	Specific gravity	Blaine fineness (cm ² /g)	SiO ₂	Al ₂ O ₃	CaO	Fe ₂ O ₃	MgO	Na ₂ O	K ₂ O	TiO ₂	Others
FA	2.24	3550	62.09	23.04	2.07	6.88	0.67	0.45	1.68	1.41	1.62
BFS30P	2.90	3200	33.82	15.11	43.64	0.28	5.67	0.26	0.25	0.56	0.41
BFS40P	2.88	4180	34.67	14.46	43.13	0.34	5.50	0.25	0.25	0.55	0.85
BFS60P	2.91	5810	34.30	14.36	43.50	0.28	5.86	0.26	0.22	0.59	0.63

Table 3.2 Alkali activator's components and density

Alkali Activator solution No.	WG : NH (by volume)	Specific gravity
AS ₁	1:0	1.270
AS ₂	3:1	1.315
AS ₃	2:1	1.320
AS ₄	0:1	1.330

Besides the fly ash that met the quality standard of JIS (Japanese Industrial Standards) fly ash grade II, three kinds of BFS with different fineness were used as active filler (AF) of GP concrete in this study, of which physical properties and chemical compositions are shown in Table 3.1. Fine aggregates used in GP concrete and GP mortar were river sand and sea sand with specific gravity of 2.60 and 2.57, respectively. Coarse aggregate used in GP concrete was crushed limestone with specific gravity of 2.70, and a maximum size of 20 mm. The specific gravity of aggregate was measured in the saturated surface-dry state. Fine and coarse aggregates were used under the saturated surface-dry condition. The retarder (R) is an inorganic compound with specific gravity of 1.78.

Four kinds of alkali activator solutions (AS), named AS₁, AS₂, AS₃ and AS₄ were used in GP concretes. They were mixtures of water glass aqueous solution (WG) and sodium hydroxide solution (NH) according to the volume ratios shown in Table 3.2. The WG was prepared by diluting JIS No.1 grade water glass with distilled water by a volume ratio of 1:1. The concentration of NH was 10 moles.

3.2.2 Mix proportions of GP concrete and mortar

According to a large number of experiments before this study, we found that the Series No. 2A (2B) has good workability and meets the requirement of compressive strength around 30 Mpa. Therefore, when designing the mix proportions of this study,

we used 2A or 2B as the control mixture. Based on the mix proportion of 2A (2B), in our experiments, 14 kinds of GP concretes and 9 kinds of mortars with different mix proportions, as summarized respectively in Table 3.3 and Table 3.4, were used to investigate the carbonation resistance and its influencing factors of GP materials. The GP concrete specimens were produced in different times, differentiating with alphabet A (June 2016) and B (Oct. 2016) in the series No.. The ratio of BFS to the total fillers is lower than 50% for the large use of FA. In case of GP mortar, the ratio of fine aggregate (S) to active filler (AF) was around 2.0 by mass, and the alkali activator to active filler ratio was 0.5.

Table 3.3 Mix proportions and compressive strength of GP concrete

Influencing factors	Series No.	AS/AF	WG/AS	BFS/AF	BFS sort	R/AF (%)	AF (kg/m ³)	AS (kg/m ³)	S (kg/m ³)	G (kg/m ³)	f_c (MPa)	Slump (cm)	
AS content	1A	0.50	0.75	0.3	40P	5	420	AS ₂ =210	721	1000	25.0	26.1	
	2A						400	AS ₂ =200	762		28.4	26.1	
	2B								762		29.7	25.0	
	3A						370	AS ₂ =185	824		27.4	24.5	
AS/AF	4B	0.45						AS ₂ =200	704		28.4	24.9	
	5B	0.55						AS ₂ =200	790		27.7	25.5	
AS sort	6B	0.50	1	0.3	30P	0	400	AS ₁ =200	749		19.1	13.1	
	7B		0.75						AS ₂ =200		752	41.8	24.5
	8B		0						AS ₄ =200		768	20.1	4.0
BFS/AF	9B		0.75	0.5	40P	5	AS ₂ =200		771		40.0	24.5	
	10A			0.4					767		31.0	25.0	
	11A			0.2					753		23.5	25.0	
	12B			0.0					723		17.7	24.0	
Retarder	13A			0.2					753	23.8	26.1		

[Notes] AS: Alkali activator, AF: Active filler, FA: JIS grade II fly ash, BFS: Ground granulated blast furnace slag, R: Retarder, S: Fine aggregate, and G: Coarse aggregate, f_c : 28days compressive strength

Table 3.4 Mix proportions and curing temperature of GP mortar

Series No.	1	2	3	4	5	6	7	8	9	
Curing temperature (°C)	20	60	80	20						
AS/AF	0.5									
S/AF	2.0									
AS sort	AS ₂			AS ₁	AS ₃	AS ₄	AS ₂			
R/AF (%)	5						0	5		
BFS sort	40P							30P	60P	

Criado, et al. [20] stated that the main reaction product of active fillers containing above 60% BFS is C-A-S-H gel, but when the replacing ratio of BFS is below 40%, the main product becomes to be N-A-S-H gel. Now there is no generally accepted definition about geopolymer, but it is thought that geopolymer has at least two features:

three-dimensional structure and amorphousness. Since the N-A-S-H gel tends to be amorphous and a three-dimensional structure, we limited the replacing ratio of BFS to 50% in this study. Another reason is to use FA in GP concrete as much as possible by limiting the BFS content.

3. 2. 3 Specimen preparation

The experimental procedure is shown in Fig. 3.1. A concrete mixer with two horizontal blades and a Hobart planetary mortar mixer were used to mix GP concrete, and GP mortar, respectively. In case of concrete, active fillers and fine aggregate were firstly put into the concrete mixer and mixed for 1 minute. Then, the alkali activator and retarder were added and mixed for 2 min. to get GP matrix mortar. Finally, coarse aggregate was added to the mortar and further mixed for 2 min. to get GP concrete. After the slump and air content were measured, fresh concrete was cast half and half into the plastic cylinder molds with a diameter of 10 cm and a height of 20 cm. Every half casting accompanied 10 seconds of vibration using a rod vibrator. Following by the vibration, the outside of mold was tapped by a wood hammer.

The mixing procedure of GP mortar was the same to GP concrete except not adding coarse aggregate. Freshly mixed GP mortar was used to produce two kinds of specimen: cylinder with a diameter of 10 cm and a height of 20 cm, and prism with 4 cm of side length of square and 16 cm of height, respectively. The former was for the accelerated carbonation test, and the latter was used to measure the mechanical properties. 1 min. vibration was applied to each of the mortar specimens with a table vibrator. The top surfaces of all the specimens were leveled by a metal spatula.

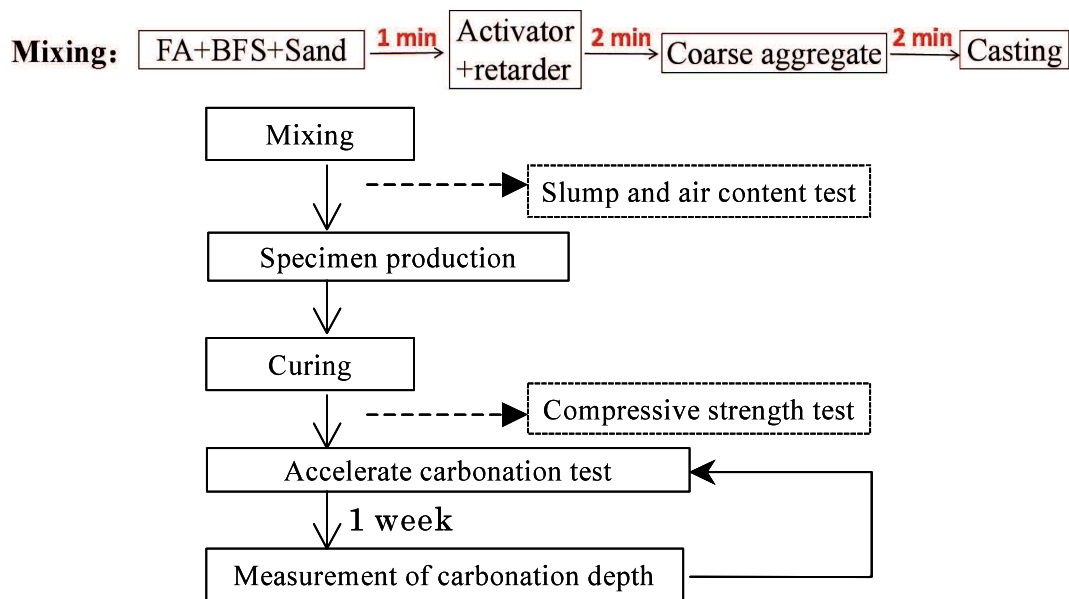


Fig. 3.1 Experimental procedure

The specimens of concrete and mortar were cured in the ambient air of $20 \pm 2^\circ\text{C}$, R.H. $60 \pm 5\%$ for 28 days except Series No.2 and No.3. GP concrete specimens were demoulded at 5 days age. However, the GP mortar specimens were demoulded at 1 day age except Series No.6 that set 2 days later.

The mortar specimens of Series No.2 and Series No.3 were cured at 60°C , and 80°C for 8 hours, respectively, following by curing in the ambient air of $20 \pm 2^\circ\text{C}$, R.H., $60 \pm 5\%$ till 28 days age. Demoulding was done after the first 3 hours curing of 60°C or 80°C .

3. 2. 4 Accelerated carbonation and compressive strength test

After the 28 days curing, the top and the base of every cylindrical specimen were sealed with waterproof tape to ensure that CO_2 diffuses into the specimens only through the circumferential surface, as shown in Fig. 3.2. Then, the specimens were placed into a carbonation test chamber with 5% of CO_2 concentration, 20°C , and R.H. 60%. At an interval of one week, the concrete or mortar specimen was cut at 35-40 mm intervals to measure the carbonation depth. It should be noted that during the cutting, in order to ensure that the alkali matters were not washed away, spraying water was not used as dust countermeasure.



Fig. 3.2 Specimen's section sealed with waterproof tape

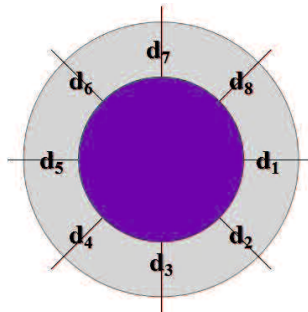


Fig. 3.3 Measurement positions of carbonation depth

After the measurement of carbonation depth, the specimens were returned into the

CO₂ chamber to continue the carbonation test, following by sealing the cut section with the tape. The accelerated carbonation test lasted 8 weeks, and 6 weeks for concrete and mortar specimens, respectively.

The method, used to measure the carbonation depth of GP specimen in this study, is the same to that usually used for OPC concrete, i.e. spraying phenolphthalein on freshly cut section, then measuring the depths of colorless region in 8 directions on the cross section of cylindrical specimen, finally calculating average value of the 8 depths, as shown in Fig. 3.3.

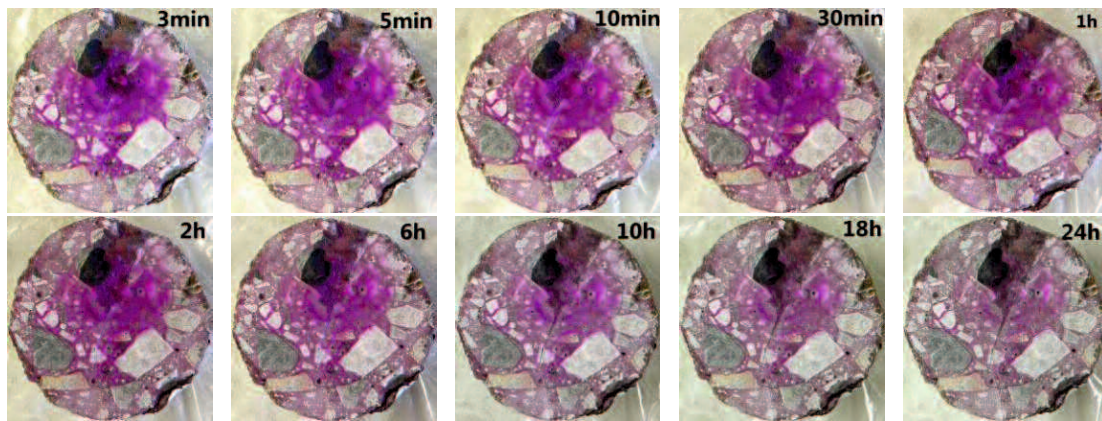


Fig. 3.4 Color change after spraying the phenolphthalein solution

Other researchers [21] [22] [23] pointed out that the interface between carbonated and non-carbonated zones of GP specimens is unstable after spraying phenolphthalein solution, we also observed that the pink color area changes with the elapsed time, as shown in Fig. 3.4. However, if the measurement is done early, it is able to distinguish the pink color boundary definitely, and measure the carbonation depth precisely. Hence, we measured the carbonation depths at 8 positions within 3~5 min. after spraying the phenolphthalein solution.

The compressive strengths (f_c) of GP concretes were measured at 28 days age according to JIS A 1108, which were average values of three specimens for each series, as shown in Table 3.3. The slump and air content of every series of specimens were conducted according to JIS A 1101 and JIS A 1118 respectively. The slump values were also shown in Table 3.3. And the air content of all these GP specimens were around 1~1.5%.

3. 3 Results and the proposing of carbonation rate function

3. 3. 1 Pink color range on the specimen section after spraying phenolphthalein solution

Table 3.5 Pink color ranges of concrete specimens before and after the accelerated carbonation

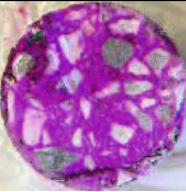


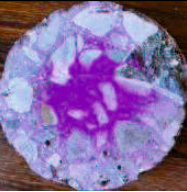

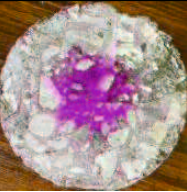
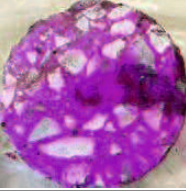
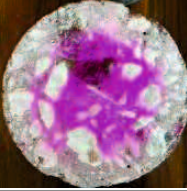


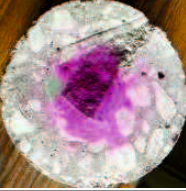
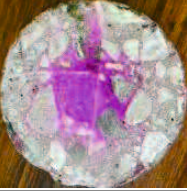

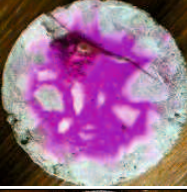


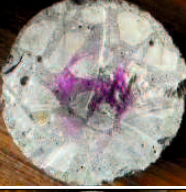
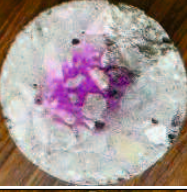

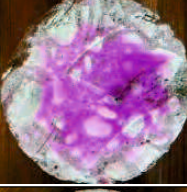



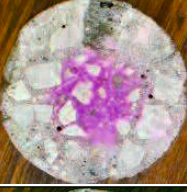
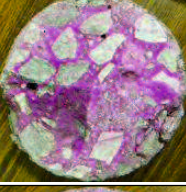
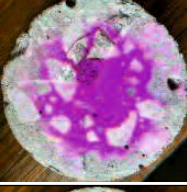



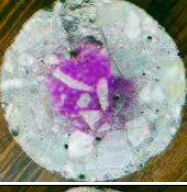
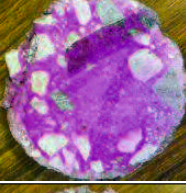
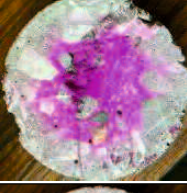





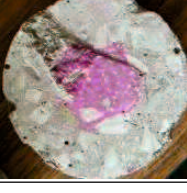




No.	Before	1 week	2 weeks	4 weeks	6 weeks	8 weeks
1A						
2A						
2B						
3A						
4B						
5B						
6B						

Table 3.5 Pink color ranges of concrete specimens before and after the accelerated carbonation (continued)

No.	Before	1 week	2 weeks	4 weeks	6 weeks	8 weeks
7B						
8B						
9B						
10A						
11A						
12B						
13A						

Table 3.5 shows the color changes on the cross sections of all the specimens at 5 min. later after phenolphthalein solution was sprayed, which were carbonated for 8 weeks. Almost all of the GP concrete specimens except Series No.12B had clear pink boundary, and the pink area decreased with the carbonation time. The pink boundary

was not in a cycle, interrupted by coarse aggregate particles.

Series No.12B was actually FA-based GP concrete, not using BFS so that its strength was small. That is to say, it had not a dense structure and thus was easily carbonated. Maybe Series No.12B was greatly carbonated during the curing, which resulted in that it had a pale pink area even before the accelerated carbonation test, as shown in Table 3.5 (continued).

3. 3. 2 Variation of carbonation depth with elapsed time

Fig. 3.5 shows the test results of the relationship between the carbonation depth (C-depth) and the elapsed time for the GP concretes. The carbonation depth increased with the elapsed time in the first three week, but after three week, the increase became smaller and smaller

The relationship between the carbonation depth of GP mortar and the elapsed time are shown in Fig. 3.6. Like as the GP concrete, the carbonation of GP mortar progressed rapidly with time in the first two weeks, and then evolved slowly.

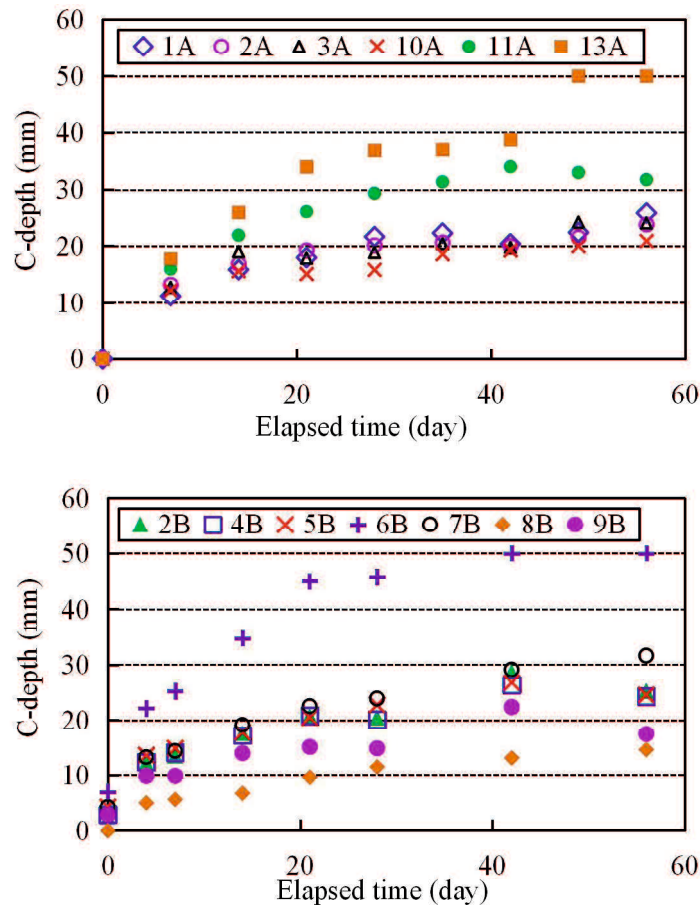


Fig. 3.5 Relationship between the carbonation depth of GP concrete and the elapsed time

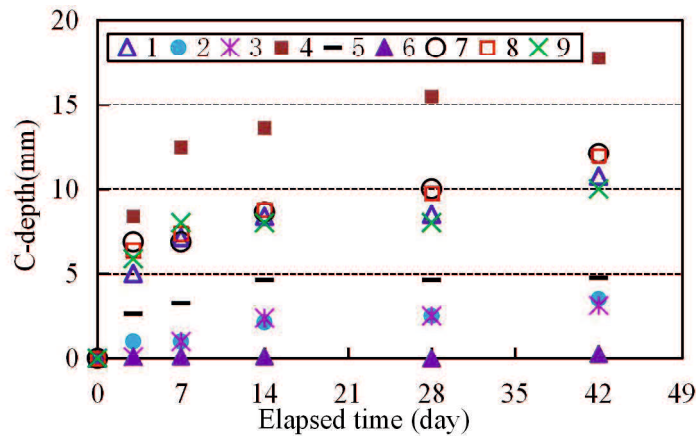


Fig. 3.6 Relationship between the carbonation depth of GP mortar and the elapsed time

3. 3. 3 Carbonation Rate of GP Concrete

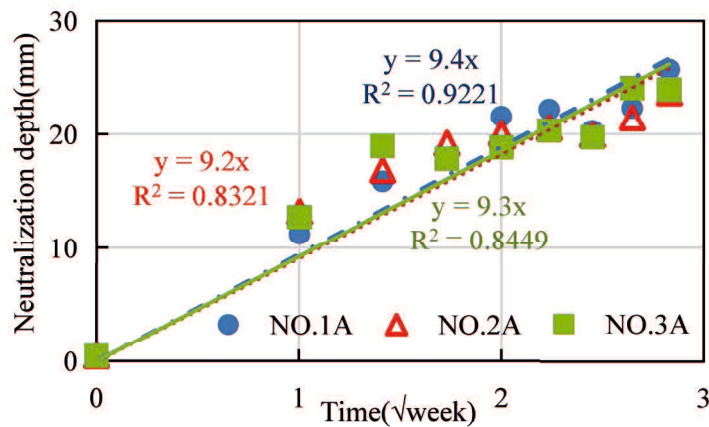


Fig. 3.7 Carbonation coefficient of GP concrete with different AS content

Section color of GP concrete specimens, before carbonation test and after 1, 3, 5 and 8 weeks carbonation in environment “E_c”, are shown in Table 3.5. In the first week, a deep carbonation was found for all the specimens. But with the time growth, the carbonation rate slowed down, as presented in Fig. 3.5. This tendency is similar to OPC concrete, but at present we can’t conclude that GP concrete’s carbonation is faster or slower than OPC concrete only according to Table 3.5 and Fig. 3.5.

I conducted regression to analyze the relation between the carbonation depth and the root of elapsed time (week) to get three carbonation depth equations for the three mixtures, as shown in Fig. 3.7. Since the coefficients of determination (R²) of three equations are near to 0.9, it can be said that the form of the relation equation between the carbonation depth and time of GP concrete coincides with that of OPC concrete, as shown in Eq.(3.1) [24].

$$x = a \cdot \sqrt{\text{CO}_2\% / 5.0} \cdot \sqrt{t} \quad (3.1)$$

where, x : Carbonation depth (mm)

t : Carbonation period (week)

$CO_2\%$: CO_2 concentration (%)

a : Carbonation rate coefficient (mm/ $\sqrt{\text{week}}$)

carbonation rate coefficients for three kinds of GP concrete were gotten from Fig.3.7, and are shown in Table 3.6. 28 days-compressive strengths of three GP concretes are also indicated in Table 3.6.

Reference [24] gives a relationship equation of the carbonation rate coefficient for normal OPC concrete, as shown in Eq.(3.2).

$$a = -0.13 f_c + 7.40, R^2 = 0.999 \quad (3.2)$$

where, a : Carbonation rate coefficient (mm/ $\sqrt{\text{week}}$)

f_c : Compressive strength (N/mm²)

Table 3.6 Carbonation rate coefficient of GP concrete and OPC concrete with same compressive strength (mm/ $\sqrt{\text{week}}$)

No.	Compressive strength (N/mm ²)	OPC concrete	GP concrete
1A	25.0	4.1	9.4
2A	28.4	3.7	9.2
3A	27.4	3.8	9.3

Using the above equation, we calculated the carbonation rate coefficients of OPC concretes with the same compressive strength as the GP concretes, as shown in Table 3.6. If comparing the carbonation rate coefficients of GP and OPC concretes, it was clearly found that the carbonation resistances of the three FA&BFS-based GP concretes were lower than those of OPC concretes. For a given strength the carbonation rate coefficient of FA&BFS-based GP concrete is two times higher than that of normal OPC concrete.

3. 3. 4 Carbonation rate model

(1) Theoretical analysis of carbonation rate

According to Fick's first law [25], the diffusion flux of carbon dioxide into concrete through unit cross section at unit time (Q , g/m²·s) is expressed by Eq. (3.3), assuming that the carbon dioxide concentration (φ) just changes with diffusing depth (x).

$$Q = -D \frac{\partial \varphi}{\partial x} \quad (3.3)$$

where, D is the diffusion coefficient of CO_2 (m²/s)

The relationship between the CO_2 concentration (φ) and the diffusing depth (x) is generally simplified as a linear relationship, i.e. the φ decreases linearly with the x . If

the CO₂ concentration at the surface of concrete is noted as φ_0 , Eq. (3.3) can be changed as Eq. (3.4).

$$Q = D \frac{\varphi_0}{x} \quad (3.4)$$

Before the CO₂ diffuses to the position x , it must be consumed or bound by the chemicals located on the diffusing route. For OPC concrete, main chemical substance reacting with CO₂ is generally Ca(OH)₂. But for GP concrete, the chemicals are not clear. The CO₂ is perhaps bound by unconsumed alkali activator.

The diffusion flux of carbon dioxide can be expressed by Eq. (3.5)

$$dJ = Q \cdot S \cdot dt \quad (3.5)$$

where, J is the mass of chemically bound CO₂ in concrete (g), t is time (s), S is the surface through which the diffusion occurs (m²).

If the CO₂ absorption capacity of concrete due to carbonation through a unit surface area in unit time is noted by q (g/m³), dJ can be given by Eq. (3.6).

$$dJ = q \cdot S \cdot dx \quad (3.6)$$

For the materials that do not react with diffusing gas, e.g. sand and soil, their gas diffusion coefficients are constant, not changing with the exposed time. However, for hardened concrete, it is generally considered that the carbonation products, such as CaCO₃ in case of OPC concrete, make concrete dense so that the porosity decreases since the volume of CaCO₃ is larger than that of Ca(OH)₂ by about 11.7% [26] [27]. Yang's model [28] shows that the diffusion coefficient of OPC concrete is directly proportional to the square of porosity, and decreases with the advance of hydration and carbonation.

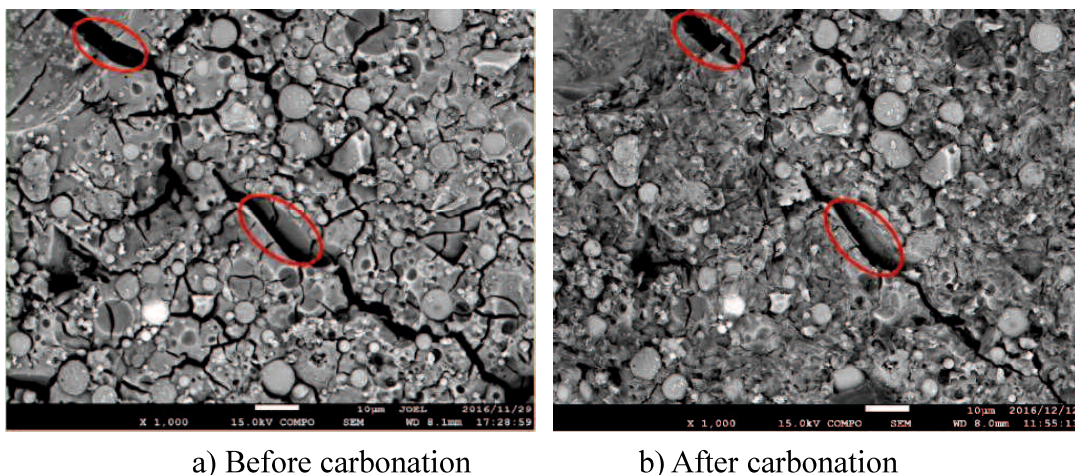


Fig. 3.8 The SEM images of series No.1 before and after carbonation

Fig. 3.8 shows the SEM images of GP mortar before and after the carbonation. It can be found that after carbonation, the fine cracks disappeared and the coarse cracks became small, i.e. the GP concrete became dense. Moreover, the compressive strengths of Series No.2B were 29.7 MPa, and 34.2 MPa before and after the carbonation,

respectively. The increase of strength also indicates that the GP concrete become dense after the carbonation. Therefore, we consider that the diffusion coefficient (D) of GP concrete would decrease with the carbonation time (t) as OPC concrete.

Czarnecki [29] investigated the relationship between the diffusion coefficient (D) and t for OPC concrete, and proposed a D - t relationship model, as shown in Eq. (3.7). The diffusion coefficient of OPC concrete decreases with the elapsed time. It is generally considered that this is because the CaCO_3 fills up the pores in concrete.

$$D = 28.085t^{-0.439} \quad (3.7)$$

It is not easy to examine how the diffusion coefficient of GP concrete changes with carbonation time. In this study, we firstly supposed that Eq. (3.7) is also applied to FA&BFS-based GP concrete since the carbonation constituent (e.g. NaOH) in GP concrete reacts with CO_2 to form Na_2CO_3 like the generation of CaCO_3 in OPC concrete.

The amount of $\text{Ca}(\text{OH})_2$, which is a kind of hydrates, depends on hydration degree of cement. $\text{Ca}(\text{OH})_2$ is also main carbonation constituent of OPC concrete. Thus, for a certain OPC concrete, the CO_2 absorption capacity increases with the age of concrete, as shown in Eq. (3.8) [28].

$$q = \frac{8.06t_c}{2.0 + t_c} \alpha_\infty \cdot C \cdot M_{\text{CO}_2} \quad (3.8)$$

where t_c is the age of concrete, α_∞ is the ultimate degree of hydration, C : cement content in 1 m^3 concrete, and M_{CO_2} is the molecular weight of CO_2 (44 g/mol.)

Now the carbonation mechanism of GP concrete is not fully clear. Remained alkali activator, C-A-S-H gel, and N-A-S-H gel are possible to react with CO_2 . As the C-A-S-H and N-A-S-H gels form, the alkali activator deceases. Hence, we can't conclude that whether the CO_2 absorption capacity of GP concrete increases with carbonation time or not. However, according to the Eq. (3.8), for a given OPC concrete (C is constant), the increase of the CO_2 absorption capacity with time is not great. Also, unless GP concrete is kept in moist state by sealing, its long-term strength growth is very small. Therefore, in this study we ignored the change of the CO_2 absorption capacity of GP concrete, i.e. treated the q as a constant for a given GP concrete.

Eq. (3.6) and Eq. (3.7) were substituted into Eq. (3.4) and Eq. (3.5) respectively, and based on the consideration that the CO_2 diffusion amount is equal to the CO_2 absorption amount, Eq. (3.9) was obtained as follows.

$$q \frac{dx}{dt} = 28.085 \cdot t^{-0.439} \cdot \frac{\varphi_0}{x}$$

$$x dx = \frac{28.085 \cdot \varphi_0}{q} t^{-0.439} dt \quad (3.9)$$

Furthermore, after integrating the two sides of Eq. (3.9) with respect to the depth x , and the elapsed time t , respectively, the relational equation of carbonation depth and time was gotten, as shown in Eq. (3.10).

$$x = 10 \sqrt{\frac{\varphi_0}{q}} \cdot t^{0.28} \quad (3.10)$$

The carbonation depth-time relational equation Eq. (3.10) was simplified as Eq. (3.11). The parameter a is defined to be the carbonation rate coefficient of GP concrete. From Eq. (3.11), we can understand that the carbonation rate of GP concrete in the early time of carbonation is greater than in the long time. Also, the carbonation depth of OPC concrete is generally thought to be the square root function of carbonation time. Hence, the increasing rate of carbonation depth of GP concrete is larger than that of OPC concrete in the early time of carbonation. When FA&BFS-based GP concrete cured in the ambient air has the same 28-days compressive strength to OPC concrete, the carbonation rate coefficient of the former, which is also a proportional coefficient of square root function like as OPC concrete, is larger than that of the latter [30].

$$x = a \cdot t^{0.28} \quad (3.11)$$

(2) Experimental analysis of carbonation rate

Since the above theoretical analysis was performed on basis of several suppositions, Eq. (3.11) should be verified by experimental results. Next, we further conducted regression analyses toward the experimental results shown in Fig. 3.5, according to root function shown in Eq. (3.12). Several n values of root equation were used in the regression analyses, which were around 0.28 besides 0.5 according to Eq. (3.11).

$$x = at^{1/n} \quad (3.12)$$

where, x means carbonation depth (mm), t represents carbonation time (day), a is proportional coefficient, i.e. carbonation rate coefficient, and n is a positive number.

The proportional coefficients (a) of six kinds of root functions ($1/n=0.50, 0.33, 0.35, 0.30, 0.28, 0.25$), and the determination coefficients (R^2) were obtained from the regressive curve equations of GP concrete, as shown in Tables 3.7 and 3.8. The standard deviation (σ) of R^2 was gotten for every series (see Table 3.8). The mean and the σ of R^2 changed with the $1/n$ used. The greater the mean of R^2 (R^2_m) and the smaller the σ of R^2 , the higher the accuracy of the regressive equation. Using the mean and the σ of R^2 for every series is to propose a carbonation rate model suiting for FA&BFS-based GP concrete with different recipes.

For getting a root function that is universally applied to describe the carbonation evolution of FA&BFS-based GP concrete cured in the ambient air, we plotted the relationships of R^2_m , σ and $1/n$, as shown in Fig. 3.9. From Fig. 3.9, we found that with the increase of $1/n$, the R^2_m increases and the σ decreases, but beyond a certain value of

$1/n$, the R_m^2 starts to decrease and the σ starts to increase. When $1/n$ is in a range of 0.28~0.33, both the R_m^2 and the σ reached each satisfactory value.

Table 3.7 The carbonation rate coefficient a of FA&BFS-based GP concrete

No.	$1/n$					
	1/4	0.28	0.30	1/3	0.35	1/2
1A	8.6439	7.7678	7.2721	6.4726	6.1042	3.5678
2A	8.4519	7.5879	7.0995	6.3125	5.9503	3.4634
2B	9.5333	8.6309	8.1139	7.2701	6.8772	4.0989
3A	8.5415	7.6700	7.1772	6.3832	6.0177	3.5064
4B	9.2485	8.3677	7.8634	7.0409	6.6582	3.9572
5B	9.5928	8.6760	8.1513	7.2960	6.8981	4.0933
6B	18.7810	17.0020	15.9830	14.3200	13.5450	8.0673
7B	10.6390	9.6386	9.0649	8.1280	7.6914	4.5985
8B	4.6471	4.2168	3.9697	3.5653	3.3765	2.0326
9B	7.0918	6.4169	6.0305	5.4003	5.1070	3.0363
10A	7.4956	6.7306	6.2981	5.6012	5.2804	3.0768
11A	12.2530	11.0100	10.3070	9.1725	8.6500	5.0529
13A	16.0940	14.4800	13.5650	12.0890	11.4080	6.7025

Table 3.8 The Determination coefficient R^2 of FA&BFS-based GP concrete

No.	$1/n$					
	1/4	0.28	0.30	1/3	0.35	1/2
1A	0.9575	0.9664	0.9697	0.9721	0.9716	0.9253
2A	0.9858	0.9810	0.9759	0.9632	0.9552	0.8398
2B	0.9254	0.9366	0.9399	0.9398	0.9370	0.8432
3A	0.9651	0.9638	0.9609	0.9522	0.9463	0.8516
4B	0.9456	0.9492	0.9475	0.9380	0.9302	0.7855
5B	0.9229	0.9211	0.9155	0.8983	0.8863	0.6942
6B	0.9208	0.9324	0.9356	0.9344	0.9307	0.8202
7B	0.9240	0.9442	0.9530	0.9620	0.9637	0.9053
8B	0.8948	0.9217	0.9357	0.9559	0.9640	0.9838
9B	0.8512	0.8559	0.8550	0.8470	0.8400	0.7043
10A	0.9866	0.9848	0.9816	0.9723	0.9661	0.8682
11A	0.9648	0.9725	0.9752	0.9761	0.9749	0.9204
13A	0.9013	0.9218	0.9326	0.9483	0.9547	0.9741
Mean (R_m^2)	0.9340	0.9420	0.9445	0.9430	0.9401	0.8550
σ	0.0307	0.0254	0.0235	0.02430	0.0271	0.0687

[Notes] σ is the Standard deviation of R^2

In order to get an optimum value of $1/n$ for the root function, the regressive analyses were conducted for the relationships between the R_m^2 , the σ and the $1/n$ to get two relational equations, as shown in Eq. (3.13) and Eq. (3.14). The determination coefficients of the two equations are larger than 0.99. This indicates that the accuracy of regressive curve equation of carbonation depth is greatly dependent on the $1/n$ value.

$$R_m^2 = -2.531 (1/n)^2 + 1.5804 (1/n) + 0.6975,$$

Determination coefficient: 0.9998 (3.13)

$$\sigma = 1.312 (1/n)^2 - 0.8285(1/n) + 0.1551,$$

Determination coefficient: 0.9975 (3.14)

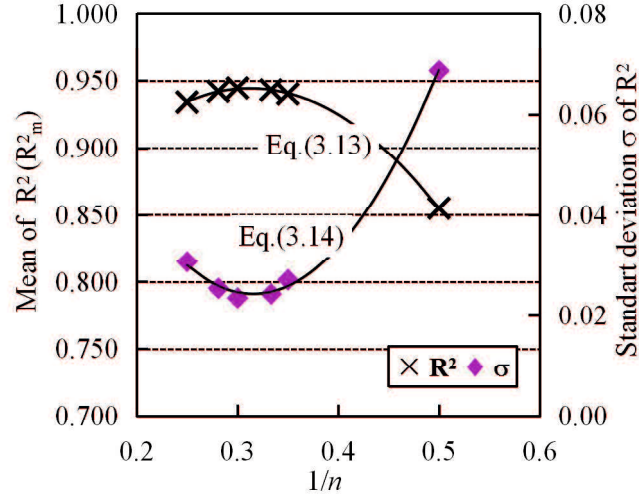


Fig. 3.9 The changes of R_m^2 and σ with $1/n$ of concrete

Through a maximum-minimum problem analysis, we found that for achieving a maximum R_m^2 , $1/n$ should be 0.3122, and for getting a minimum σ , the $1/n$ should be 0.3157. Hence, the optimum value of $1/n$ is about 0.31.

Based on the above theoretical analysis and the discussion on the experimental results, in case of FA&BFS-based GP concrete, as an universal model, we proposed to use the root function shown in Eq. (3.15) to describe the carbonation progress with time.

$$x = at^{0.31} \tag{3.15}$$

The n value of Eq. (3.15) is different from the theoretical result shown in Eq. (3.11). This is because the theoretical analysis was conducted on basis of several suppositions and there are errors in the experiment. However, the n values in Eq. (3.11) and Eq. (3.15) are very close. This means that the results of theoretical analysis and experimental discussion are reliable.

On the other hand, considering that the carbonation resistance of GP concrete is greatly dependent on that of GP matrix mortar, and in order to avoid the interference from coarse aggregate so that we can easily guarantee the accuracy of carbonation test and reduce experimental works, toward the experimental results of FA&BFS-based GP mortar shown in Fig. 3.6, we also conducted the regression analysis on the relationship between carbonation depth and time, using 6 kinds of root functions (see Eq. (3.12), $1/n=0.15, 0.20, 0.25, 0.28, 0.33, 0.50$). The proportional coefficient (a), i.e. carbonation rate coefficient and determination coefficient (R^2) were obtained, as shown in Tables 3.9 and 3.10.

Table 3.9 The carbonation rate coefficient a of FA&BFS-based GP mortar

No.	$1/n$					
	0.15	0.20	1/4	0.28	1/3	1/2
1	5.4330	4.7253	4.0866	3.7249	3.1719	1.8457
4	9.2604	8.0541	6.9653	6.3486	5.4060	3.1448
5	2.7077	2.3523	2.0319	1.8507	1.5739	0.9118
7	6.0708	5.2783	4.5639	4.1597	3.5422	2.0624
8	6.0381	5.2498	4.5390	4.1367	3.5222	2.0495
9	5.3890	4.6706	4.0258	3.6620	3.1082	1.7916

Table 3.10 The Determination coefficient R^2 of FA&BFS-based GP mortar

No.	$1/n$					
	0.15	0.20	1/4	0.28	1/3	1/2
1	0.9457	0.9712	0.9784	0.9744	0.9744	0.8081
4	0.9561	0.9817	0.9887	0.9845	0.9641	0.8136
5	0.9498	0.9648	0.9606	0.9492	0.9164	0.7258
7	0.9531	0.9760	0.9814	0.9767	0.9564	0.8123
8	0.9624	0.9852	0.9901	0.9848	0.9632	0.8125
9	0.9685	0.9601	0.9328	0.9073	0.8515	0.5972
Mean(R^2_m)	0.9559	0.9732	0.9720	0.9628	0.9377	0.7616
σ	0.0064	0.0078	0.0169	0.0230	0.0358	0.0667

[Notes] σ is the Standard deviation of R^2

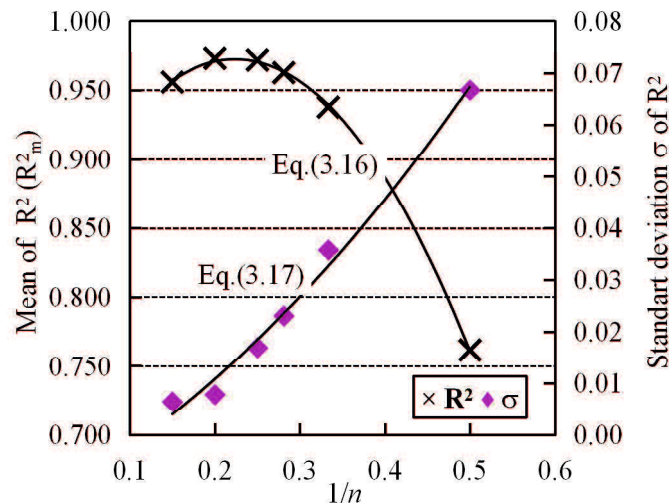


Fig. 3.10 The changes of R^2_m and σ with $1/n$ of mortar

Except the square root function ($1/n=0.50$), almost all the determination coefficients (R^2) of other regressive root functions are more than 0.90. That is to say, the root functions of $1/n=0.15\sim 1/3$ can nearly describe the experimental relationship between carbonation depth and time. For determining an optimum value of $1/n$ for GP

mortar, the relationship between the mean of determination coefficient (R^2_m), the standard deviation (σ) and $1/n$ were plotted, as shown in the Fig. 3.10. Like as GP concrete, the R^2_m increases with increasing the $1/n$, but beyond a certain $1/n$ value, the R^2_m starts to decrease with the $1/n$. However, the standard deviation (σ) of R^2 increases with the $1/n$.

The regressive curve equation of R^2_m , $\sigma \sim 1/n$ relationship were gotten, as shown in Eq. (3.16) and Eq. (3.17).

$$R^2_m = -2.7664 (1/n)^2 + 1.2372 (1/n) + 0.8342,$$

$$\text{Determination coefficient: } 0.9996 \tag{3.16}$$

$$\sigma = 0.1466 (1/n)^2 + 0.0858 (1/n) - 0.0122,$$

$$\text{Determination coefficient: } 0.9892 \tag{3.17}$$

Through a maximum-minimum problem analysis of Eq. (3.16), we found that in case of GP mortar, for achieving a maximum R^2 , $1/n$ should be 0.224. And when $1/n$ is equal to 0.224, According to Eq. (3.17) the σ is 0.0078, which is small enough. Hence, we proposed to use the root function shown in Eq. (3.18) to describe the relationship between carbonation depth and elapsed time in case of FA&BFS-based GP mortar.

$$x = at^{0.22} \tag{3.18}$$

3. 4 Influencing factors of carbonation resistance

In order to investigate influencing factors of the carbonation resistance of GP concrete, it is usual to use the experimental results of GP concrete specimens. The root functions used to describe exactly the carbonation rate of GP concrete and mortar are different, as shown in Eq. (3.15) and Eq. (3.18). However, it is considered that the carbonation resistance of GP concrete is greatly dependent on that of GP matrix mortar. It is possible to use GP mortar specimens instead of GP concrete to discuss the influencing factors, excluding aggregate type and content, through comparing the carbonation rate coefficient a of GP mortar.

Due to the coarse aggregate particles' existence, the pink area boundary on the GP concrete's section is a jagged line rather than a circle. The jagged pink area boundary reduces the accuracy of carbonation depth's measurement. For easily guaranteeing the accuracy of carbonation test and reducing experimental works, GP mortar specimens were used for the investigation of some of influencing factors, including curing temperature, BFS fineness, alkali activator sort, and addition of retarder. It should be noted that when investigating a certain influencing factor, we compared the carbonation rate coefficient (a) of the same kind of GP material (mortar or concrete) with different recipes. That is to say, we did not confuse the “ a ” of mortar and concrete to do the factor analysis. The carbonation rate coefficients of concrete and mortar were gotten according to Eq. (3.15), and Eq. (3.18), respectively.

3. 4. 1 Addition of retarder

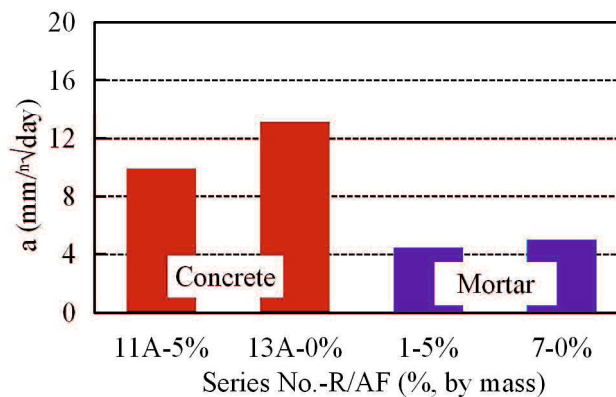


Fig. 3.11 Effect of retarder on the a value of GP concrete and mortar

Fig. 3.11 demonstrates the carbonation rate coefficients (a) of GP concrete and GP mortar with or without adding the retarder. In case of adding the retarder, the dosage was 5% of active fillers by mass. From this figure, it can be found that whether the GP concrete or the GP mortar specimen adding 5% retarder had a smaller carbonation rate coefficient, compared to the specimens without adding the retarder. At present, the reason is not clear. The retarder prolongs the setting time of GP through slowing down

the dissolution of Ca^{2+} from BFS so that the GP structure forms slowly but densely [19]. Dense GP structure may be of benefit to the improvement of the carbonation resistance of GP concrete.

3. 4. 2 WG to AS ratio

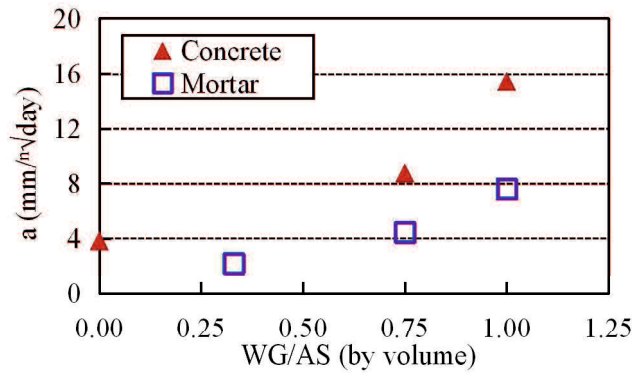


Fig. 3.12 The a -WG/AS ratio relationship of GP concrete and mortar

Fig. 3.12 shows the change of the a value of GP concrete with WG/AS ratio by volume. It clearly shows that as the volume ratio of water glass solution to alkali activator solution increased from 0 to 1.0, the carbonation rate coefficients (a) increased greatly. That is to say, the more the water glass (WG) in the WG-NaOH solution (AS), the lower the carbonation resistance of FA&BFS-based GP concrete.

Although the GP concrete specimen using NaOH solution as alkali activator showed a better carbonation resistance than the specimens using a combination of NaOH and water glass, the compressive strength of the former at 28 days age was smaller than that of the latter when cured at room temperature [18]. Pinto, et al. [31] also reported the similar results that using the alkaline activator containing water glass causes a higher mechanical strength. Criado et al.[14] explained the reason to be that water glass favors the polymerization process to lead to the reaction products with more Si.

3. 4. 3 AS to AF ratio and AS content

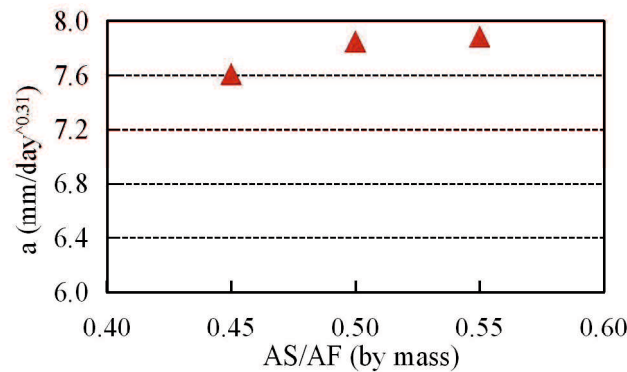


Fig. 3.13 The a -AS/F ratio relationship of GP concrete

The relationship between the a values of FA&BFS-based GP concrete and AS/AF ratio is shown in Fig. 3.13. The carbonation rate coefficient of GP concrete increased with the AS/AF ratio. This result is the similar to OPC concrete. OPC concrete's carbonation resistance generally decreases with the increase of water-cement ratio. The increase of AS/AF ratio causes the increases of Na/Si ratio and the W/AF ratio. Much water would yield more pores in hardened GP concrete. That is to say, W/AF ratio affects the carbonation resistance of GP concrete. P. Nath ^[17] also stated that the W/AF ratio affects the strength of GP concrete. As explained in Chapter 5, the greater the strength of GP concrete, the higher its carbonation resistance.

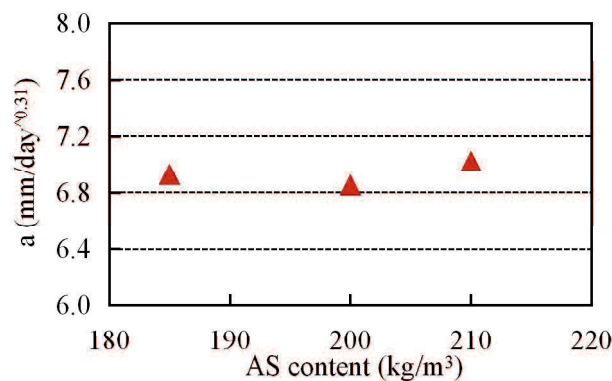


Fig. 3.14 The a -AS content relationship of GP concrete

However, from Fig. 3.14, we didn't find the effect of AS content on the carbonation resistance of GP concrete.

3. 4. 4 BFS to AF ratio

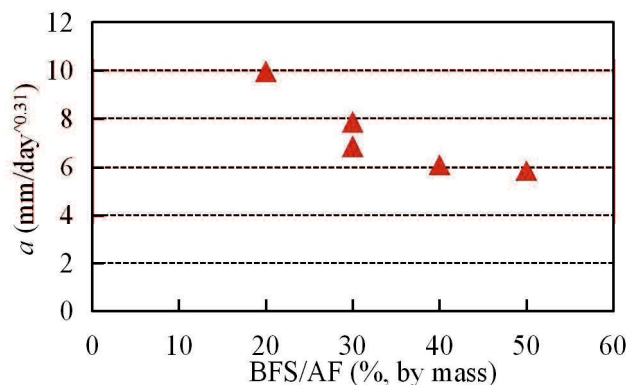


Fig. 3.15 The a -BFS/F ratio relationship of GP concrete

The a values of GP concretes, blended with 20%, 30%, 40% and 50% BFS by mass respectively, are shown in Fig. 3.15. In this figure, the a values corresponding to 30% BFS were gotten by different specimens produced in June and October, 2016, respectively. Though the data varies widely, it can be found that the a value decreased with increasing the ratio of BFS to the active filler (AF), i.e. the carbonation resistance

of FA&BFS-based GP concrete becomes high as the BFS content increases. This attributes to that the increase of BFS content improves the compressive strength of the FA&BFS-based GP concrete that becomes more compact [17]. However, we also found that the relationship between the a value and the BFS/AF ratio is not proportional, with the increase of BFS/AF ratio, especially over 40% the decrease of the a value became small.

It should be noted that we also tried to investigate the carbonation resistance of GP concrete without mixing BFS in this study. But because the boundary of pink color area was so vague that the carbonation depth could be measured properly (see Series No.12B in Table 3.5), we have to give up this discussion here.

3. 4. 5 BFS fineness

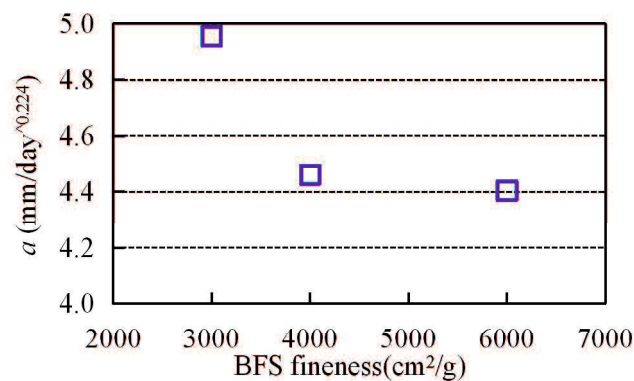


Fig. 3.16 The effect of BFS fineness on the a value of GP mortar

The BFS with Blaine fineness of 3000, 4000, and 6000 cm²/g were used to investigate the effect of BFS fineness on the carbonation resistance of FA&BFS-based GP concrete. Obtained results are shown in Fig. 3.16. The carbonation rate coefficient a of the GP concrete using the BFS with 3000 cm²/g of Blaine fineness was the largest. But the a values of the GP concretes using BFS 40P and BFS 60P were almost the same. Therefore, we can say that when the fineness of BFS reaches a certain level, e.g. 4000 cm²/g in this study, its effect on the carbonation resistance of FA&BFS-based GP concrete becomes unobvious.

From the viewpoint of strength, Talling, et al. [32] pointed out that the optimum Blaine fineness of slag is 4000 cm²/g, and Wang et al. [33] stated that the optimum Blaine fineness of slag depends on the type of slag and varies between 4000 and 5500cm²/g. If referring to the results shown in the Chapter 5 that the carbonation resistance of GP concrete correlates closely with its strength, the results shown in Fig. 3.16 are reasonable.

3. 4. 6 Curing temperature

Since the best $1/n$ values of the root functions for GP mortar cured at ambient

temperature and high temperatures are different, as shown in Table 3.8 (see Series No.1~3). Hence, instead of carbonation rate coefficient, we directly compared the carbonation depths at the same carbonation time for different curing temperatures, as shown in Fig. 3.17. It can be clearly found that GP mortars cured at 60°C and 80°C had almost the same carbonation depth, but 20°C curing yielded about 3 times carbonation depth of heat curing. That is to say, heat curing can improve the carbonation resistance of FA&BFS-based GP concrete.

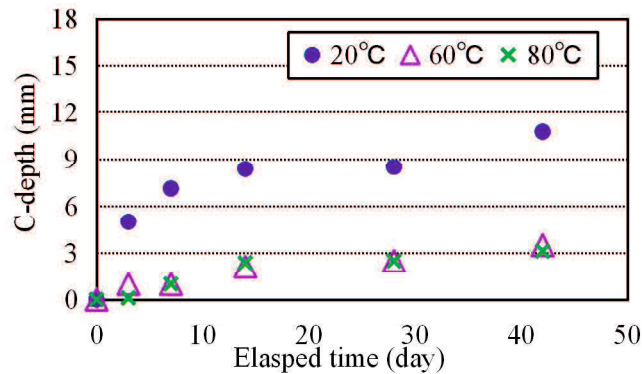


Fig. 3.17 The effect of curing temperature on the carbonation resistance of GP mortar

3. 4. 7 Na to Si ratio

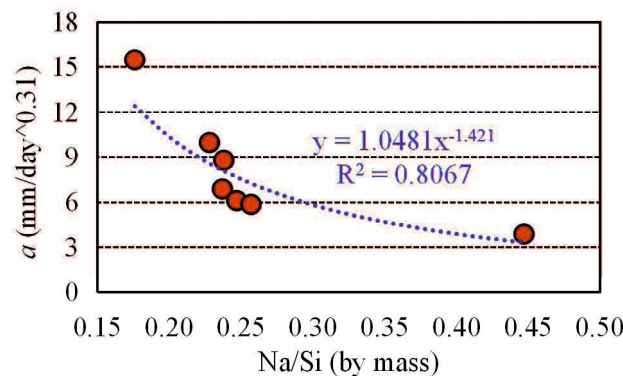


Fig. 3.18 The change of the a value of GP concrete with Na/Si ratio

Fig. 3.18 shows the influence of Na/Si ratio by mass on the carbonation resistance of FA&BFS-based GP concrete with 0.50 of AS/AF ratio. The larger Na/Si ratio, the smaller the a value. The relationship between the a value and Na/Si ratio can be roughly described by a power function.

3.5 Relationship between compressive strength and carbonation resistance

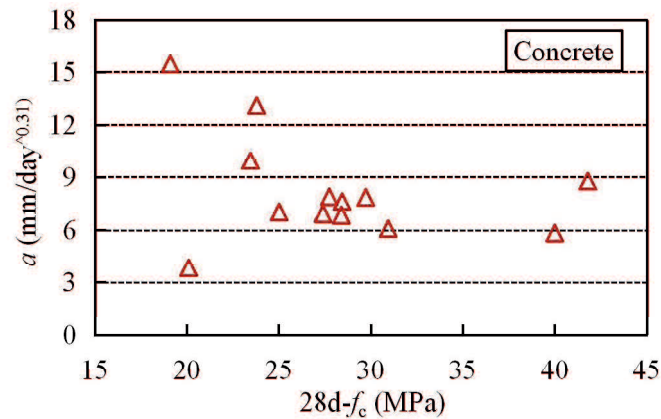


Fig. 3.19 Relationship between the a value and compressive strength

The relationship between the 28-days compressive strength and the carbonation rate coefficient (a) are shown in Fig. 3.19 for 13 series of GP concrete, which were cured in the 20 °C air. Though the a values dropped as the compressive strength increased on the whole, they ranged widely even for the same compressive strength. This is because although the compressive strength depends on the denseness degree of concrete, the carbonation resistance of GP concrete is affected by not only the denseness degree, but also the sort of alkali activator, and pore characteristics, etc. For example, even if the pores' amount and size distribution are the same, the concrete with the pores that are connected with the outside would have a low carbonation resistance.

3.6 Conclusions

In order to clarify the carbonation resistance of FA&BFS-based GP concrete, in this study the accelerated carbonation tests of GP concrete and GP mortar were performed. The carbonation depth was measured within 5 minutes later after spraying phenolphthalein solution. The relationship between the carbonation depth and time was further examined based on the experimental results and by theoretical analysis. Finally, we discussed the influencing factors of the carbonation resistance of FA&BFS-based GP concrete in detail through comparing the carbonation rate coefficients of different specimens. Main conclusions are as follows.

(1) FA&BFS-based GP concrete, using 30% BFS, has a lower carbonation resistance than OPC concrete with the same compressive strength to the GP concrete.

(2) The relationship between carbonation depth and elapsed time of FA&BFS-based GP concrete and GP mortar, which are cured in the ambient air, can be expressed by root functions, shown in Eq.(13) and Eq.(16) where $1/n$ values are 0.31, and 0.22 respectively. The increasing rate of carbonation depth of FA&BFS-based GP concrete in the early time is larger than that of OPC concrete.

(3) As the effects of raw materials on the carbonation resistance of FA&BFS-based GP concrete, the addition of the retarder mainly composed of potassium sodium tartrate can improve the carbonation resistance of FA&BFS-based GP concrete cured in the ambient air. The finer the BFS, the smaller the carbonation rate coefficient (a) of FA&BFS-based GP concrete. However, the decrease of a value with the increase of BFS fineness becomes smaller and smaller when the Blaine fineness of BFS is larger than 4000g/cm^2 .

(4) As the effects of mix proportions on the carbonation resistance of FA&BFS-based GP concrete, with the increase of BFS ratio in active fillers (AF), the carbonation rate coefficient of FA&BFS-based GP concrete decreases. However, the decrease becomes small when the BFS ratio is above 40%. The higher the NaOH content in the alkaline activator (AS) composed of sodium silicate and NaOH, the higher the carbonation resistance. The compressive strength of FA&BFS-based GP concrete only using sodium hydroxide is, however, lower than that using sodium silicate and NaOH together. Also, with increasing the AS/AF ratio or Water-AF ratio, the carbonation rate coefficient increases. However, the effect of AS content was not clearly found from the experimental results. Moreover, for the same AS/AF ratio, the carbonation rate coefficient declines with the increase of Na/Si ratio.

(5) Curing temperature greatly influences the properties of FA&BFS-based GP concrete. Curing at room temperature yields a lower carbonation resistance, compared to heat curing. There is, however, no great difference between 60°C and 80°C curing, if the curing duration is the same.

(6) The carbonation resistance of GP concrete is related to its compressive strength. The concrete having a higher strength generally tends to have a higher carbonation resistance. But the carbonation resistance of GP concrete is also affected by other factors, such as alkaline activator type. The experimental results in this study showed that the carbonation rate coefficient of FA&BFS-based GP concrete doesn't always decrease with its compressive strength, as shown in Fig. 3.19.

References

- [1] J. Davidovits, Geopolymers of the first generation: silicate-process, Geopolymer'88: First European Conference on Soft Mineralogy, Compiègne, France. 2 (1988) 49-67.
- [2] D. A Crozier, J. G. Sanjayan, Chemical and physical degradation of concrete at elevated temperatures, *Concrete in Australia*. 25(1) (1999) 18-20.
- [3] S. Thokchom, P. Ghosh, S. Ghosh, Performance of fly ash based geopolymer mortars in sulphate solution, *Journal Engineering Technology Review*. 3(1) (2010) 36-40.
- [4] B. V. Rangan, Geopolymer concrete for environmental protection, *The Indian Concrete Journal*. 88(4) (2014) 41-59.
- [5] D. N. Huntzinger, T. D. Eatmon, A life-cycle assessment of Portland cement manufacturing: comparing the traditional process with alternative technologies, *Journal of Cleaner Production*. 17 (7) (2009) 668-675.
- [6] C. Meyer, The greening of the concrete industry, *Cement and Concrete Composites*. 31 (8) (2009) 601-605.
- [7] Z. Li, Z. Ding, Y. Zhang, Development of sustainable cementitious materials. *International Workshop on Sustainable Development and Concrete Technology*. (2004) 55-76.
- [8] P. Duxson, J. L. Provis, G. C. Lukey, J. S. J. van Deventer, The role of inorganic polymer technology in the development of green concrete, *Cement and Concrete Research*. 37(12) (2007) 1590-1597.
- [9] A. A. Adam, Strength and durability properties of alkali activated slag and fly ash-Based geopolymer concrete, RMIT University Melbourne, Australia. (2009)
- [10] D. W. Law, A. A. Adam, T. K. Molyneaux, I. Patnaikuni, A. Wardhono, Long term durability properties of class F fly ash geopolymer concrete, *Materials and Structures*. 48(3) (2015) 721-731.
- [11] J. Davidovits, Geopolymer, *Green Chemistry and Sustainable Development Solutions: Proceedings of the World Congress Geopolymer 2005*. Geopolymer Institute. (2005) 9-15.
- [12] K. I. Song, J. K. Song, B. Y. Lee, K. H. Yang, Carbonation characteristics of alkali-activated blast-furnace slag mortar, *Advances in Materials Science and Engineering*. (2014) 1-11.
- [13] S. A. Bernal, J. L. Provis, B. Walkley, R. San Nicolas, J. D. Gehman, D. G. Brice et al., Gel nanostructure in alkali-activated binders based on slag and fly ash, and effects of accelerated carbonation, *Cement and Concrete Research*. 53 (2013) 127-144.
- [14] M. Criado, A. Palomo, A. Fernández-Jiménez, Alkali activation of fly ashes. Part 1:

- Effect of curing conditions on the carbonation of the reaction products, *Fuel*. 84(16) (2005) 2048-2054.
- [15] K. Pasupathy, M. Berndt, A. Castel, J. Sanjayan, R. Pathmanathan, Carbonation of a blended slag-fly ash geopolymer concrete in field conditions after 8 Years, *Construction and Building Materials*. 125 (2016) 661-669.
- [16] S. Sundar Kumar, J. Vasugi, P. S. Ambily, B. H. Bhaskar, Development and determination of mechanical properties of fly ash and slag blended geopolymer concrete, *International Journal of Scientific & Engineering Research*. 4(8) (2013).
- [17] P. Nath, P. K. Sarker, Effect of GGBFS on setting, workability and early strength properties of fly ash geopolymer concrete cured in ambient condition, *Construction and Building Materials*. 66 (2014) 163-171.
- [18] T. Nagai, Z. Li, H. Takagaito, A. Suga, Experimental study on the mechanical properties of geopolymer concrete using fly ash and ground granulated blast furnace slag, *Proceedings of the Japan Concrete Institute*. 39(1) (2017) 2077-2082.
- [19] T. Okada, Z. Li, S. Hashizume, T. Nagai, Experimental study on the properties of fly ash and ground granulated blast furnace slag based geopolymer concrete using retarder, *Proceedings of the Japan Concrete Institute*. 38(1) (2016) 2295-2300.
- [20] M. Criado, W. Aperador, I. Sobrados, Microstructural and mechanical properties of alkali activated Colombian raw materials, *Materials*. 9(3) (2016) 158.
- [21] K. Harada, I. Ichimiya, S. Tsugo, K. Ikeda, Fundamental study on the durability of geopolymer mortar, *Proceedings of the Japan Concrete Institute*. 33(1) (2011) 1937-1942.
- [22] D. W. Law, A. A. Adam, T. K. Molyneaux, I. Patnaikuni, A. Wardhono, Long term durability properties of class F fly ash geopolymer concrete, *Materials and Structures*. 48(3) (2015) 721-731.
- [23] M. S. Badar, K. Kupwade-Patil, S. A. Bernal, J. L. Provis, E. N. Allouche, Corrosion of steel bars induced by accelerated carbonation in low and high calcium fly ash geopolymer concretes, *Construction and Building Materials*. 61 (2014) 79-89.
- [24] S. Suzuki and M. Hisaka, Study on Mechanical Properties and Durability of High Fluidity Concrete (part12 carbonation), *Architecture Institute of Japan*. 1995 (1995) 303-304.
- [25] E. Vesikari, Carbonation and chloride penetration in concrete with special objective of service life modelling by the factor approach, *Research Report*. (2009) 4-6.
- [26] T. Sasaki, I. Shimabukuro, H. Oshita, Analytical study on prediction of pore volume changes due to carbonation of concrete based on detailed carbonation model introduced chemical equilibrium theory, *Journal of Japan Society of Civil Engineers E*. 62(3) (2006) 555-568.
- [27] T. Ishida, K. Maekawa, Modeling of pH profile in pore water based on mass transport and chemical equilibrium theory. *Journal of Japan Society of Civil*

- Engineers. 47(648) (2000) 203-215.
- [28] K. H. Yang, E. A. Seo, S. H. Tae, Carbonation and CO₂ uptake of concrete, Environmental Impact Assessment Review. 46 (2014) 43-52.
- [29] L. Czarnecki, P. Woyciechowski. Modelling of concrete carbonation; is it a process unlimited in time and restricted in space?, Bulletin of the Polish Academy of Sciences Technical Sciences. 63(1) (2015) 43-54.
- [30] S. Li, Z. Li, T. Nagai, T. Okata, Neutralization resistance of fly ash and blast furnace slag based geopolymer concrete, Proceedings of the Japan Concrete Institute. 39(1) (2017) 2023-2028.
- [31] A. T. Pinto, Alkali-activated metakaolin based binders, PhD Thesis, University of Minho. (2004).
- [32] B. Talling, J. Brandstetr, Present state and future of alkali-activated slag concretes. Proceedings of 3rd International Conference on Fly Ash, Silica Fume, Slag And Natural Pozzolans In Concrete. Trondheim Norway. (1989) 1519-1546.
- [33] S. D. Wang, K. Scrivener, P. Pratt, Factors affecting the strength of alkali-activated slag, Cement Concrete Research. 24 (1994) 1033-1043.

4 The Neutralization Resistance of FA&BFS-based GP Concrete in Conditions with Water Movement

4.1 Introduction

Geopolymer (GP) has been shown great advantages in less CO₂ emission, waste recycling, high early compressive strength, high fire and acid resistances, and no alkali aggregate reaction etc.^{[1][2][3][4][5][6]}. However, the carbonation resistance of GP concrete is proven to be lower than that of OPC concrete by accelerated carbonation test^{[7][8][9]}. Considering the difference of mixing solution between GP and cement concrete, and for the use of GP concrete in reinforced concrete structure, it is necessary to clarify the neutralization resistance in various environments.

Fly ash (FA) and blast furnace slag (BFS) are usually blended as the most available source materials of geopolymer. Comparing to OPC, the source materials of GP have low calcium content. In addition, The usually used alkali activators are Na⁺, K⁺ based silicate, hydroxide, or their blend. Therefore, the alkali activator, which remains in the porosity of hardened GP concrete, would affect the alkalinity of GP concrete. This is very different from the OPC concrete, of which the alkalinity is mainly depended on Ca(OH)₂ that is one of the hydrates of cement.

Water moves in the concrete with the humidity fluctuation in the air, and the concrete of underground and marine structures may immerse into water. However, the carbonation reaction is always considered as main reason of the alkalinity decline of OPC concrete. According to the reaction mechanism of GP from Davidovtis^[4], it can be found that the dissolution of aluminosilicate uses water, but the polymerization releases water. Releasing water during dehydration polymerization reaction of GP (in the hardening time) may cause connected open-pores in GP. Through the continuous pores in moisture environment, alkali activating matters, remained in the pores of GP concrete, may dissolve out opening to the outside. If the alkalinity of GP concrete is mainly attributed to the alkali activator matters remained in the pores of concrete, it is reasonable to consider that drying and water immersion may bring some alkali matters out of concrete to reduce its alkalinity. In fact, the study of Bernal et al. has reported that the main carbonation reaction substance in the FA-based GP concrete was alkali pore solution^[10]. That is to say, that the alkali matters in GP concrete dissolve out into water or move out with water evaporation is another reason of neutralization except carbonation. But up to now, there is no study on the effects of drying and wetting on the alkalinity change of GP concrete.

Therefore, in this study, we investigated the neutralization resistance of FA&BFS-based GP concrete and GP mortar caused by water movement besides the

Chapter 4 Neutralization Resistance of GP Concrete in Conditions with Water Movement

carbonation. Four kinds of environmental conditions were designed, which were water immersion, wet-dry repeating, carbonation in the atmosphere with 5% or 10% concentration of CO₂, and carbonation-dry repeating, respectively. The GP concrete specimens were cured in the ambient air or with heating, The used GP mortar specimens were cured in the ambient air.

4.2 Experimental program

4.2.1 Raw materials

The binder materials of GP concrete and mortar used in this experiment is FA and BFS40P (JIS 4000 class) as described in chapter 3. The alkali activator solution used was AS₂ with specific gravity of 1.315. As chapter 3, the river sand with a specific gravity of 2.60, and crushed limestone with a specific gravity of 2.70, and a maximum size of 20 mm, were employed in GP concrete as the fine and coarse aggregate respectively. But, the fine aggregate used in GP mortar was sea sand of which the specific gravity was 2.57. Fine and coarse aggregates were in the saturated surface-dry state. The retarder used was also as shown in chapter 3.

Table 4.1 shows the physical properties and the chemical compositions of the OPC mortar. The fineness aggregate used in OPC mortar was same to the GP mortar.

Table 4.1 Chemical compositions and physical properties of OPC

Binder	Chemical compositions (wt %)									Physical properties	
	SiO ₂	CaO	Al ₂ O ₃	Fe ₂ O ₃	MgO	K ₂ O	NaO	SO ₃	Others	Specific gravity	Blaine Fineness (cm ² /g)
OPC	21.80	63.90	4.49	2.90	1.84	0.38	0.20	2.26	2.23	3.16	3110

4.2.2 Mix proportions

In this study, GP concrete (GPC), GP mortar (GPM) and OPC mortar (OPCM) were prepared according to the mix proportions shown in Table 4.2. GPC and GPM had the same alkali activator solution (AS)-active filler (AF) ratio by mass, but had different BFS-AF ratios, being 0.3 and 0.4, respectively. The sand to AF ratio of GP mortar was 2.0 by mass.

Table 4.2 Mixtures of GP mortar and GP concrete

Sample ID	AS/AF	Unit weight (kg/m ³)					
		AS	FA	BFS	S	Crushed limestone	Retarder
AGPC/HGPC	0.5	200	280	120	756	1000	20
GPM	0.5	316	379	253	1264	-	32

Notes: AGPC: GP concrete (GPC) cured in the ambient air, HGPC: heat-cured GPC.

Table 4.3 Mixtures of OPC mortar

Sample ID	W/C	S/C	R-WRA/C	Unit weight (kg/m ³)			
				W	C	S	R-WRA
OPCM	0.45	3	0.005	229	509	1527	2.5

Notes: W: water, C: OPC cement, R-WRA: AE retarding type water-reducing agent.

For the OPC mortar, the water-cement ratio and the sand-cement ratio were 0.45 and 3.0, respectively, as shown in Table 4.3. Also, retarding type AE water-reducing agent was added at the dosage of 0.5% of cement.

4. 2. 3 Production and curing of specimens

(1) GP concrete

The mix procedure of the GP concrete was conducted as shown in chapter 3. After measuring the air content and slump, the fresh concrete were cast into molds with diameter of 10 cm and height of 20 cm by rod vibration.

The GP concrete specimens were cured at different temperatures. The AGPC specimens, as described in the notes of Table 4.2, were cured at the ambient air of 20°C, R.H. 60 ± 5% for 28 days. The HGPC specimens were cured in the chamber of 60 °C for 6 hours, then in the ambient air of 20°C, R.H. 60 ± 5% until 28 days age. The ages before demoulding were 3 days for the AGPC specimens used in the environmental condition “e_{w+d}”, but 1 day for the specimens used in the environmental conditions “e_c” and “e_{c+d}”. The HGPC specimens were demoulded after 6 hours curing at 60 °C. After the 28 days’ curing, the AGPC and HGPC specimens were placed in the lab room of 20 ± 5 °C for about 100 days. Then, we moved them into the accelerated carbonation chamber or other environments to conduct the neutralization experiments.

(2) GP mortar and OPC mortar

The mixing process of GP mortar was the same to the GP concrete before adding the coarse aggregate, but a Hobart planetary mortar mixer was used. For producing the OPC mortar, the cement and sand was first mixed for 1 min., then the water and admixture were fed into the mixer and mixed for other 3 min. The GP mortar or OPC mortar was cast into three smaller prism molds, with a size of 4×4×16 cm, for measuring the its compressive strength, and a larger prism mold with a size of 10×10×40 cm for neutralization test. The specimens were vibrated on a vibrating table.

All the mortar specimens were cured in the ambient air with temperature of 20°C, R.H. 60±5% for 28 days. They were demoulded after 1 day curing, and their neutralization experiment began after 28 days curing.

4. 2. 4 Neutralization environment conditions

The four kinds of environmental conditions of neutralization were shown in Table 4.4 in detail. It should be noted that the environmental conditions used for AGPC and GPM were different. In the environments “E_w”, “E_{w+d}”, and “e_{w+d}”, the electrolyzed water with pH of 7.7 was used. The water content ratios of the specimens were the same in the beginning of every circle. The environment, marked as “E_w”, is a wetting

Chapter 4 Neutralization Resistance of GP Concrete in Conditions with Water Movement

environment. The mortar specimens were immersed into the water of 20 °C for 8 days per circle. The “E_{w+d}” environmental condition is a wet-dry repeating. The specimens were first soaked into the water for 3 days, then they were dried in a chamber of 60°C or 80°C for 2 days, and soaked into the water again for 3 days, before measuring the neutralization depth and pH. However, for GP concrete, there was no the process of the second water immersion of 3 days. Hence, the water contents of GPM and GP concrete were different when measuring the neutralization depth and pH value.

Table 4.4 Environment conditions of neutralization (one cycle)

Specimen	Code	Environment		
		A water immersion (pH=7.7, 20°C)	B Drying (B ₁ : 60°C or B ₂ : 80°C)	C: Carbonation (C ₁ : CO ₂ =5±0.5%, 20°C, R.H.=60±5%, or C ₂ : CO ₂ =10±0.5%, 20°C, R.H.=60±5%,)
GPM and OPCM	E _w	A (8 days) → Measurement		
	E _{w+d}	A (3 days) → B ₁ (2 days) → A (3 days) → Measurement		
	E _c	C ₁ (8 days) → Measurement		
	E _{c+d}	C ₁ (3 days) → B ₁ (2 days) → C ₁ (3 days) → Measurement		
GPC	e _{w+d}	A (3 days) → B ₂ (2 days) → Measurement		
	e _c	C ₂ (7 days) → Measurement		
	e _{c+d}	C ₂ (7d) → B ₂ (2d) → Measurement		

The environmental conditions, briefly called as “E_c” and “e_c”, were referred to the environment of accelerated carbonation test with 20 °C, R.H. 60 ± 5%. The CO₂ concentration was 5 ± 0.5%, and 10 ± 0.5%, respectively for mortar specimens and GP concrete specimens. A lower CO₂ concentration was used in case of the mortar specimens for increasing the neutralization test cycle. After 7 days or 8 days carbonation, we measured respectively the neutralization depths and the pH values of the mortar and GP concrete specimens.

The fourth environmental condition, noted by “E_{c+d}”, was a carbonation-dry repeating. After 3 days carbonation in environment “E_c”, the mortar specimens were dried for 2 days at 60°C, then returned back into the carbonation chamber for other 3 days. After each cycle, we measured the mortar’s neutralization depth and pH value in an air-dried state of R.H. 60 ± 5%. However, the GP concrete specimens in the “e_{c+d}” condition were carbonated for 7 days then dried for about 2 days until their mass became nearly constant. The neutralization depths and the pH values of the GP concrete specimens were measured in a dried state.

In the conditions “E_{w+d}” and “e_{w+d}”, the reasons why we soaked the specimens in the water for 3 days and 2 days for drying these specimens were determined by experiments. The mass of the specimens were almost unchanged in the water after three days, and it took about two days for drying until the quality tended to be stable. For GP mortar specimens, lasting 8 days in water and carbonation conditions was to ensure a same neutralization period with the other conditions. But for GP concrete, the same neutralization period among different conditions was not considered. The carbonation

was cycled every 7 days.

4. 2. 5 Measurement methods of neutralization depth, pH and compressive strength

The phenolphthalein solution method was adopted to measure the neutralization depth of GPC, GPM and OPCM. But the measurement was limited within 5 min. after spraying the phenolphthalein indicator on the cutting section, as the carbonation depth's measurement [11].

Fig. 4.1 presents the pH measurement positions of GP concrete specimen. The powder was drilled from two positions: edge of specimen section, and central zone with a diameter of 4 cm, which are briefly noted as O, and I. For. However, for the mortar specimens, three positions where the powder samples were gathered were 0, 1, and 3 cm from the edge of specimen section, as shown in Fig. 4.2.

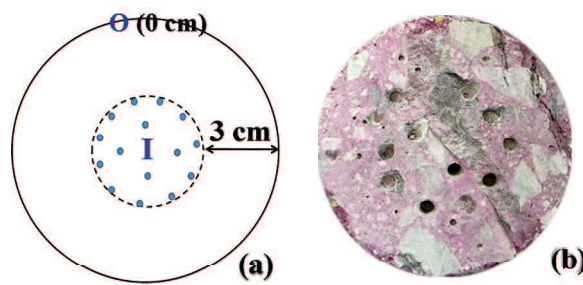


Fig. 4.1 pH measurement positions for GP concrete
 ((a) diagrammatic sketch, and (b) photograph of specimen's section)

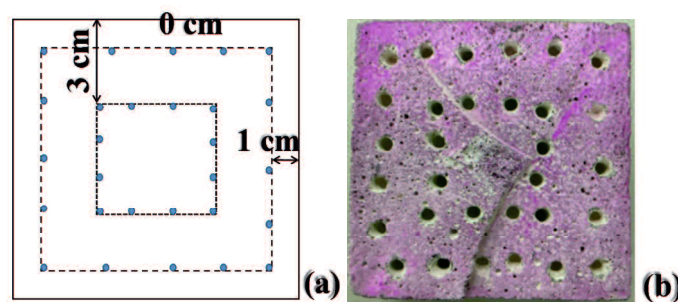


Fig. 4.2 Three pH measurement positions for mortar
 ((a) diagrammatic sketch, and (b) photograph of specimen's section)

The drilled powder samples, were firstly sieved with a sieve of 150 μ m opening, then dissolved in the ion water with pH of 7.7. Finally, a pH meter with 0.1 of precision was used to measure pH of the solutions dissolved the powder samples. The effects of concentration of powder-ion water solution and the dissolving time of the powder sample on the test result of pH value were investigated as shown in Figs. 4.3 and 4.4.

For avoiding the influence of coarse aggregate, the powder samples of the mortar specimens were used in the investigation.

From Fig. 4.3(a), it is found that the pH value of GPM, dissolving in the ion water for 1 hour and 8 hours, increased with the growth of powder-ion water solution concentration. But the increase became smaller and smaller when the powder concentration is above 7%. This is consistent with the previous result using GP concrete powder [13]. Like as the pH measurement of GP concrete [15], 8% of powder concentration was selected for all the GP specimens in this study.

In case of OPC mortar, we found that the pH didn't increase when the powder concentration exceeded 6%, as shown in Fig. 4.3(b). However, in order to avoid the influence of different measurement methods, we also used 8% of solution concentration to measure the pH value of OPC mortar.

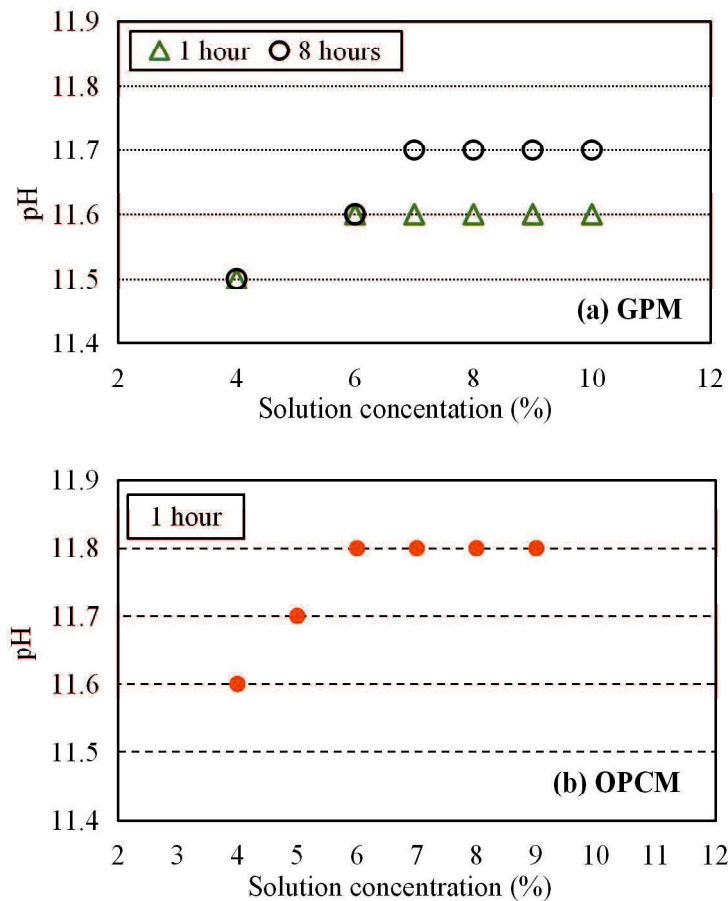


Fig. 4.3 The effect of sample concentration on the pH values of GP and OPC mortar
(Notes: The samples were drilled from the edge of GPM and OPCM specimens)

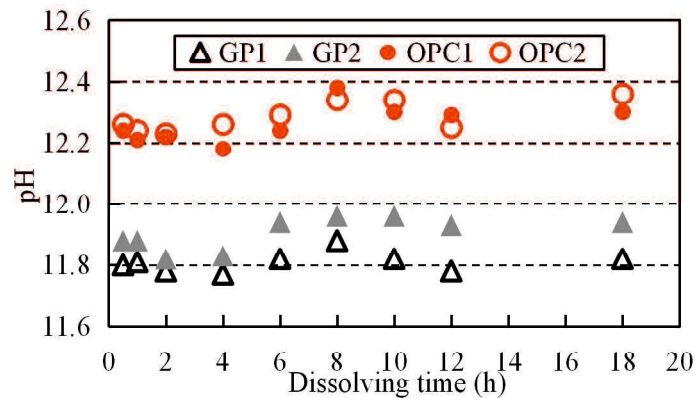


Fig. 4.4 The effect of dissolving time in water on the pH values

(Notes: The samples were drilled from 2 different positions around the position 1 cm as shown in Fig. 4.2(a))

We also investigated the effect of the powder dissolving time on the pH value of OPCM and GPM. Fig. 4.4 shows that the pH value fluctuated with the growth of dissolving time. However, the fluctuation was within ± 0.2 . It is considered that this fluctuation was nearly caused by the measuring error. Hence, in order to shorten test period and guarantee test precision, we measured the pH value 1 hour later after dissolving the powders in water.

The 28d-compressive strengths of GP concrete specimens were measured as chapter 3 introduced. What should be noted is that the samples used to measure the 28d-compressive strength of mortar specimens were prism with $4 \times 4 \times 16$ cm of size. As shown in Fig. 4.5, firstly, three prism specimens was divided into 6 after flexural strength test. Then compressive strength were obtained as a average value of 6 samples.

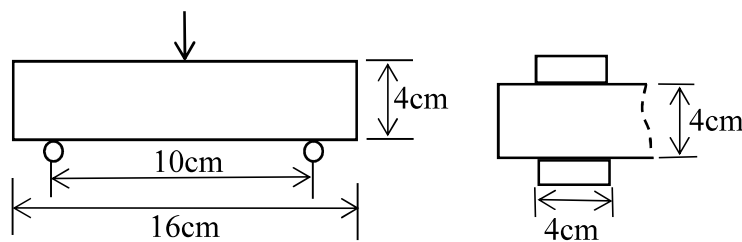


Fig. 4.5 The flexural strength test (left) and compressive strength test (right) for mortar specimens

4.3 Neutralization resistance of GP concrete

Table 4.5 Color change and neutralization depth of GP concrete specimens in three neutralization environments

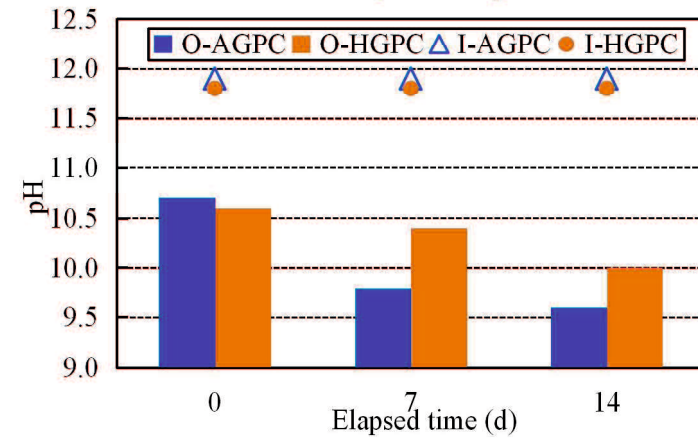
Period	AGPC			HGPC		
	e_{w+d}	e_c	e_{c+d}	e_{w+d}	e_c	e_{c+d}
Cycle 0		 $D_n=12.2\text{mm}$			 $D_n=0.0\text{mm}$	
Cycle 1		 $D_n=25.0\text{mm}$			 $D_n=9.4\text{mm}$	
Cycle 2		 $D_n=29.6\text{mm}$			 $D_n=18.0\text{mm}$	

[Notes:] D_n : neutralization depth. The neutralization depth of the specimens in the environments “ e_{w+d} ” and “ e_{c+d} ” couldn’t be measured.

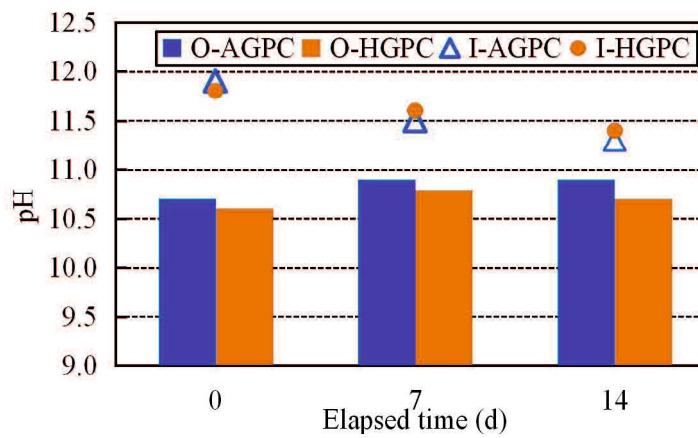
Table 4.5 presents the neutralization situation of AGPC and HGPC specimens in different environments. It was found that only the specimens in the environment “ e_c ” presented clear boundaries of pink area. The heat-cured GP concrete (HGPC) had a higher carbonation resistance than the ambient-cured GP concrete (AGPC). Before the accelerated carbonation test, the neutralization depth of the AGPC specimen had already reached to about 12 mm, the HGPC specimen was however zero. With the increase of carbonation time, the neutralization depth of the AGPC specimen increased faster than HGPC. Under the conditions “ e_{c+d} ” and “ e_{w+d} ”, the pink areas on the cutting sections of the AGPC and HGPC specimens faded away with the increase of cycle so that we couldn’t measure their neutralization depth.

Fig. 4.6 describes the pH change with neutralization time of GP concrete specimens in the three environments. The pH of AGPC’s outside (position “O”) was 10.7 before the neutralization test. In the environment “ e_c ”, as shown in Fig. 4.6(a), the pH value in the position “O” decreased with the carbonation time, but it was stable in the inner area. The pH of AGPC after 2 weeks of the accelerated carbonation became below 9.6. Comparing the pH values of position “O” of AGPC and HGPC in the environment “ e_c ”, it was clearly found that the pH value of HGPC, cured at 60°C for 6 hours, was higher than that of AGPC at the same neutralization time. Heat curing can

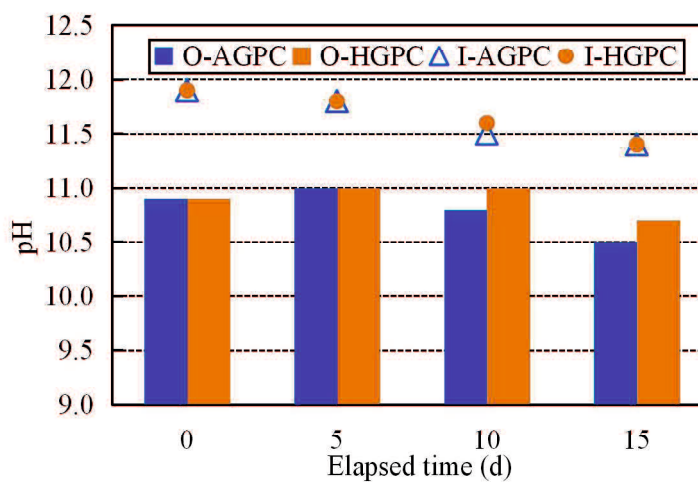
improve the compressive strength of GP concrete [12]. The higher neutralization resistance of HGPC is thus attributed to its higher compactness.



(a) "e_c" condition



(b) "e_{c+d}" condition



(c) "e_{w+d}" condition

Fig. 4.6 The pH change with the elapsed time of the GP concretes under three conditions

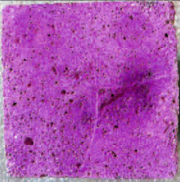
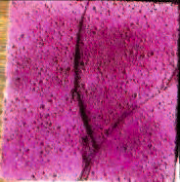
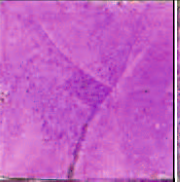
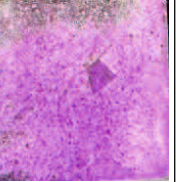
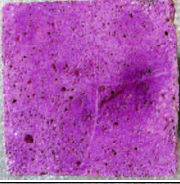
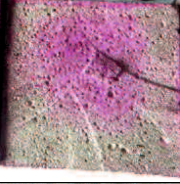
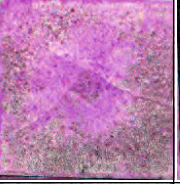
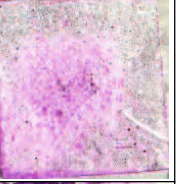
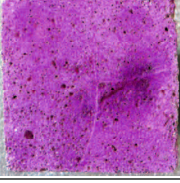
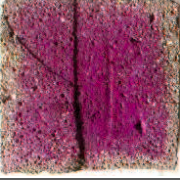
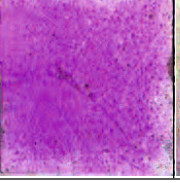
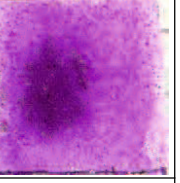
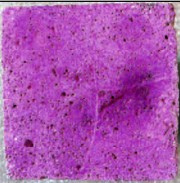
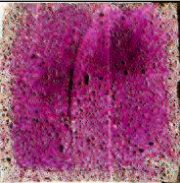
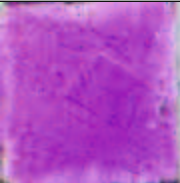
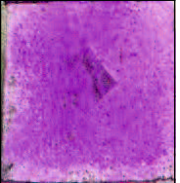



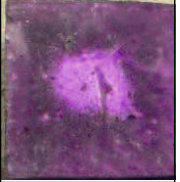
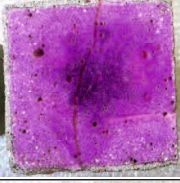
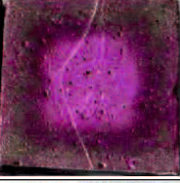
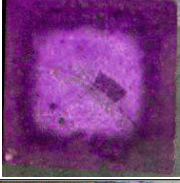
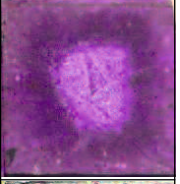
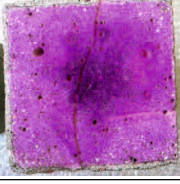
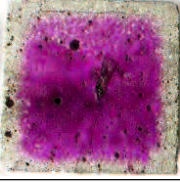
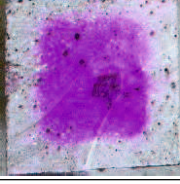
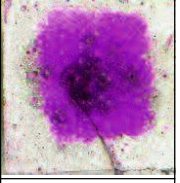
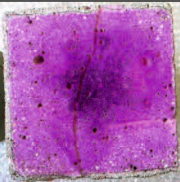
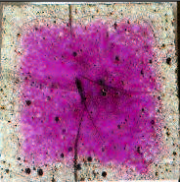

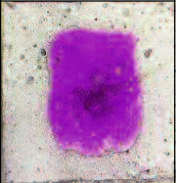
Fig. 4.6(b) shows the pH value change of GP concrete specimens in the environment “ e_{c+d} ”. The pH in the outer zones of the specimens kept around 10.9 or even increased with cycles increase. However, in the inner zones, the pH decreased greatly with the cycle. This may be explained that the alkali matters in the inner zone moved to the outer zone, even to the surface of concrete with water movement. This movement led to an indistinct boundary of color area and the neutralization of inner zone.

According to Fig. 4.6(c), in the environment “ e_{w+d} ”, the pH values in the outside zones of the GP concrete specimens were maintained as their initial values, but slight decrease occurred in their inner zones in the first cycle (5 days). With the elapsed time, the pH decreased obviously no matter in the outside zone or in the inside zone. This can explain why the pink color of the inside zone became shallow with the wet-dry repeating.

If comparing the pH of the specimens in the environment “ e_{c+d} ” and “ e_{w+d} ”, we found that the specimens had near pH values after 2 weeks. This suggests that water movement can neutralize GP concrete as well even not in CO_2 environment. This would be because that the alkali matters, which weren't consumed for in the poly-condensation reaction and existed in the pores of GP concrete, easily dissolve in the water and leach out during the wet-dry repeating.

Chapter 4 Neutralization Resistance of GP Concrete in Conditions with Water Movement

Table 4.6 Color change of mortar specimens processed in the four environments

Series	Specimen	Environment	Circle 0	Circle 1	Circle 3	Circle 5
OPC mortar	O _w	E _w				
	O _{w+d}	E _{w+d}				
	O _c	E _c				
			D _n (mm)	0	9.0	Unclear
	O _{c+d}	E _{c+d}				
			D _n (mm)	0	6.4	Unclear
GP mortar	G _w	E _w				
	G _{w+d}	E _{w+d}				
	G _c	E _c				
			D _n (mm)	3.3	10.1	17.4
	G _{c+d}	E _{c+d}				
			D _n (mm)	3.3	10.5	21.3

4.4 Neutralization resistance of GP mortar comparing with OPC mortar

Although we investigated the effect of environment condition on the neutralization of GP concrete, coarse aggregate powder may be contained in the drilled powder samples, and influence the test results. For surely clarifying the neutralization resistance of GP, we further investigated the neutralization depth and pH value of GP mortar processed in the four kinds of environments shown in Table 4.4, and made a comparison with OPC mortar.

Table 4.6 shows the color changes on the cutting section of GPM and OPCM specimens with the increase of cycle. It was found that, after cured for 28 days in the ambient air, the GP mortar specimens had been already neutralized to about 3.25 mm depth. But, for the OPC mortar specimens, the whole cutting sections presented pink color, the neutralization depth was almost zero. The GP mortar specimens in the environments “E_w” and “E_{w+d}” didn’t show a clear boundary to distinguish the neutralized and non-neutralized regions. In contrast, in the environments “E_c” and “E_{c+d}”, the GP and OPC mortars had clear pink color boundary, the neutralization depths were measured and shown in Table 4.6. However, as the increase of carbonation period, the pink color boundary of OPC mortar became difficult to find. we noted “unclear” in Table 4.6 for OPC mortar specimens under the conditions “E_c” and “E_{c+d}” after 3 cycles. Even so, it is not doubted that the neutralization of GP mortar is faster than OPC mortar in the environments “E_c” and “E_{c+d}”.

For the GP mortar specimens processed in environments “E_w” and “E_{w+d}”, it can be found that the color in the inner zone was paler than that in the outer zone. It may be because that the inside and outside zones had different water contents. However, this phenomenon was not found in the OPC mortar specimens.

On the other hand, due to the influence of drying, the G_{c+d} specimens showed a relatively smaller pink color area than G_c. But we didn’t find this phenomenon from the O_c and O_{c+d} specimens. This means that the water movement exerted more effect on the neutralization of GPM than that of OPCM in the carbonation environment. That may be due to the carbonation products of GP more easily dissolve and leach out with water.

Figs. 4.7 and 4.8 present the change of pH with the increase of experimental period, of the four positions of the OPC and GP mortar specimens, in the four environments: “E_w”, “E_{w+d}”, “E_c”, and “E_{c+d}”. It can be found from Fig. 4.7 that the pH value of OPC mortar slightly decreased only in the edge position (0 mm) at 8 days, but this decrease didn’t almost occur at 24 days and 40 days. Also, the pH values in the 10 mm and 30 mm positions of OPCM almost didn’t change. But for the GP mortar, the decrease occurred in the 0 mm position and the inner zone. And the pH value in the 0 mm

position of GPM decreased faster than OPCM. Though the pH values in the 10 mm position of GP mortar at 40 days showed a different trend, we could still conclude that drying would promote the decrease of pH.

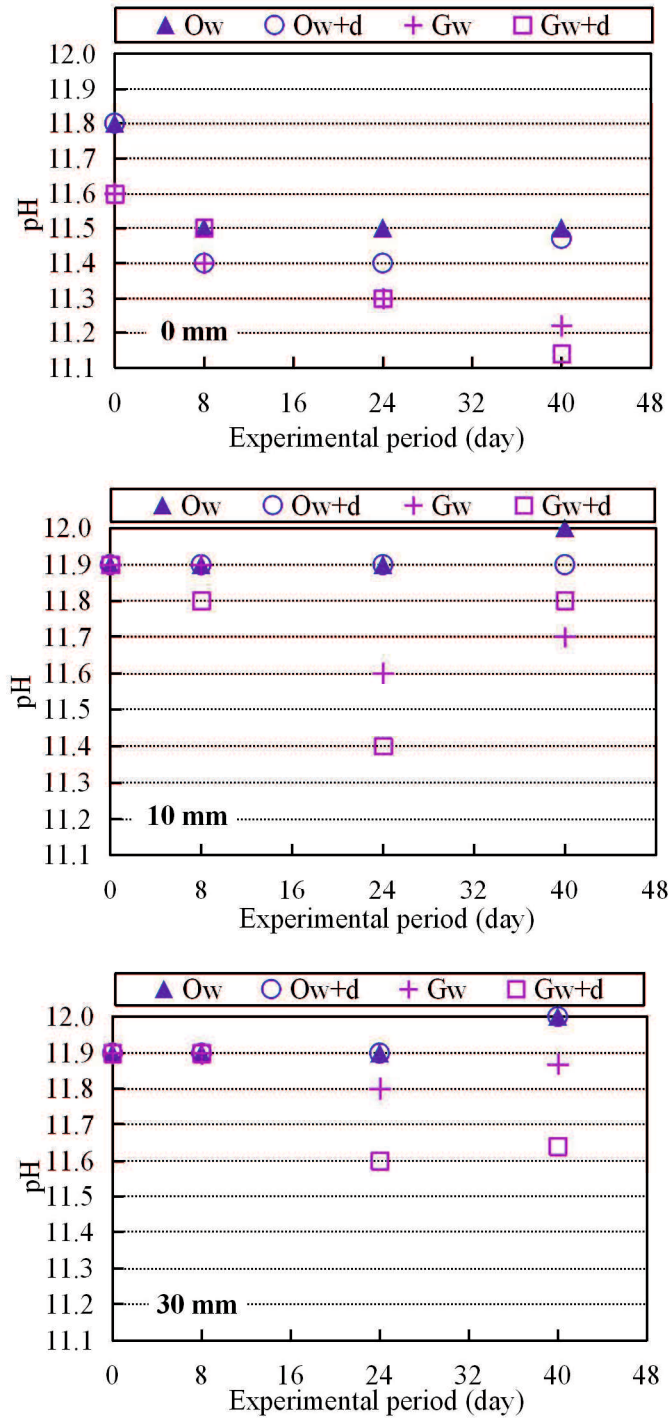


Fig. 4.7 The pH change with the elapsed time in the three positions: 0 mm, 10mm, and 30mm of OPCM and GPM in the environments “E_w” and “E_{w+d}”

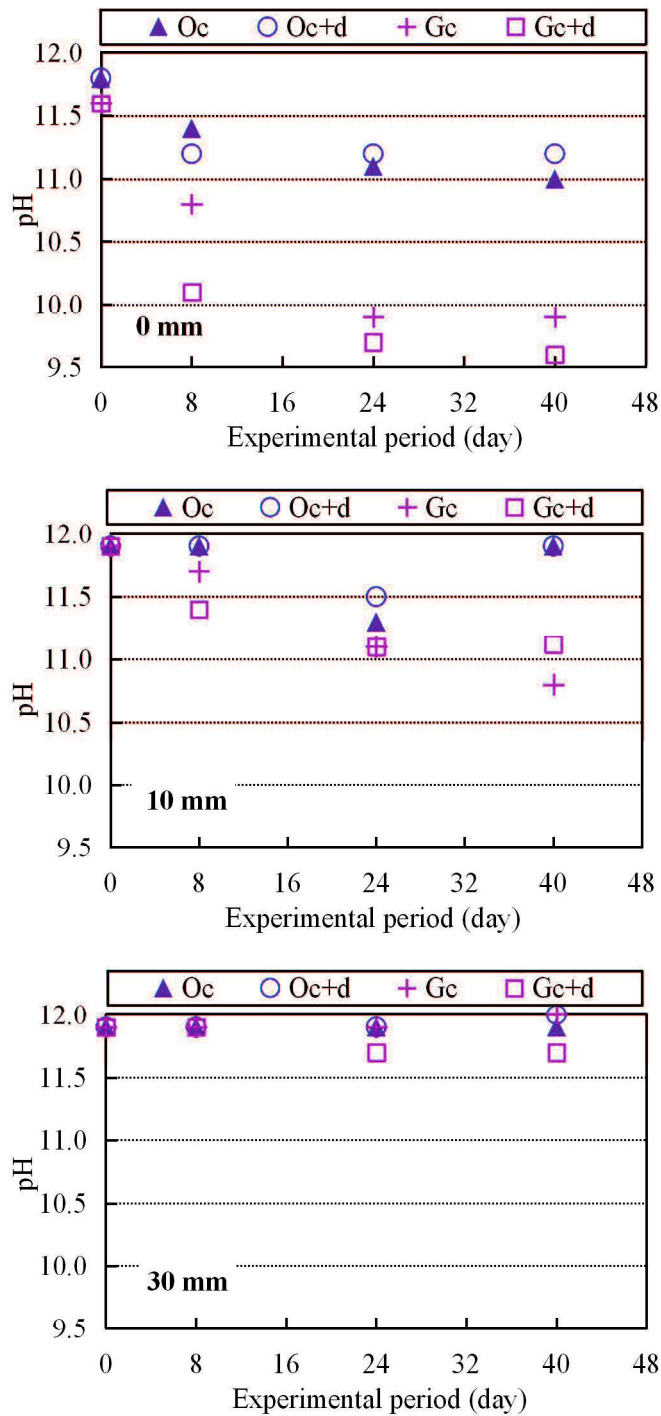


Fig. 4.8 The pH change with the elapsed time in the three positions: 0 mm, 10mm, and 30mm of OPCM and GPM in the environments “E_c” and “E_{c+d}”

From the experimental results of the 0 mm position, as shown in Fig. 4.8, it can be clearly found that the neutralization of GP mortar proceeded faster than OPC mortar, even though the 28d-compressive strength of GP mortar is 47.03 MPa, 2 times higher

than 24.76 MPa of OPC mortar. After 40 days carbonation, the pH of GP mortar decreased below 10. The pH values of the G_c specimen after carbonation, in the 10 mm position, decreased with the elapsed time, but kept constant in the 30 mm position. This is because the carbonation depth of the G_c specimen didn't yet reach to the 30 mm position. However, for the G_{c+d} specimen, even though the neutralization depth reached to 25.75 mm, the pH values in the 10 mm and 30 mm positions slightly decreased. And the decrease became very slow after 24 days. The decrease of the pH in the 30 mm position is because that the drying drove some alkali matters to move from the inner zone. In summery, the GP mortar under the condition " E_{c+d} " showed a lower neutralization resistance, compared to the condition " E_c ". The pH decrease in the position 10 mm of the O_c and O_{c+d} , specimens at 24 days can't be explained now. It might be test error.

4.5 Conclusions

The study in this chapter aims to clarify the neutralization resistance of GP concrete in different environments and the property change after neutralization. We investigated the pH values and neutralization depths of GP concrete and mortar after processed in water (“E_w”), wet-dry repeating (“E_{w+d}”, or “e_{w+d}”), carbonation (5% or 10% concentration of CO₂) (“E_c”, or “e_c”), and carbonation-dry repeating environment (“E_{c+d}”, or “e_{c+d}”), respectively. Compared with the experimental neutralization results of OPC mortar, we conclude this chapter as follows.

(1) The adopted pH measurement of FA&BFS-based GP concrete was investigated by experiment. It is found that measuring the pH value 1 hour later after dissolving the powders in water, with 8% of sample-water solution concentration, was suitable.

(2) In the environments “e_c”, “e_{c+d}”, “e_{w+d}”, the neutralization resistance of FA&BFS-based GP concrete, which has history of heat curing, is higher than that cured only in the ambient air. The pH value in the outer zone of GP concrete or mortar in the environment “e_{w+d}” after two cycles of wet-dry repeating was lower, compared to two cycles of carbonation-dry repeating. This indicates that GP concrete can also be neutralized by water movement except carbonation.

(3) Even though the 28 days-compressive strength of GP mortar in this study was higher than that of OPC mortar, the GP mortar had about 2 times neutralization depth of the OPC mortar, and the pH in the outer position of the G_{c+d} specimen decreased greatly even below 10.0 in the same environment conditions “E_c” and “E_{c+d}”. In the environment of carbonation-dry repeating, the neutralization of GP mortar was quite faster than in the environment of only carbonation. The pH change of GP mortar in the environments “E_w” and “E_{w+d}” also indicates that water movement would result in the neutralization of GP solid.

References

- [1] C. Meyer, The greening of the concrete industry, *Cement and Concrete Composites*. 31 (8) (2009) 601-605.
- [2] B. V. Rangan, Geopolymer concrete for environmental protection, *The Indian Concrete Journal*. 88(4) (2014) 41-59.
- [3] Z. Li, Z. Ding, Y. Zhang, Development of sustainable cementitious materials. *International Workshop on Sustainable Development and Concrete Technology*. (2004) 55-76.
- [4] J. Davidovits, Geopolymers of the first generation: siliface-process, *Geopolymer'88: First European Conference on Soft Mineralogy, Compiègne, France*. 2 (1988) 49-67.
- [5] D. A Crozier, J. G. Sanjayan, Chemical and physical degradation of concrete at elevated temperatures, *Concrete in Australia*. 25(1) (1999) 18-20.
- [6] S. Thokchom, P. Ghosh, S. Ghosh, Performance of fly ash based geopolymer mortars in sulphate solution, *Journal Engineering Technology Review*. 3(1) (2010) 36-40.
- [7] P. Duxson, J. L. Provis, G. C. Lukey, J. S. J. van Deventer, The role of inorganic polymer technology in the development of green concrete, *Cement and Concrete Research*. 37(12) (2007) 1590-1597.
- [8] A. A. Adam, Strength and durability properties of alkali activated slag and fly ash-Based geopolymer concrete, *RMIT University Melbourne, Australia*. (2009) 79-89.
- [9] B. M. Suffian et al., Corrosion of steel bars induced by accelerated carbonation in low and high calcium fly ash geopolymer concretes, *Construction and Building Materials*. 61 (2014) 79-89.
- [10] S. A. Bernal, J. L. Provis, B. Walkley, R. San Nicolas, J. D. Gehman, D. G. Brice et al., Gel nanostructure in alkali-activated binders based on slag and fly ash, and effects of accelerated carbonation, *Cement and Concrete Research*. 53 (2013) 127-144.
- [11] Z. Li, S. Li, Carbonation resistance of fly ash and blast furnace slag based geopolymer concrete, *Construction and Building Materials*. 163 (2018) 668-680.
- [12] T. Nagai, Z. Li, H. Takagaito, A. Suga, Experimental study on the mechanical properties of geopolymer concrete using fly ash and ground granulated blast furnace slag, *Proceedings of the Japan Concrete Institute*. 39 (1) (2017) 2077 - 2082.

5 The Post-Neutralization Properties of FA&BFS-based GP Concrete

5.1 Introduction

The carbonation lowers the alkalinity of OPC concrete, but improves the compactness of concrete and in turn increases its strength [1][2]. The recognized explanation is that the carbonation reaction consumes and decreases the alkalinity of pore solution, but at the same time produces calcium carbonate that can fill some cracks, pore volumes and decrease the permeability of OPC concrete. That can be verified from the research of Claisse et al. [3], who investigated the effect of carbonation on pore and permeability of OPC mortar with different water/cement ratio and curing condition, and reported that carbonation greatly reduces the permeability and porosity, especially for the poor quality concrete.

However, for GP concrete, the carbonation effect on mechanical properties up to now is seldom studied. There are few researchers stated that the compressive strength of GP concrete after carbonation decreased. Song et al [4], who reported that the AAS based specimens lose more compressive strength as carbonation period expanding. But the experimental study of Hedge et al. [5], about accelerated carbonation effects on lightly reinforced FA and 50% BFS blended GP concrete slabs, inversely found a increasing flexure strength during increasing the carbonation period.

Moreover, it have been proven that water curing will improve the pore structure and reduce porosity resulting from greater degree of cement hydration and pozzolanic reaction without any loss of moisture from the concrete cubes [6]. But, for the alkali activated GP concrete, water curing is reported leading to a compressive strength decrease [7]. The reason was guessed due to the high alkalinity and easy dissolution in water of alkali activators. Water can dissolve and decrease the alkalinity in GP concrete and lower GP's degree of polymerization, then reduce the compressive strength of GP concrete.

Additionally, carbonation is not the only way, during “real life” service, that can decrease the alkali of concrete. The variations in temperature, humidity, wet-dry cycling, and other conditions may also neutralize the alkali in concrete [8]. Considering these above, it becomes necessary to assess the effect of water dissolving and wet-dry cycling etc. on compressive strength of GP concrete.

Hence, in this study, we firstly investigated the compressive strength change of FA&BFS-based GP concrete and mortar specimens with different mixtures affected by carbonation (The mixture proportions of these specimens were shown in the chapter 3).

Then SEM and EDS test was used to further understand their changes in the ingredient and micro-structure of GP mortar. Besides, following the neutralization resistance research of FA&BFS-based GP mortar as described in chapter 4, the compressive strength, micro-structure and ingredient changes of GP and OPC mortar under water immersion, wet-dry repeating etc. four kinds of neutralization environments were also compared and analyzed.

5.2 Experimental program

For investigating the effect of carbonation, the changes in compressive strength and micro-structure of GP concrete series 2B, 6B, 8B, 9B and GP mortar series 1, 3, 4, 8. (had been used in chapter 3), with and without carbonation, were also discussed in this experiment. Except these specimens mentioned above, GP concrete marked as series 14B was added with mixture proportion as shown in table 5.1. Meanwhile, the compressive strength and micro-structure changes of FA&BFS-based GP mortar and OPC mortar in four neutralization conditions were also compared and discussed, after assessing their neutralization resistance in chapter 4.

Table 5.1 Mix proportions of FA&BFS-based GP concrete (C)

Series No.	AS(kg/m ³)	AS/AF	BFS sort	BFS/AF	R/AF (%)	RS (kg/m ³)	G (kg/m ³)
14B	AS ₂ =200	0.5	40P	0	0	723	1000

The compressive strengths of OPCM and GPM specimens were measured at 28 days and around 68 days ages, also after neutralization in the four kinds of environments. However, for GP concrete, 28 days and 84 days ages' compressive strength and compressive strength after 56 days carbonation were measured. All of the compressive strength are average values of three specimens.

Scanning electron microscopy (SEM) equipped with an Energy Dispersive Spectroscopy (EDS) analyzer (providing the elements and oxide analysis of samples) was used to investigate the micro-structure of GPM and OPCM specimens before and after neutralization under four kinds of environmental conditions. Samples were used with a smooth observation surface and a height lower than 3 mm.

What should be noted is that we observed the same positions on the OPCM and GPM specimens before and after neutralization.

5.3 The post-carbonation properties

5.3.1 The compressive strength of specimens with and without carbonation

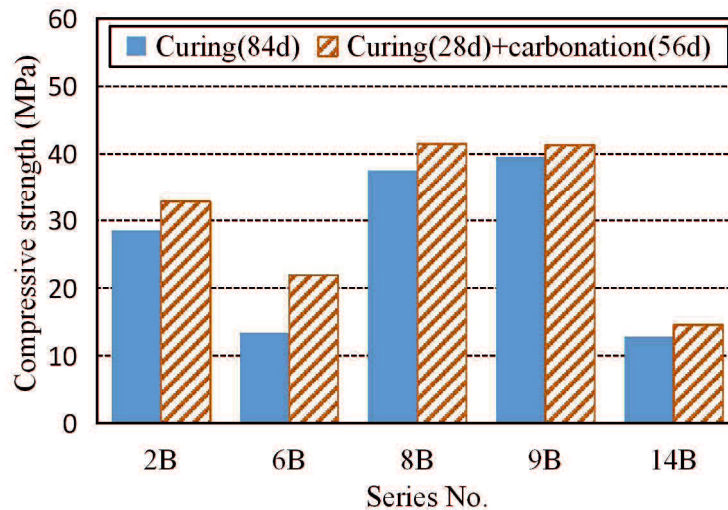


Fig. 5.1 The compressive strength of GP concrete with and without 56 days carbonation

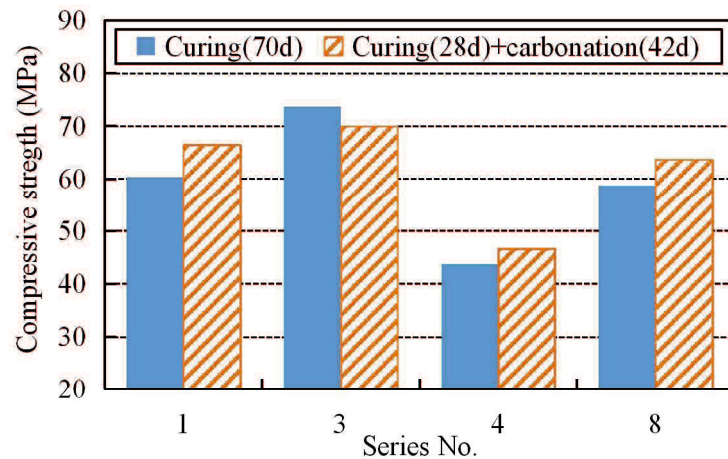


Fig. 5.2 The compressive strength of GP mortar with and without 42 days carbonation

Figs. 5.1 and 5.2 introduce the compressive strength of the GP concrete and GP mortar with and without carbonation. Generally speaking, the compressive strength of FA&BFS-based GP concretes and GP mortars with different mixture after carbonation increased to different extent, except the series No.3 that was cured at a high temperature. That the compressive strength of FA&BFS-based GP concrete after carbonation increased shows different with the conclusion regarding to alkali activated slags (AAS)

made by Song et al [4]. Who concluded that AAS based specimens were with a more loss of compressive strength as carbonation period expanding. From this to say, FA&BFS-based GP concrete may present more advantages than AAS and FA-based GP concrete.

The influencing factors in this study mainly considered BFS/AF ratio, AS sort and curing temperature, that have been thought as the great influencing factors to carbonation resistance of GP based materials.

Firstly, considering the effect of AS sort, from the compressive strength change of Series No.1 and No.4 of GP mortar and Samples 2B, 6B and 8B of GP concrete, it can be found that the compressive strength of specimens, activated by AS with more NH, is higher than that of specimens with lesser NH. This is not contradictory to the carbonation front result, mentioned in chapter 3, which stated that the more NH in the AS solution the better carbonation resistance of GP concrete. However, after carbonation, the increase of compressive strength of the GP concrete with less NH is higher than the one activated by AS with more NH. This may be because that the higher NH/AS ratio in GP concrete, the less carbonation depth, and lead to a small compressive strength increase.

Secondly, the influencing factor of BFS content were considered based on the compressive strength results of Series 2B, 9B and 14B, with BFS/AF ratio of 0.3, 0.5 and 0, respectively. As shown in Fig. 5.1, it can be found the more BFS in the AF, the higher compressive strength of GP concrete. After carbonation, the compressive strength of specimens using AF blended with BFS increased to different extent according the BFS/AF ratio. The increase of compressive strength of GP concrete with BFS/AF ratio of 0.3 showed higher than that of GP concrete with BFS/AF ratio of 0.5. The reason may due to the more dense structure of specimens blended with 50% BFS than that only mixed with 30% BFS. The FA-based GP concrete after carbonation showed a more slight compressive increase than GP concrete blended 30% BFS. That may due to the heat curing of FA-based GP concrete.

Meanwhile, the specimens curing at high temperature have a higher compressive strength than ambient-cured GP specimens no matter before or after carbonation. However, the compressive strength of heat-cured GP mortar after 6 weeks became lower than that of specimens without carbonation. That can be explained by the SEM analysis shown in the Section 5.3.2. This results is agree with the conclusion of Criado et al.[9], who reported that the mechanical strength become lower after carbonation than that of non-carbonated binders cured at 80 °C.

BFS fineness of 3000 and 4000 cm²/g didn't show great effect on the carbonation resistance of GP concrete as described in chapter 3. Hence, it can be easily understood that the increase of compressive strength of the two kinds of GP mortar were closed

after carbonation.

5. 3. 2 The micro-structure of specimens before and after carbonation

The SEM and EDS test were conducted to investigate the changes of micro-structure and products of FA&BFS-based GP specimens before and after carbonation. The microscope images of Series No.1, No.3, No.4 and No.8 carbonated and non-carbonated were shown in Table 5.2. What should be noted is that, in order to observe the micro-structure changes more easily and more correctly, the observing positions of GP pastes after carbonation were tried to keep the same as before carbonation.

Table 5.2 The SEM images of 4 kinds of GP mortars before and after carbonation

Series No.	1	3	4	8
Non-carbonated				
Carbonated				

As the Table 5.2 shows, after 6 weeks carbonation, there appeared many small substances in the Series No.1, and the cracks become minute and less. It was guessed that the cracks might be filled by the new carbonation products. This phenomenon was also surveyed in the No.8. But for No.3, cured at a high temperature, carbonation didn't result in any new substances. On the contrary, the cracks of specimens Series No.3 after carbonation seem to become much longer and wider. Considering that, the compressive strength decrease of GP concrete with heat curing, after carbonation, can be easily understood. For Series No.4, activated only using the WG solution, there are also some substances appeared on the surface of specimens. However, this substance was considered different to the diamond structure of No.1, based on not only their shape, but also for the products of Series No. 4 didn't change any cracks of the GP mortar after carbonation. That can explain why Series No.1, using blended WG and NH as alkali activator, presented a better carbonation resistance than Series No.4 activated only by WG solution.

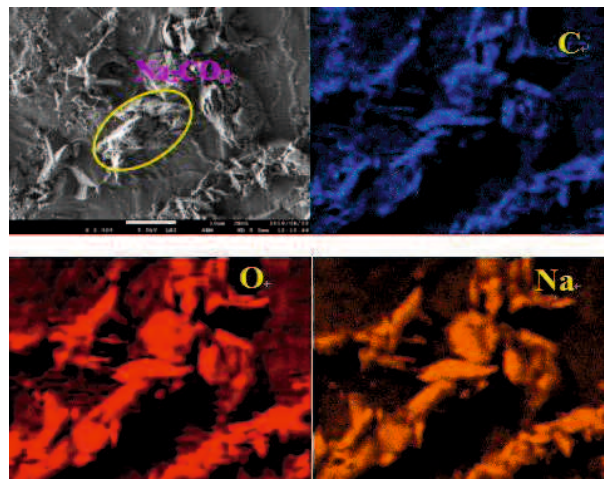


Fig. 5.3 The EDS mapping of GP concrete Series 11A carbonated 2 weeks

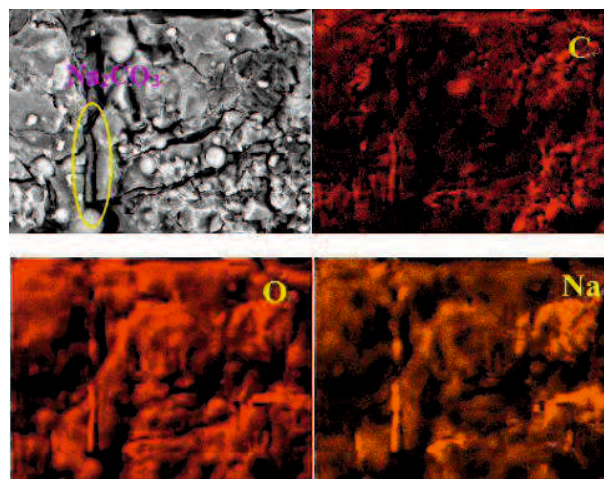


Fig. 5.4 The EDS mapping of GP concrete Series 11A carbonated 6 weeks



Fig. 5.5 Micro-structure of Na_2CO_3

Further, the carbonation products occurred in Series No. 1 and 8 were also observed in the Series No.11A as shown in the Figs. 5.3 and 5.4. From the EDS result, the diamond material may be defined as Na_2CO_3 , as mainly consist of element C, O and Na. It is guessed that the CO_2 moves along the crack and reacts with the alkali solution in crack into some kind of oxycarbide. In fact, this production is closely like as the micro-structure of Na_2CO_3 shown in Fig. 5.5. Also, Criado et al. [10], in assessing the effect of different curing conditions on alkali-activated fly ash, identified the carbonation of sodium containing crystalline products in pore solution during open curing. Because of the product, the cracks of GP mortar after carbonation become narrow and short.

5.4 The post-neutralization properties

Continuing to the chapter 4 about the neutralization resistance of FA&BFS-based GP mortar under 4 kinds of neutralization environments, we also investigated the effects of neutralization conditions on the compressive strength, micro-structure and ingredients of FA&BFS-based GP mortar by experiment.

5.4.1 The compressive strength of specimens neutralized and non-neutralized

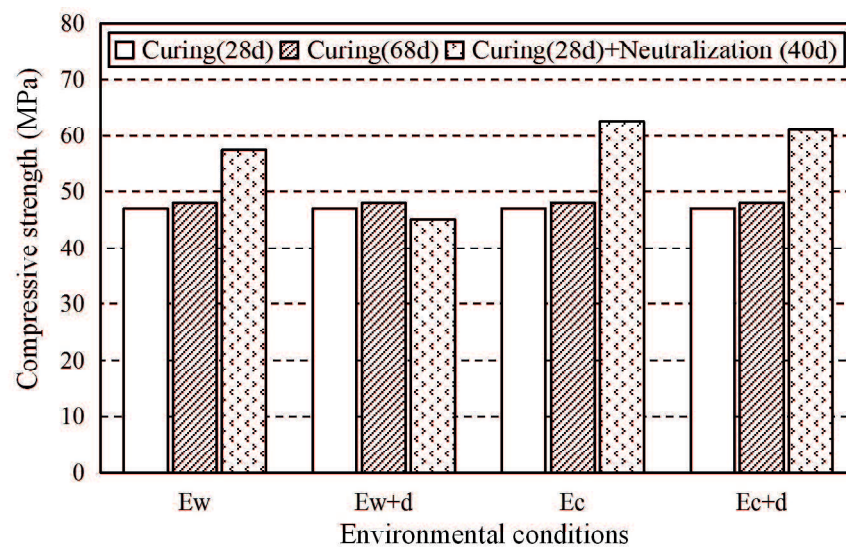


Fig. 5.6 The compressive strengths of specimens at the age of 28days, 68days, and after neutralizing in the four environments

Fig. 5.6 shows the compressive strengths of mortar specimens before and after neutralization in four kinds of environments. It was found that the compressive strength of GP mortar at the age of 68 days was larger than at 28 days age. But the compressive strength of OPC mortar didn't almost increase after 28 days.

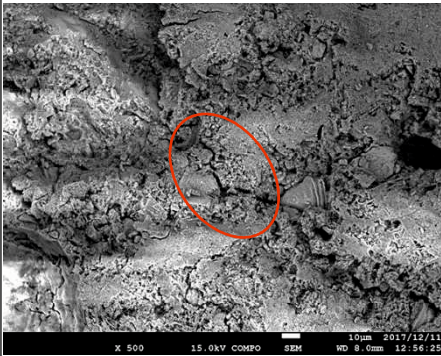
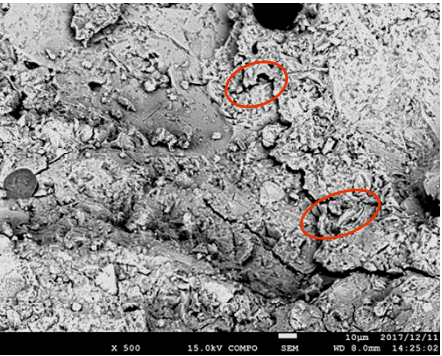
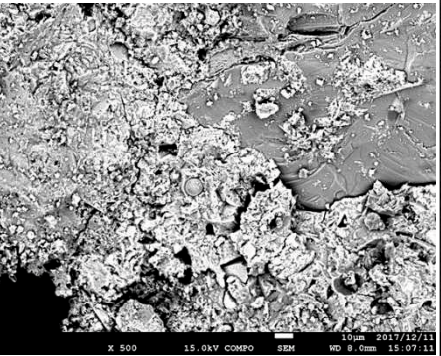
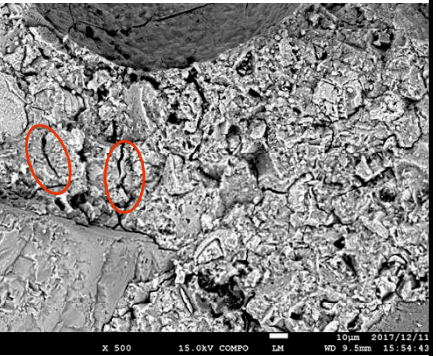
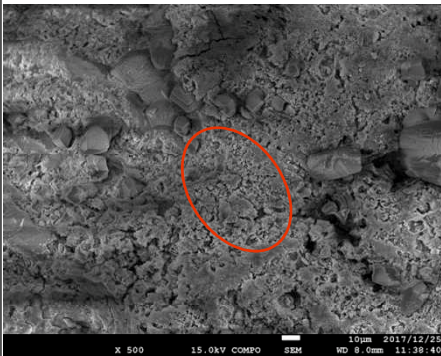
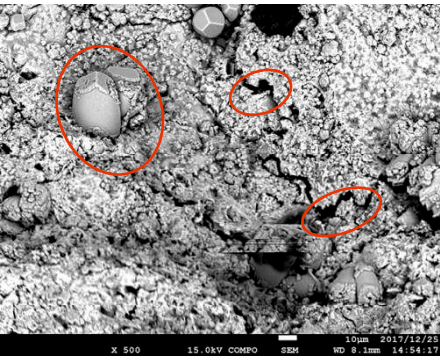
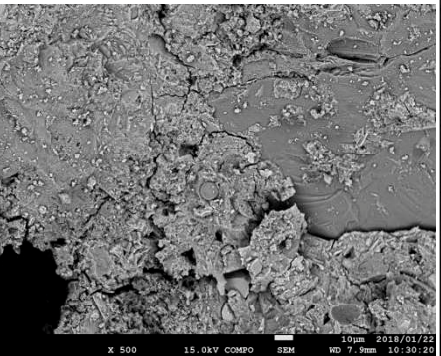
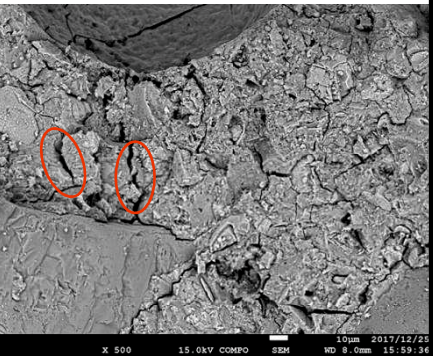
After neutralization, except the environment "E_{w+d}", the compressive strengths of no matter GP mortar or OPC mortar increased, especially in the environmental conditions "E_{c+d}", and "E_c". The increase of OPC mortar's compressive strength was higher than that of GP mortar in the environments "E_c" and "E_{c+d}". And due to drying process, the increase of compressive strength of the mortar in the environment "E_{c+d}" was less than that that caused by only the carbonation in the environment "E_c".

The compressive strength of GPM (G_w in Fig. 5.6) increased after immersed into the water for 40 days from 28 days age, compared to the compressive strength at the age

of 28 days. This result is inconsistent with the general knowledge that water curing harms the strength growth of GP concrete. However, the water immersion in this study was begun after 28 days ambient curing rather than right after demoulding. The GPM already gained an ability to keep the alkali matters into it, and the polymerization reaction would last in the moisture environment to increase the compactness and compressive strength. That is to say, though the water immersion and the carbonation reduce the alkalinity of GP, its compressive strength would increase after the neutralization.

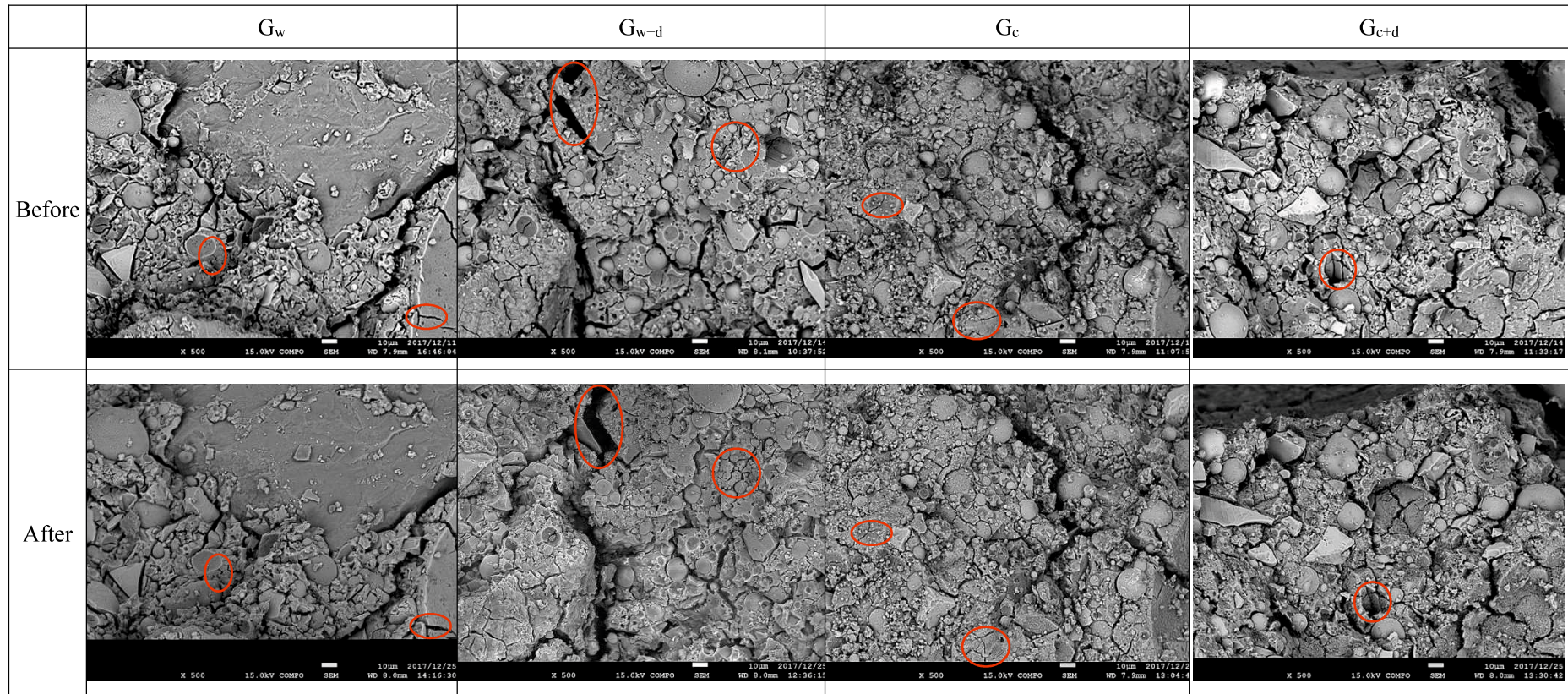
However, the compressive strength of GP mortar after the neutralization in the environment “ E_{w+d} ” decreased, compared to before the neutralization. It can be concluded that the decrease of compressive strength due to drying was higher than the increase of compressive strength caused by the water immersion.

Table 5.3 The SEM images ($\times 500$) of GPM and OPCM before and after neutralization in the 4 kinds of environments

	O_w	O_{w+d}	O_c	O_{c+d}
Before				
After				

Notes: The length of scale is 10 μm

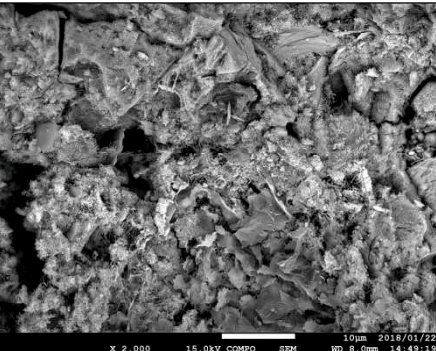
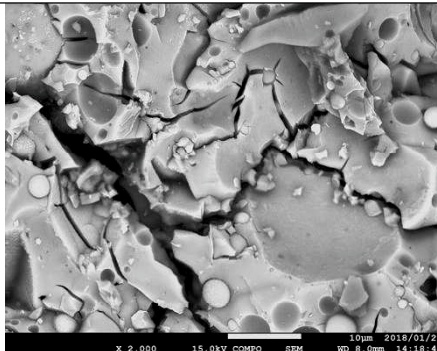
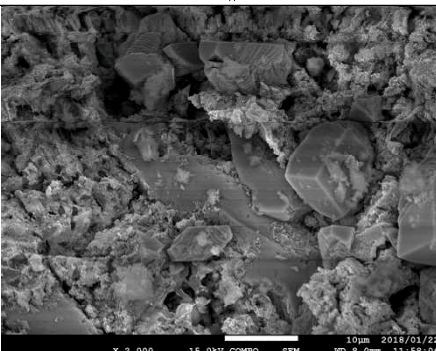
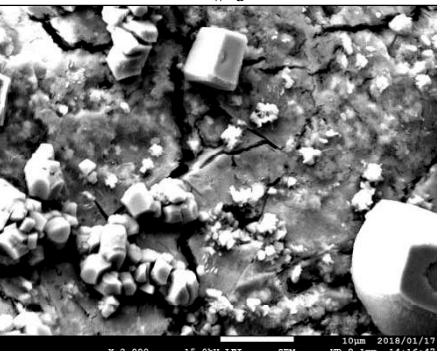
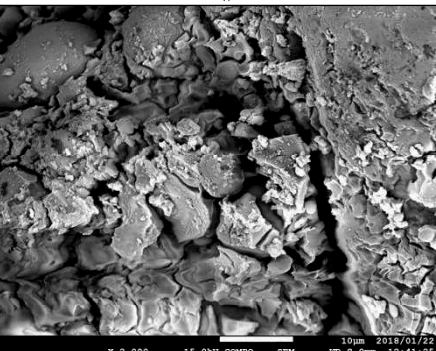
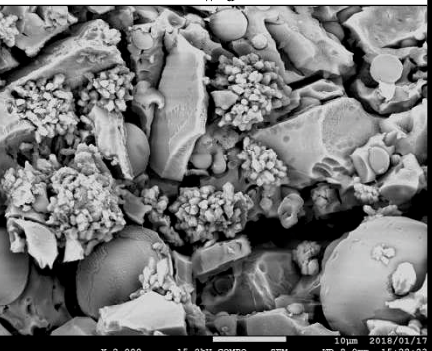
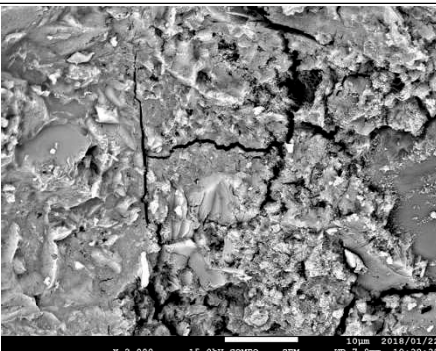

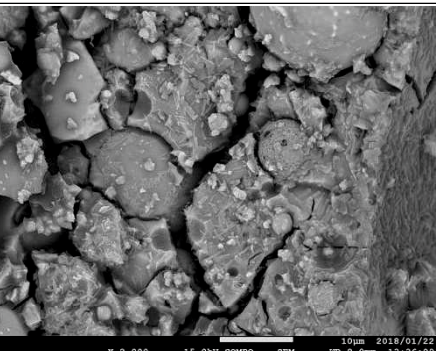
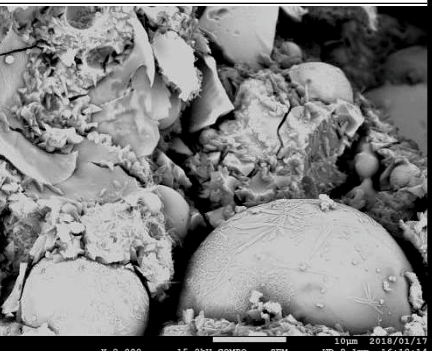
Table 5.3 The SEM images ($\times 500$) of GPM and OPCM before and after neutralization in the 4 kinds of environments (continued)



Notes: The length of scalar in each SEM image is 10 μm

Chapter 5 The Post-Neutralization property of FA&BFS-based GP Concrete

Table 5.4 The SEM images ($\times 2000$) of GPM and OPCM before and after neutralization in the 4 kinds of environments

	OPCM		GPM	
Before				
After	O_w 	O_{w+d} 	G_w 	G_{w+d} 
	O_c 	O_{c+d} 	G_c 	G_{c+d} 

Notes: The length of scale is 10 μm

5. 4. 2 *The changes in micro-structure after neutralization*

For further making the effect of neutralization on GP clear, we examined the changes in internal crack and compositions of GP mortar before and after the neutralization process of 2 cycles, based on the SEM-EDS analysis. Table 5.3 shows the SEM images of GPM and OPCM before and after neutralization in the four environments. It was found that the cracks in the OPC mortar neutralized in the environment “E_w” (the O_w specimen) became fewer and narrower, compared to before the neutralization. But for the OPC mortar (the O_{w+d} specimen) that was suffered the wet-dry repeating, some cracks, e.g. those in the red ellipses, were widened after neutralizing. On the other hand, for the GP mortar, the cracks of GPM became more and wider under the conditions “E_w” and “E_{w+d}”, especially the condition “E_{w+d}”. This result helps us to understand why the neutralized G_{w+d} specimen had a lower compressive strength than the specimen having the same age but not suffered the wet-dry repeating.

In the environment “E_c”, we couldn’t find clear crack change in OPC mortar after carbonation. But we observed some cracks became slightly wide in the OPC mortar specimens (O_{c+d}) after neutralization in the environment “E_{c+d}”. In the case of GPM, it can be found that some cracks shown in the red circles in Table 5.3 (continued) were slightly extended after neutralization in the environment “E_c”. Also, there were more exudates on the surface of the G_{c+d} specimen than the G_c specimen after neutralization, and these substances filled many surface cracks. This is caused by the drying, some alkali matters moved out to the surface of the G_{c+d} specimen along with the water movement. However, if based on the test results of pH and neutralization depth stated above, it can be understand that even though drying caused the exudates to fill surface cracks, the G_{c+d} specimen still showed a lower neutralization resistance than the G_c specimen. This is obviously because the loss of alkali matters reduced the alkalinity and the porousness of GP mortar.

Further, we compared the micro-structures and compositions of OPCM and GPM processed in the 4 environments, on basis of the SEM images shown in Table 5.4 and the EDS analysis results. After neutralization in the environment “E_w”, there were regular crystals in the O_w sample, and the crystals were thought to be calcite according to the EDS mapping shown in Fig. 5.7 and the crystal shape. This kind of crystal was also found in the O_{w+d} sample, which was smaller than that in the O_w sample. The shape and size of the crystal appeared in the O_w and O_{w+d} samples can be clearly seen from Fig. 5.8.

On the other hand, for the GP mortar neutralized in the environment “E_w”, few products were generated in the G_w sample, and they were in fragments. For the G_{w+d} sample neutralized in the environment “E_{w+d}”, the product appeared in clusters look like

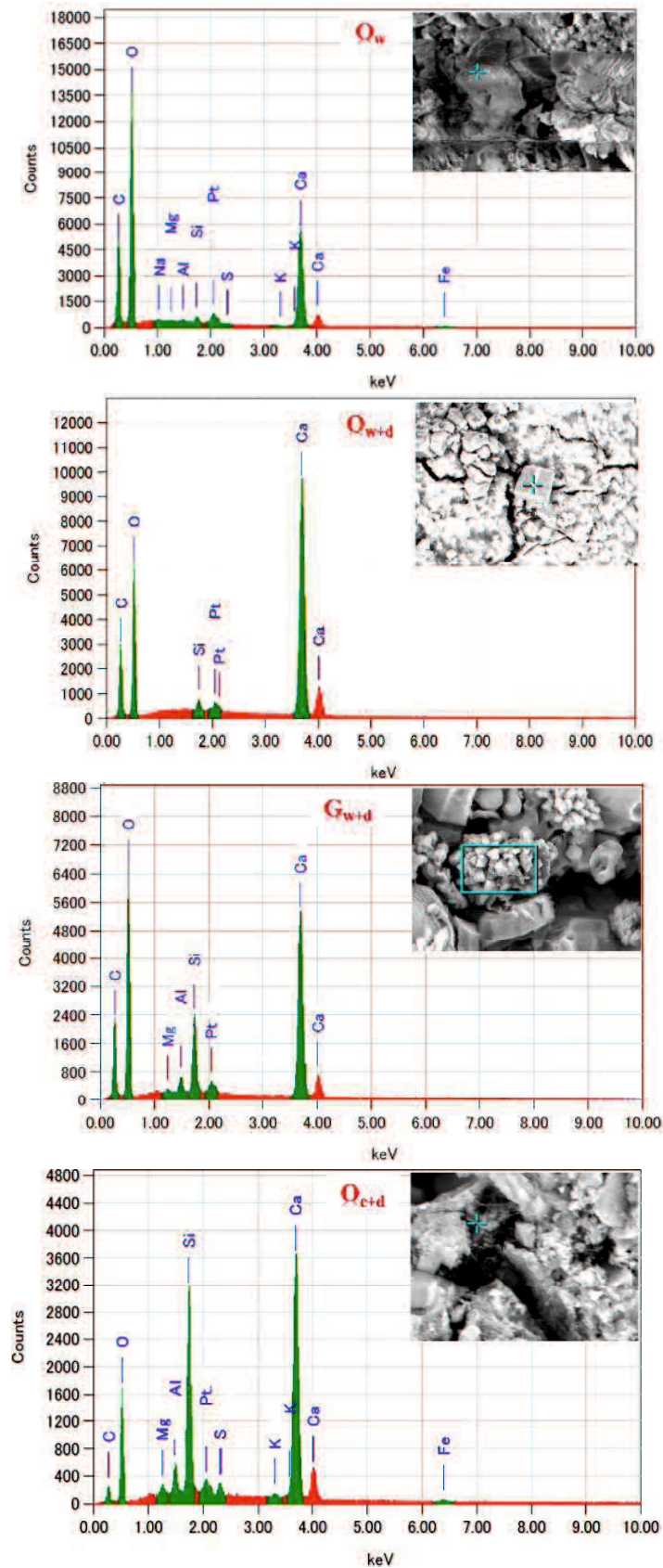


Fig. 5.7 The element distribution of the crystals in the O_w , O_{w+d} , G_{w+d} and O_{c+d} samples

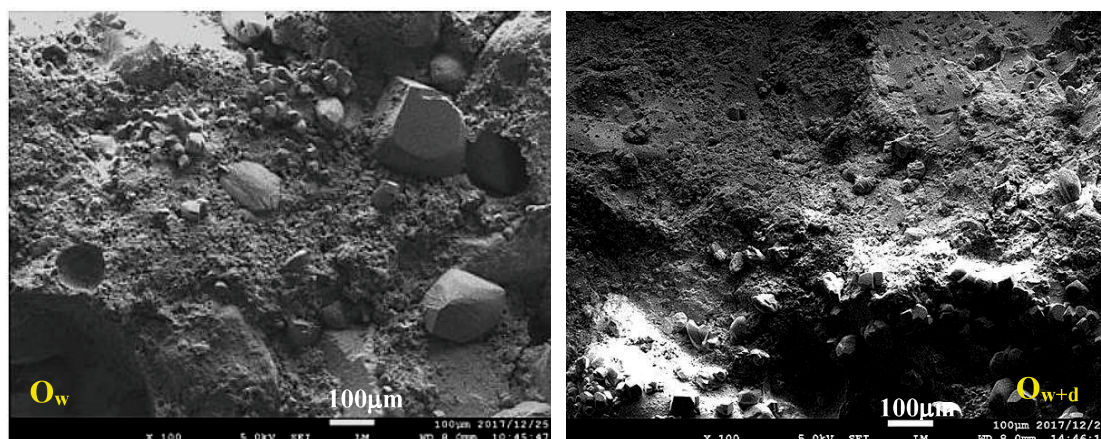


Fig. 5.8 The SEM images ($\times 100$) of O_w and O_{w+d}

flower in bloom, ranging in the G_{w+d} sample (see Fig. 5.7 G_{w+d}). According to the EDS results given in Fig. 5.7, this product is mainly composed of C, O, Si, Al, and Ca elements. That the GPM specimen was carbonated during the air curing is considered as one reason of the existence of C element. The similar phenomenon was found by P. He who investigated the effect of water curing on the micro-structure of CO_2 -cured concrete [11]. Another finding is that the Na^+ content in the GPM decreased greatly to be rough zero after neutralizing in the environment “ E_w ” and “ E_{w+d} ”.

After 2 cycles process in the environment “ E_c ”, we found needle-shaped and white block-shaped substances in the G_c samples. The EDS mapping of main elements in these substances is shown in Fig. 5.9. According to the Fig. 5.9, the block-shaped substance was carbonation product of abundant C element. However, Na^+ was the most abundant element in the needle-shaped substance, instead of C element.

The G_{c+d} sample had more crystal substance on its surface, compared to the G_c sample, which contained more C element with the same distribution to Na element, as shown in Fig. 5.10. It indicates that some Na^+ included into the crystal substance were carbonated in the environment “ E_{c+d} ”. According to its shape, the crystal substance should be Na_2CO_3 . However, in the cracks of the O_{c+d} sample, we found some needle-shaped substance. It was thought as one kind of C-S-H gel [12], and the element distribution was presented in Fig. 5.7.

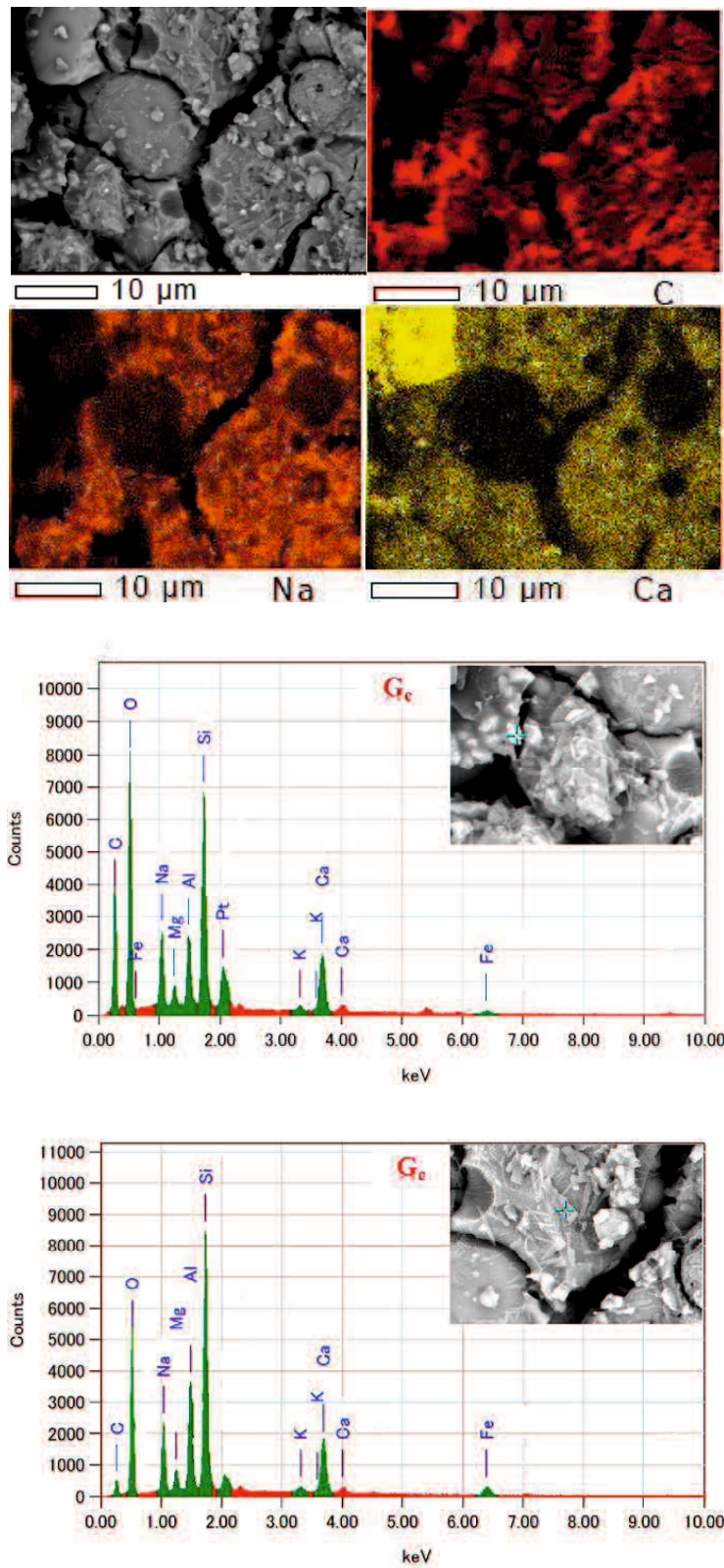


Fig. 5.9 EDS mapping of the G_c sample after carbonation

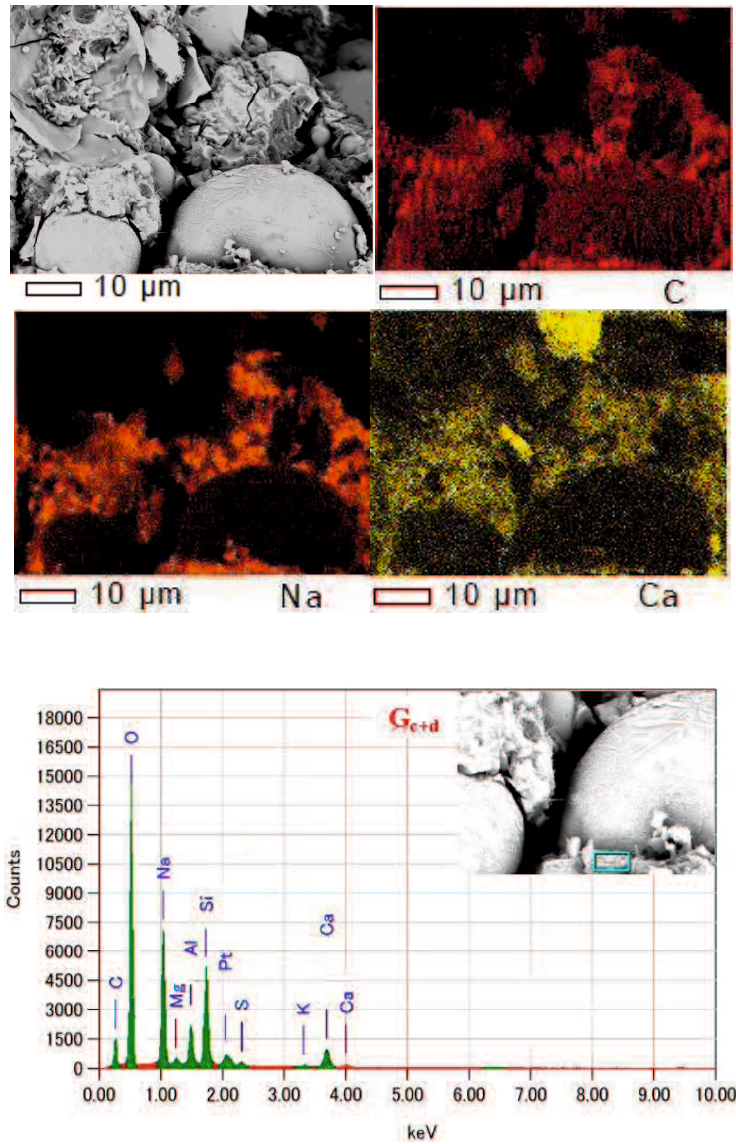


Fig. 5.10 EDS mapping of the G_{c+d} sample after carbonation-dry repeating

5.5 Conclusions

This chapter introduced the neutralization effect on the compressive strength and micro-structure of FA&BFS-based GP concrete. Firstly, the compressive strength of the GP concrete with and without carbonation were measured and compared. Then, for meeting the real condition, the compressive strength change effected by neutralization in water, wet-dry repeating, carbonation, and carbonation-dry repeating environment, respectively, were also investigated. Meanwhile, SEM and EDS were used to survey the micro-structure and ingredient changes of GP concrete after neutralization. After analyzing, we concluded all the findings below.

(1) The compressive strength of FA&BFS-based GP concretes and GP mortars with different mixture after carbonation increased to different extent, except the GP mortar curing at a high temperature. The experimental results, effected by AS sort, BFS content and curing temperature, showed a regularity that the deeper carbonation depth of a GP concrete or mortar, the more increase of its compressive strength after carbonation. This also confirm the effect of carbonation on increasing compressive strength of FA&BFS-based GP concrete.

(2) The micro-structure change of FA&BFS-based GP mortar after carbonation, measured by SEM, further illustrated the compressive strength change. And the main carbonation products of FA&BFS-based GP concrete can be judged as Na_2CO_3 from EDS analysis.

(3) The compressive strength of OPC mortar after neutralization in any of the four environments increased. However, the strength increase of GP mortar after the neutralization was little in the environments “ E_c ”, “ E_{c+d} ”, and “ E_w ”. In the environment “ E_{w+d} ”, The GP mortar even inversely had a lower compressive strength after the neutralization than the non-neutralized specimen at the same age. And the compressive strength of the G_{c+d} specimen was smaller than that of G_c specimen after the neutralization. That is to say, the carbonation and water immersion can also improve the compressive strength of GP slightly. But drying harms the strength property of GP.

(3) According to the crack changes from the SEM images, wetting and drying harmed the structure of GP mortar in a greater degree than OPC mortar. From the result that the pH values of G_w and G_{w+d} decreased with the experimental period, it is thought that the loss of alkali matters may be a reason of crack enlargement. There were the cubic-shaped calcite crystals appeared in the O_w and O_{w+d} samples after neutralization. But the size of calcite crystal in the O_w sample was bigger than that in the O_{w+d} sample. The products occurred in the G_{w+d} sample were arranged like flower in bloom, of which the main elements were C, Ca, O and Si elements. Na_2CO_3 crystal was found in the GP mortar sample after processed in the environments “ E_c ” and “ E_{c+d} ”.

Reference

- [1] K. You, H. Jeong, W. Hyung, Effects of accelerated carbonation on physical properties of mortar, *Journal of Asian Architecture and Building Engineering (JAABE)*. 13(1) (2014) 217-221.
- [2] M. C. Jack, H. Ran, and C. C. Yang, Effects of carbonation on mechanical properties and durability of concrete using accelerated testing method, *Journal of Marine Science and Technology*. 10(1) (2002) 14-19.
- [3] P. A. Claisse, H. El-Sayad, I. G. Shaaban, Permeability and pore volume of carbonated concrete, *ACI Materials Journal*. 96 (1999) 378-381.
- [4] K. I. Song, J. K. Song, K. H. Yang, B. Y. Lee, Carbonation characteristics of alkali activated blast-furnace slag mortar, *Journal of the Korea Concrete Institute*. 24(3) (2012) 315-322.
- [5] S. S. M. N Hedge, Experimental study of accelerated carbonation effects on lightly reinforced geopolymer concrete slabs, *International Journal of Engineering Research & Technology (IJERT)*. 3(7) (2014) 1061-1067.
- [6] P. Sandor. Effect of curing method and final moisture condition on compressive strength of concrete. *Journal Proceedings*. 83(4) (1986) 650-657.
- [7] K. Andrea, H. Harald. Investigation of geopolymer binders with respect to their application for building materials. *Ceram-Silic*. 48(3) (2004) 117-120.
- [8] M. A. Sanjuán, C. Andrade, M. Cheyrezy, Concrete carbonation test in natural and accelerated conditions, *Advances in Cement Research*. 15 (2003) 171-180.
- [9] M. Criado, A. Palomo, A. Fernández-Jiménez, Alkali activation of fly ashes. Part 1: Effect of curing conditions on the carbonation of the reaction products, *Fuel*, 84 (2005) 2048-2054.
- [10] M. Criado, A. Palomo, A. Fernández-Jiménez, Alkali activation of fly ashes. Part 1: Effect of curing conditions on the carbonation of the reaction products, *Fuel*, 84 (2005) 2048-2054.
- [11] P. He, C Shi et al., Effect of further water curing on compressive strength and micro-structure of CO₂-cured concrete, *Cement and Concrete Composites*. 72 (2016) 80-86.
- [12] A. P. M. Trigo; J. B. L. Liborio, Doping technique in the interfacial transition zone between paste and lateritic aggregate for the production of structural concretes, *Materials Research*. 17(1) (2014) 17-22.

6 Conclusions and Future Works

This chapter summarizes the main conclusions drawn from the investigation of neutralization depth and pH changes with the growth of neutralization time, and the investigation of 4 kinds of neutralization environment effect on the neutralization resistance, compressive strength and micro-structure of FA&BFS-based GP concrete with different mixtures. Meanwhile, the future works are also talked about.

6.1 Conclusions

1. The carbonation rate coefficients (a) of OPC concretes, with the same compressive strength as the GP concretes, were calculated and compared to that of the GP concrete. The higher carbonation rate coefficient of GP concrete indicated that FA&BFS-based GP concrete, cured at ambient temperature, had a lower neutralization resistance than OPC concrete.

2. After investigating the carbonation resistance of FA&BFS-based GP concrete in detail by theoretical analysis and the accelerated carbonation experimental analysis, carbonation rates of the ambient-cured GP concrete and GP mortar were modeled by two root functions ($x=at^{1/n}$, a : carbonation rate coefficient). The reciprocal number of root values ($1/n$) of the carbonation rate function of FA&BFS-based GP concrete and GP mortar are respectively 0.31 and 0.22, that is lower than the 0.5 usually used for OPC concrete. That is to say, the increasing rate of carbonation depth of FA&BFS-based GP concrete in the early time is larger than that of OPC concrete.

3. The influencing factors of carbonation rate of GP concrete were clarified, including retarder addition, BFS's ratio and fineness, NaOH content, and curing temperature, etc. It can be concluded that the carbonation resistance increases with the increase of BFS ratio in active fillers (AF), NaOH content in active activator solution (AS), and BFS fineness, or with the decrease of AS/AF ratio, and water/AF ratio. Moreover, heat curing and the use of the retarder are benefit to the carbonation resistance of FA&BFS-based GP concrete. The carbonation resistance of GP concrete is related to its compressive strength. But the carbonation rate coefficient of FA&BFS-based GP concrete doesn't always decrease with its compressive strength. The carbonation resistance of GP concrete may also be affected by other factors, such as alkaline activator type.

4. The pH value in the outer zone of GP concrete after cycles of wet-dry repeating was lower, compared to cycles of carbonation-dry repeating. This indicates that GP concrete can also be neutralized by water movement except carbonation, due to the elution of alkali matters and water movement from inside. Drying would accelerate neutralization of inside of GP concrete. And the neutralization resistance of

FA&BFS-based GP concrete, which has history of heat curing, is higher than that cured only in the ambient air.

5. The GP mortar had about 2 times neutralization depth of the OPC mortar, even though the 28 days-compressive strength of GP mortar in this study was higher than that of OPC mortar. In the environment of carbonation-dry repeating, the neutralization of GP mortar was quite faster than in the environment of only carbonation. The pH in the outer position of the carbonated GP mortar decreased even below 10.0. The pH change of GP mortar in water immersion and wet-dry repeating environments also indicate that water movement would result in the neutralization of GP solid.

6. The compressive strength of ambient-cured FA&BFS-based GP concretes and GP mortars after carbonation, carbonation-dry repeating and water immersion environment increased. The GP mortar curing at a high temperature, or in the wet-dry repeating environment, inversely had a lower compressive strength after the neutralization than the non-neutralized specimen at the same age. And the compressive strength of the GP specimen, in carbonation-dry repeating condition, was smaller than that of GP specimen only carbonated. That is to say, the carbonation and water immersion can also improve the compressive strength of GP slightly. But drying harms the strength property of GP.

7. Wetting and drying harmed in a greater degree to the structure of GP mortar than OPC mortar according to SEM results. It is thought that the pH values of GP mortar, in the water immersion and wet-dry repeating environments, decreased with the experimental period lead to the crack enlargement. And after neutralizing under the two environments, the cubic-shaped calcite crystals appeared in the OPC samples. But the size of calcite crystal in water immersion environment showed bigger than in wet-dry repeating environment. GP mortar in wet-dry repeating environment after neutralization also appeared some products arranged like flower in bloom, the main elements of which were C, Ca, O and Si. In the environments carbonation and carbonation-dry repeating, Na_2CO_3 crystal was judged as the main product of GP mortar.

6.2 Future works

- The effect of carbonation on the mechanical properties, including compressive strength, sulfuric and fire resistance, dry shrinkage change etc. of FA&BFS-based GP mortar, will be conducted in detail. The FA&BFS-based GP mortar samples of the experiment, for investigating the carbonation effect on mechanical properties, have been prepared. After curing and carbonation, the carbonation effect can be clearly understood.
- The countermeasures for improving the neutralization resistance of FA&BFS-based GP concrete will be looked for. It has been got some achievements, by using the dry shrinkage agent, adding admixtures like crushed stone and red mud, and coating the surface of GP concrete by one kind of waterproof materials. But, the results were supported by only few data. Much wider and deeper experiments are necessary. The countermeasures will directly determine whether GP can be widely used in the reinforced concrete.
- The alkaline activator for GP concrete is more expensive than water for OPC concrete. The expensive price will limit the application of GP concrete to a large extent. Searching for new and cheap alkali activators, and finding the methods decreasing AS price will be a subject that needs long-term research in the future works.
- The accelerated carbonation may have some difference to the natural carbonation. That is to say, the carbonation resistance of FA&BFS-based GP concrete suffering natural carbonation need to be tested and compared with the accelerated carbonation results.

Paper List

(a) 査読のある雑誌

1. Sha Li, Zhuguo Li, Tomohide Nagai, Tomohisa Okada, Neutralization resistance of fly ash and blast furnace slag based geopolymer concrete, コンクリート工学年次論文集, (2017) Vol.39 No.1 pp.2023-2028.
2. Zhuguo Li, Sha Li, Carbonation resistance of fly ash and blast furnace slag based geopolymer concrete, Construction and Building Materials, (2017), Vol.163, pp. 668-680. (2016 IF: 3.169)
3. Sha Li, Zhuguo Li, Neutralization behaviors and post-neutralization property of geopolymer concrete in the CO₂ atmosphere and under the conditions of wetting and drying, Construction and Building Materials, (査読中)

(b) 査読のある国際会議の会議録等

1. Sha Li, Zhuguo Li, Neutralization resistance of fly ash and slag based geopolymer concrete, Proceedings of 14th ICACTS. (採用、印刷中)

(c) その他

1. Sha Li, Zhuguo Li, Carbonation Resistance of Fly Ash And Blast Furnace Slag Based Geopolymer Concrete, 2017 年度日本建築学会中国支部研究報告集, Vol.40 pp.41-44.
2. Sha Li, Zhuguo Li, Experimental Study on the Properties of Geopolymer Concrete Using Fly Ash and Ground Granulated Blast Furnace Slag (Part 5: Neutralization Resistance), 2016 年度日本建築学会大会学術講演梗概集, pp. 1491-1492.
3. Sha Li, Zhuguo Li, Experimental Study on the Properties of Geopolymer Concrete Using Fly Ash and Ground Granulated Blast Furnace Slag (Part 9: carbonation Resistance), 2017 年度日本建築学会大会学術講演梗概集, pp. 741-742.
4. Sha Li, Zhuguo Li, FEM Analysis of the Precision of Hinge-joint Plate Method Used to Calculate Transverse Distribution Coefficient, 2016 年度日本建築学会中国支部研究報告集, Vol.39 pp.57-60.
5. 田青, 李柱国, 李莎, ジオポリマー系軽量耐火被覆材料に関する基礎研究, 2016 年度日本建築学会中国支部研究報告集, Vol.39, pp.41-44。
6. 堀田 悠一, 李 柱国, 李莎, 都市ごみ焼却灰溶融スラグを用いたジオポリマー硬化体に関する実験的研究, 2017 年度日本建築学会中国支部研究報告集, Vol.40 pp.49-52。